SwRI-7531

UCRL-15605
P. O. 9877001

12

AD-A141 259

"DO-IT-YOURSELF" FALLOUT/BLAST SHELTER EVALUATION

FINAL REPORT
MARCH 1984

Prepared for
FEDERAL EMERGENCY MANAGEMENT AGENCY
WASHINGTON, D. C. 20472

20030110006

Approved for public release;
distribution unlimited.

Contract No. EMW-E-0883
Work Unit 1617C

SOUTHWEST RESEARCH INSTITUTE
SAN ANTONIO HOUSTON

DISCLAIMER

FEMA Review Notice

Unclassified

SECURITY CLASSIFICATION OF THIS PAGE (When Data Entered)

REPORT DOCUMENTATION PAGE		READ INSTRUCTIONS BEFORE COMPLETING FORM
1. REPORT NUMBER	2. GOVT ACCESSION NO. AD-A141 259	3. RECIPIENT'S CATALOG NUMBER
4. TITLE (and Subtitle) "Do-It-Yourself" Fallout/Blast Shelter Evaluation		5. TYPE OF REPORT & PERIOD COVERED Final Report
		6. PERFORMING ORG. REPORT NUMBER UCRL- 15605
7. AUTHOR(s) P. T. Nash, W. E. Baker, E. D. Esparza, P. S. Westine, N. W. Blaylock, Jr., R. E. White, M. G. Whitney		8. CONTRACT OR GRANT NUMBER(s) P.O. 987001
9. PERFORMING ORGANIZATION NAME AND ADDRESS Southwest Research Institute 6220 Culebra Road San Antonio, Texas 78284		10. PROGRAM ELEMENT, PROJECT, TASK AREA & WORK UNIT NUMBERS Work Unit 1617C
11. CONTROLLING OFFICE NAME AND ADDRESS Federal Emergency Management Agency Washington, D.C. 20472		12. REPORT DATE March 1984
		13. NUMBER OF PAGES 164
14. MONITORING AGENCY NAME & ADDRESS(if different from Controlling Office) Lawrence Livermore National Laboratory P. O. Box 808 Livermore, CA 24550		15. SECURITY CLASS. (of this report) Unclassified
		15a. DECLASSIFICATION/DOWNGRADING SCHEDULE

16. DISTRIBUTION STATEMENT (of this Report)

Approved for Public Release; Distribution Unlimited

17. DISTRIBUTION STATEMENT (of the abstract entered in Block 20, if different from Report)

18. SUPPLEMENTARY NOTES

19. KEY WORDS (Continue on reverse side if necessary and identify by block number)

Expedient Fallout Shelters
Shelter Occupant Survival
Shock Tunnel Testing
Scale Modeling
Nuclear Blast Protection
Trench Shelters

20. ABSTRACT (Continue on reverse side if necessary and identify by block number)

Expedient fallout shelters recommended to the general public were evaluated for their potential to provide safety to occupants during nuclear blast. The blast threat was in the 2 to 50 psi overpressure range from a 1 megaton (MT) yield weapon. Research included a literature search for expedient shelter designs and evaluations of the designs to certify their ability to protect occupants. Shelters were evaluated systematically by first analyzing each design for expected failure loads. Next, scale model tests

DD FORM 1 JAN 73 1473 EDITION OF 1 NOV 65 IS OBSOLETE

Unclassified

SECURITY CLASSIFICATION OF THIS PAGE (When Data Entered)

(Continued)
were planned and conducted in the Fort Cronkhite shock tunnel. Structural responses and blast pressures were recorded in a series of twelve experiments involving 96 structural response models. Two rigid models were included in each test to measure internal blast pressure leakage. Probabilities of survival were determined for each of the shelters tested.

In a search of the U. S. literature, eight candidate shelters were identified for evaluation. The expedient shelters utilize, in general, an excavation with a soil-covered roof to provide protection from fallout. Load-bearing members are timbers, household doors, or automobiles. Limited previous testing had concluded only one of the shelters, small-pole, was practical for blast loadings greater than 15 psi. Not all of the recommended shelters had been tested. Inquiries to several foreign countries found only Sweden has developed shelter designs.

Expected failure mechanisms were identified for each of the eight U. S. shelters. One shelter, tilt-up doors and earth, was eliminated from consideration because of uncertainties for the associated permanent structure. Failure loads of the remaining seven shelters were determined through analysis. Analyses included failure by overturning/translation, trench collapse, or roof collapse. A car-over-trench shelter was evaluated solely through analysis. Other shelters were tested in the Fort Cronkhite shock tunnel facility. The threshold for human tolerance to blast pressures (lung damage) was calculated as 8 psi with a 99 percent survival rate at 28 psi. Thresholds for trench wall stability were calculated based on material strengths and shelter geometries.

Several physical modeling procedures were recommended to evaluate the expedient shelters. However, limitations of the Fort Cronkhite facility eliminated all but replica modeling. Using replica modeling, blast overpressures were limited to approximately 9 psi. Model scale factors were selected so achievable load durations were long enough to consider shelter responses in the quasi-static realm. Using wooden dowels and high-quality plywood to represent poles and doors, respectively, a number of models were fabricated and tested in the shock tunnel. An elevated soil test section was used to install the buried and partially buried shelters. Shelters were tested at nominal 2.8, 4.6, and 8.8 psi overpressures. The predominant mode of failure was soil instability, even though the soil passed the "thumb pressure" test recommended in the shelter design literature. Pressures measured inside the shelters were virtually the same as the surface pressures measured outside.

The small-pole and aboveground ridge-pole shelters survived each overpressure level, although soil erosion greatly decreased the fallout protection of the aboveground ridge-pole shelter. Aboveground door-covered and crib-walled shelters survived the 2.8 psi loads, failed at 8.8 psi, and were marginal at 4.6 psi. Both the trench shelters (door-covered and log-covered) were marginal at 2.8 psi and failed for higher overpressures. However, minor modifications to the shelters noticeably improved their survivability.

SOUTHWEST RESEARCH INSTITUTE
Post Office Drawer 28510, 6220 Culebra Road
San Antonio, Texas 78284

"DO-IT-YOURSELF" FALLOUT/BLAST SHELTER EVALUATION

by
P. T. Nash
W. E. Baker
E. D. Esparza
P. S. Westine
N. W. Blaylock, Jr.
R. E. White
M. G. Whitney

FINAL REPORT
MARCH 1984

Prepared for
FEDERAL EMERGENCY MANAGEMENT AGENCY
WASHINGTON, D. C. 20472

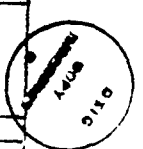

Approved:

Alex B. Wenzel

Alex B. Wenzel, Director
Department of Energetic Systems

ACKNOWLEDGEMENTS

The authors are grat[illegible] to Doctors Robert G. Hickman, Shyam N. Shukla, and Sang-Wook Kang for their program and technical guidance throughout the course of this research.

Also, special recognition is given to Messrs. Chuck Wilton, James V. Zaccor, and other personnel from Scientific Service, Inc., for their outstanding support during testing at the Fort Cronkhite shock tunnel.

Finally, the authors recognize Messrs. Ernest R. Garcia, Jr., Alfonso C. Garcia, and Mark R. Castle for their contributions to the preparation and test efforts.

TABLE OF CONTENTS

LIST OF ILLUSTRATIONS

LIST OF TABLES

EVALUATION OF DO-IT-YOURSELF FALLOUT/BLAST SHELTERS

SUMMARY

Expedient fallout shelters recommended to the general public were evaluated for their potential to provide safety to occupants during nuclear blast. The blast threat was in the 2 to 50 psi overpressure range from a 1 megaton (MT) yield weapon. Research included a literature search for expedient shelter designs and evaluations of the designs to certify their ability to protect occupants. Shelters were evaluated systematically by first analyzing each design for expected failure loads. Next, scale model tests were planned and conducted in the Fort Cronkhite shock tunnel. Structural responses and blast pressures were recorded in a series of twelve experiments involving 96 structural response models. Two rigid models were included in each test to measure internal blast pressure leakage. Probabilities of survival were determined for each of the shelters tested.

In a search of the U. S. literature, eight candidate shelters were identified for evaluation. The expedient shelters utilize, in general, an excavation with a soil-covered roof to provide protection from fallout. Load-bearing members are timbers, household doors, or automobiles. Limited previous testing had corcluded only one of the shelters, small-pole, was practical for blast loadings greater than 15 psi. Not all of the recommended shelters had been tested. Inquiries to several foreign countries found only Sweden has developed shelter designs.

Expected failure mechanisms were identified for each of the eight U. S. shelters. One shelter, tilt-up doors and earth, was eliminated from consideration because of uncertainties for the associated permanent structure. Failure loads of the remaining seven shelters were determined through analysis. Analyses included failure by overturning/translation, trench collapse, or roof collapse. A car-over-trench shelter was evaluated solely through analysis. Other shelters were tested in the Fort Cronkhite shock tunnel facility. The threshold for human tolerance to blast pressures (lung damage) was calculated as 8 psi with a 99 percent survival rate at 28 psi. Thresholds for trench wall stability were calculated based on material strengths and shelter geometries.

Several physical modeling procedures were recommended to evaluate the expedient shelters. However, limitations of the Fort Cronkhite facility eliminated all but replica modeling. Using replica modeling, blast overpressures were limited to approximately 9 psi. Model scale factors were selected so achievable load durations were long enough to consider shelter responses in the quasi-static realm. Using wooden dowels and high-quality plywood to represent poles and doors, respectively, a number of models were fabricated and tested in the shock tunnel. An elevated soil test section was used to install the buried and partially buried shelters. Shelters were tested at nominal 2.8, 4.6, and 8.8 psi overpressures. The predominant mode of failure was soil instability, even though the soil passed the thumb pressure test recommended in the shelter design literature. Pressures measured inside the shelters were virtually the same as the surface pressures measured outside.

The small-pole and aboveground ridge-pole shelters survived each overpressure level, although soil erosion greatly decreased the fallout protection of the aboveground ridge-pole shelter. Aboveground door-covered and crib-walled shelters survived the 2.8 psi loads, failed at 8.8 psi, and were marginal at 4.6 psi. Both the trench shelters (door-covered and log-covered) were marginal at 2.8 psi and failed for higher overpressures. However, minor modifications to the shelters noticeably improved their survivability.

INTRODUCTION

The purpose of this research was to evaluate recommended expedient fallout/blast shelters and determine shelter adequacies for protecting occupants against blast loadings.

A number of do-it-yourself fallout/blast shelters have been designed and recommended to provide protection from deadly radiation and radioactive fallout generated by a nuclear detonation (References 1 and 2). Shelter designs vary to accommodate local conditions and available materials. Several of the shelters have been blast loaded in nuclear blast simulation tests, but information on their blast resistance has been more qualitative than quantitative. Although the shelters were designed primarily for fallout protection, some blast-resistant capabilities have been observed.

This research program was designed to quantify overpressure levels within which the recommended fallout/blast shelters provide a safe environment for occupants. The scope of the research included a review of applicable literature, analyzing candidate shelters for expected failure loads, designing and conducting tests to determine acceptable pressure levels, and determining confidence levels for the test results. Testing was intended to simulate loadings from a 1 megaton (MT) yield weapon in the 2 to 50 psi overpressure range. Overpressure and dynamic pressure threats from a 1 MT nuclear weapon detonated at its optimum height of burst (HOB), calculated from curves in Reference 3, are listed in Table 1. Estimates of the free-field soil displacements, velocities and accelerations produced by the 1 MT blast overpressures, calculated from methods in Reference 4, are given in Table 2. The Fort Cronkhite shock tunnel, located in the Golden Gate National Recreation Area near San Francisco Bay, was specified as the test facility for this project. The facility, as described in Reference 5, presented limitations to testing which will be discussed later. A cutaway view of the shock tunnel is given in Figure 1.

TABLE 1

BLAST THREATS FROM A 1-MT AIR BURST

Ground Range (ft)	Optimum HOB (ft)	Overpressure Peak (psi)	Overpressure Duration (sec)	Dynamic Overpressure Peak (psi)	Dynamic Overpressure Duration (sec)	Wind Speed (mph)
42,000	11,000	2	3.7	0.1	4.4	70
26,000	11,000	4	3.3	0.4	4.1	163
14,600	7,500	10	2.6	2.2	3.6	294
9,200	6,000	20	2.1	8.1	3.4	502
6,400	5,400	30	1.7	17.0	3.3	669
4,900	4,000	50	1.1	41.0	2.7	934

TABLE 2

FREE-FIELD SOIL DISPLACEMENT, VELOCITY, AND ACCELERATION PRODUCED BY A 1-MT BLAST (6 FEET SOIL DEPTH)

Peak Overpressure (psi)	Peak Displacement (inches)	Peak Velocity (in/sec)	Peak Acceleration (G's)
2	3.1	2.5	1.6
4	4.3	4.9	3.2
10	6.9	12.3	7.9
20	9.7	24.5	15.8
30	11.9	36.6	23.5
50	15.3	55.6	35.7

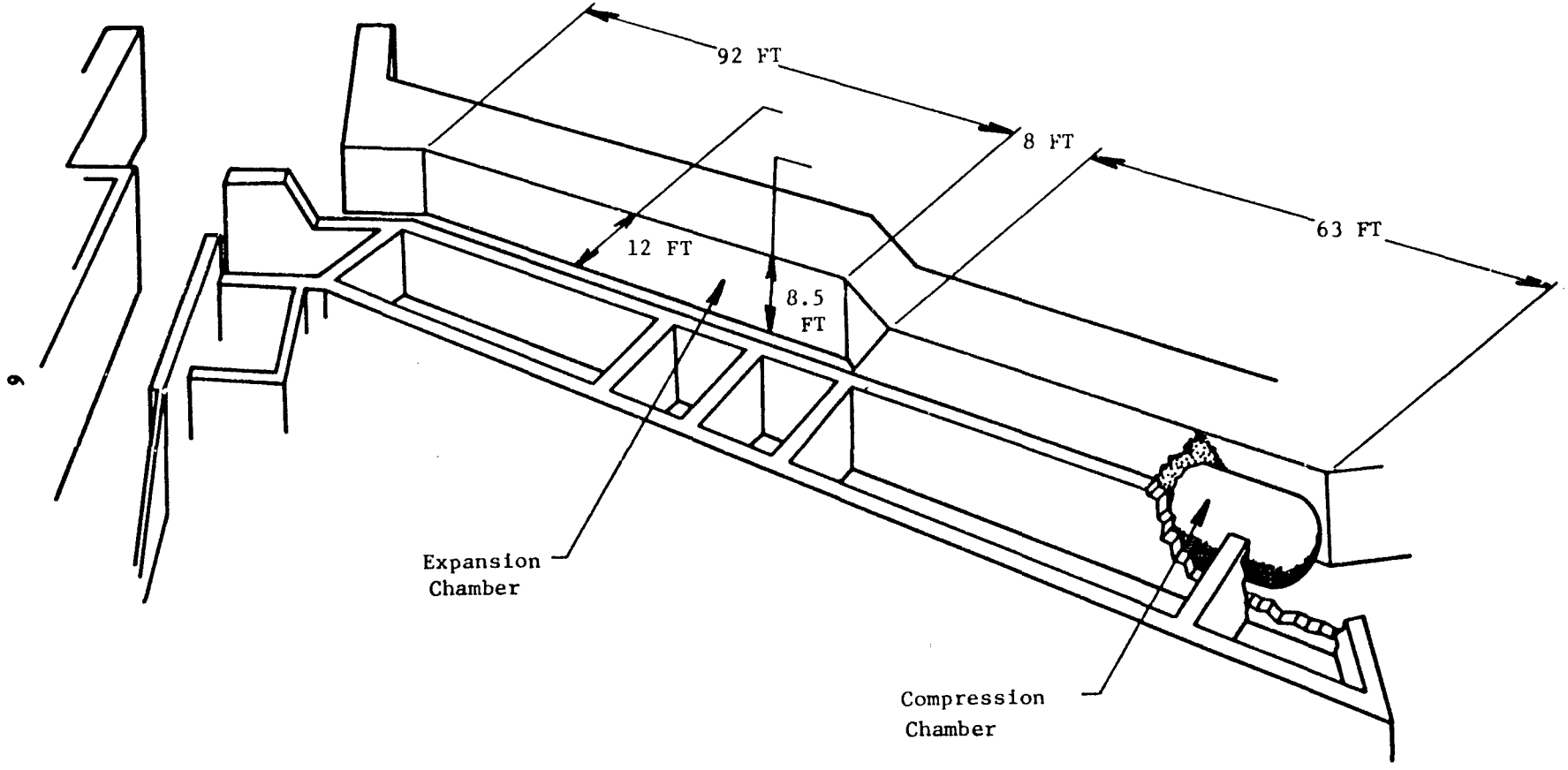

Figure 1. Cutaway View of Shock Tunnel

LITERATURE REVIEW

Using several abstracting and literature retrieval services and reference lists from a number of source documents, references were compiled and reviewed to:

- o Identify recommended do-it-yourself fallout/blast shelter descriptions
- o Determine available qualitative and quantitative information to assess shelter adequacies
- o Identify information deficiencies requiring further study for shelter certification.

A compilation of the literature reviewed is given in the reference list. Do-it-yourself shelters detailed in References 1 and 2 or some variations of the shelters are repeated in most of the literature. Eight shelters, as shown in Figures 2 through 9 were identified for evaluation. The expedient shelters utilize, in general, an excavation with a soil-covered roof to provide protection from fallout. The earth cover is generally 12 to 24 inches deep and is supported on a load-bearing roof of timbers, household doors, or automobile. The excavations are generally 3 to 5 feet deep with vertical walls. Shelters without excavations (aboveground door-covered, aboveground ridge-pole and aboveground crib-walled) utilize the earth-covered load-bearing roof and earth-mounded or earth-filled walls made of household doors or timbers.

In addition to searching the U. S. literature, several countries were written requesting any expedient shelter concepts. Organizations contacted and a summary of responses are given in Table 3.

As shown in Table 3, only the Royal Fortifications Administration in Sweden provided plans for fallout/blast shelters. Although most of the Swedish reports are not translated into English, illustrations from the reports give an idea of the Swedish philosophy toward shelter design.

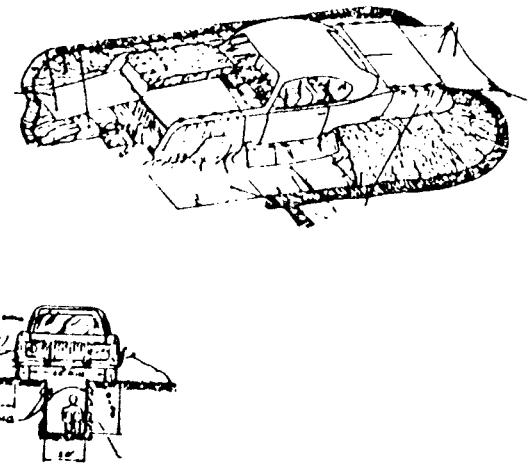

Figure 2. Car-Over-Trench Shelter

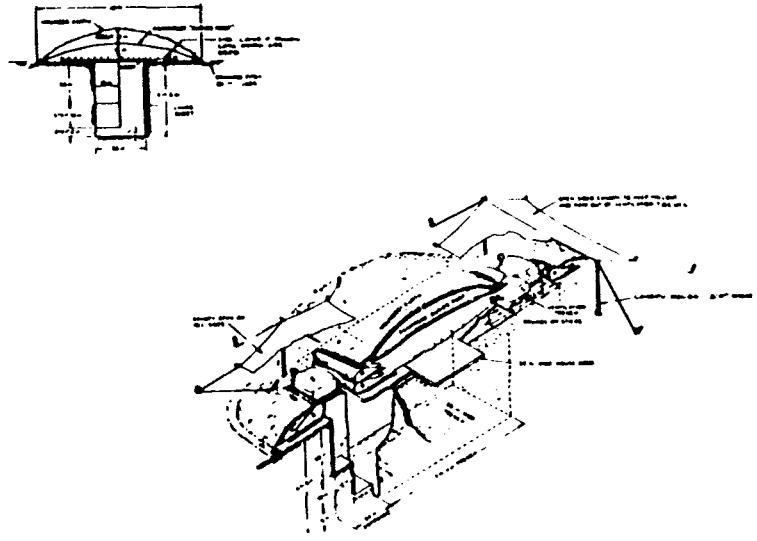

Figure 3. Door-Covered Trench Shelter

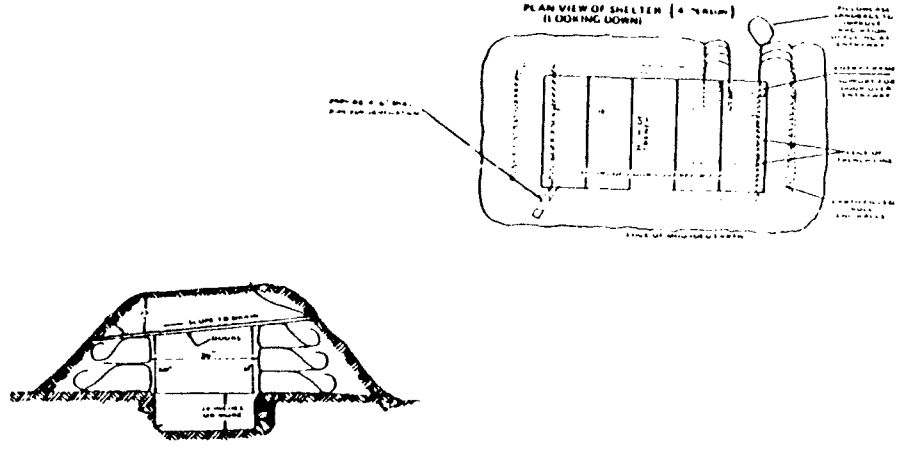

Figure 4. Above-Ground Door-Covered Shelter

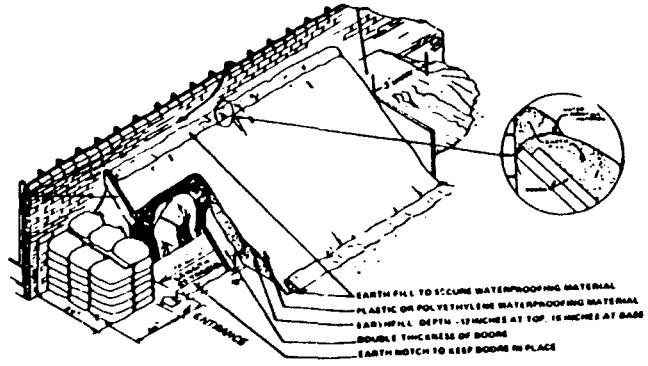

Figure 5 Tilt-Up Doors and Earth Shelter

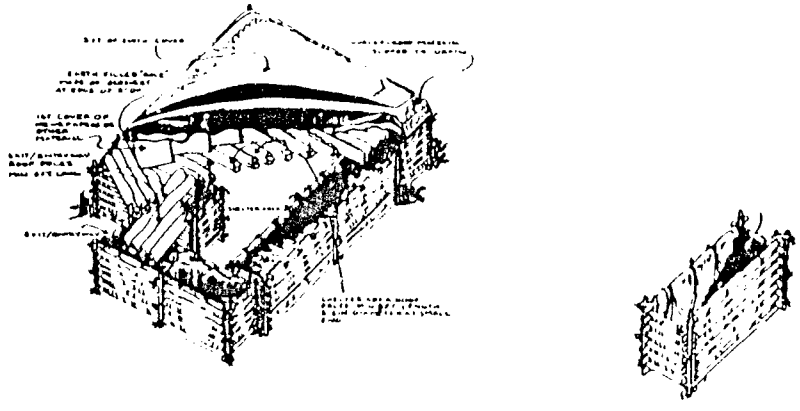

Typical Crib

Figure 6. Crib-Walled Shelter (Above Ground)

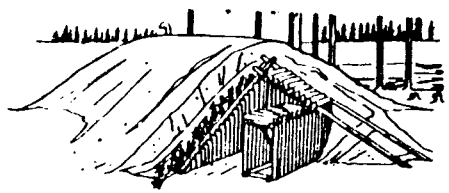

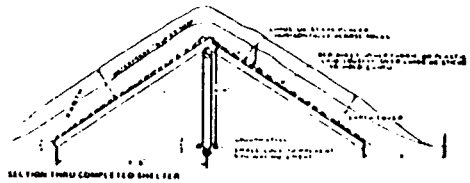

Figure 7. Above-Ground Ridge-Pole Shelter

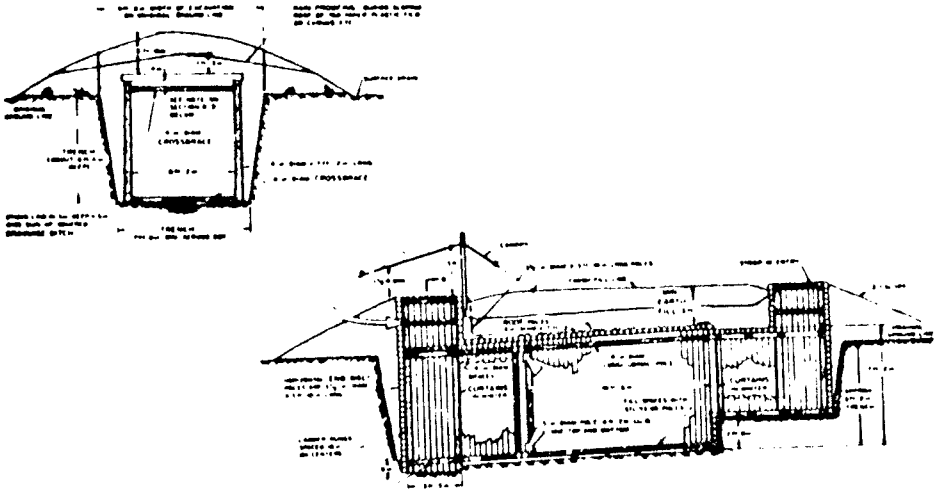

Figure 8. Small-Pole Shelter

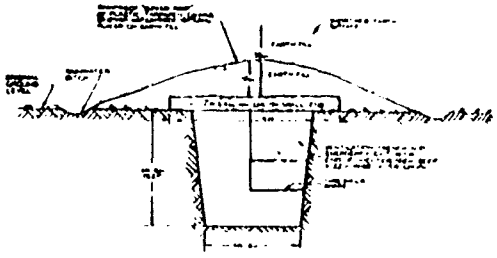

Figure 9. Log-Covered Trench Shelter

TABLE 3. FOREIGN ORGANIZATIONS CONTACTED

Country	Organization	Response
England	Royal Armament Research and Development Establishment	Still searching at the time of this report
Norway	Norwegian Defense Construction Service	No response
The Netherlands	Technological Laboratory TNO	Initial response - no work being done. Continuing search.
Germany (Federal Republic)	Ernst-Mach-Institut	None existing or planned
Switzerland	Head of Department for Safety Planning and Protective Structures	No response
Sweden	National Defense Research Institute	No response
Sweden	Royal Fortifications Administration	Eighteen documents received detailing shelter plans
Israel	Ministry of Defense	No plans for expedient shelters

Most of the shelters employ structural elements and buried designs similar to those of the U. S. However, they seem to require construction times outside of expediency, and some require heavy construction equipment to place prefabricated concrete sections. It appears structural members are always used to provide shoring of shelter earth walls. In some cases, roof members are attached to shelter walls with metal strips to resist uplift forces. Several of the concepts are given in Appendix A. More detail for each of these shelters and others is in the Swedish literature received.

Several of the U. S. concepts shown in Figures 2 through 9 or variations thereof have been included in nuclear blast simulation testing. Reference 2 briefly discusses past tests against expedient blast shelters. Damages to shelters built of lumber and soil included broken structural members, earth wall collapse, blast wind erosion of the soil cover and blast pressure leakage into the shelter. Pertinent shelter damage information was compiled from available nuclear blast simulation test reports (References 6 and 7) and is shown in Tables 4 through 8. Although blast testing has included some shelter types somewhat different from those shown in Figures 2 through 9, the ones shown are most commonly recommended to the public (References 1 and 2). Only those eight shelters were identified for evaluation; however, many of the conclusions and recommendations apply to a broad class of expedient blast/fallout protection shelters.

General conclusions from blast tests against the expedient shelters are given in Table 9. Reviewing available test information and conclusions, a shelter certification plan was developed to evaluate the recommended blast/fallout shelters. The primary information required which was lacking from previous testing included:

- o overpressure limits to which shelters provide safe environment for occupants
- o better description of required engineering properties for shelter materials
- o responses under longer duration loading
- o leakage pressure measurements inside shelters without closure systems
- o evaluations of previously untested shelters.

TABLE 4. PREVIOUS TEST RESULTS
DOOR-COVERED TRENCH SHELTER

Event	Equivalent HE Yield	Overpressure (psi)	Results	Comments
Dice Throw	1 kt	31	o Roofing doors collapsed	o Extra 2-1/2 feet soil overburden
Dice Throw	1 kt	15	c Roofing doors cracked	o Extra 2-1/2 feet soil overburden
			o Vertical caliche walls partially collapsed	
			o Inside overpressure 5 psi	

TABLE 5. PREVIOUS TEST RESULTS
ABOVE-GROUND DOOR-COVERED SHELTER

Event	Equivalent HE Yield	Overpressure (psi)	Results	Comments
Dice Throw	1 kt	15	o Roofing doors lower 1/8 inch veneer broken o One inch of earth scoured by blast winds o Interior reduced from 36 to 14 inch width due to earthroll distortions o Inside overpressure 6 psi	o Shelter axis on radius from ground zero o Entrances at each end of the shelter
Dice Throw	1 kt	5.8	o Shelter survived o Only minor earth scouring from blast winds o Inside overpressure 3 psi	o Roofing doors lower veneer broken during construction

TABLE 6. PREVIOUS TEST RESULTS
ABOVE-GROUND RIDGE-POLE SHELTER

Event	Equivalent HE Yield	Overpressure (psi)	Results	Comments
Dice Throw	1 kt	15	o Main room undamaged o Nine inches of earth scoured from top by blast winds o Plastic liner broke exposing shelter interior o Entranceways rotated o Inside overpressure 3 psi (collapsed entranceways)	o Ridge pole perpendicular to a radius from ground zero o Entrances at each end of the shelter
Dice Throw	1 mt	15	o Extreme earth scouring	o 1/10 scale model tested for 1 kt implies 1 mt yield
Dice Throw	1 kt	5.8	o Undamaged frame o Six to twelve inches of earth scouring o Plastic liner broken o Inside overpressure 2 psi	o Ridge pole perpendicular to a radius from ground zero

TABLE 7. PREVIOUS TEST RESULTS
SMALL-POLE SHELTER

Event	Equivalent HE Yield	Overpressure (psi)	Results	Comments
Dice Throw	1 kt	53	o Roof and walls moved downward approximately 2-6 inches o Floor, puffed up 2-8 inches o Earthmound and roof displaced 4-1/4 inches horizontally o Inside overpressure 1.5 psi o Blast winds blew away 12 inches of dry earth o Cracks formed in plastic liner after earth scouring	o Length of shelter perpendicular to radius from ground zero o Roof covered with an additional 2 feet of earth o Entrance covered with blast door o Excavation in hard caliche o Five inch diameter roof and wall poles

TABLE 7. PREVIOUS TEST RESULTS
SMALL-POLE SHELTER (CONTINUED)

Event	Equivalent HE Yield	Overpressure (psi)	Results	Comments
Dice Throw	1 mt	53	o Undamaged as was full-scale counterpart	o 1/10 scale model tested for 1 kt implies 1 mt yield
Dice Throw	1 mt	106	o Failed by collapsing a vertical entry o No blast wind scouring of earth	o 1/10 scale model tested for 1 kt implies 1 mt yield o Earth mounds shaped at 10^{o} rather than 36^{o}
Dice Throw	1 mt	180	o Survived o Wall poles pushed into earth 1/3 height o Lower cross bracing broke, would have injured occupants	o Main room only

TABLE 7. PREVIOUS TEST RESULTS
SMALL-POLE SHELTER (CONCLUDED)

Event	Equivalent HE Yield	Overpressure (psi)	Results	Comments
Misers Bluff	.2 kt	90	o Roof and walls undamaged o Pressure inside 4 psi o Some dust inside o Six inches of side sway o Room with bare floor suffered soil uplifting	o Additional two feet of earth cover o Solid floor of poles o Blast door included o Separate shelter room

TABLE 8. PREVIOUS TEST RESULTS
LOG-COVERED TRENCH SHELTER

Event	Equivalent HE Yield	Overpressure (psi)	Results	Comments
Dice Throw	1 kt	53	o No poles broken o Earth walls (unshored) collapsed o Maximum deflection in Chinese half 1-1/2 inch (7/8 inch permanent o Significant blast wind scouring of earth	o Half of structure was Russian design, half was Chinese design o Extra two feet of soil o Five inch diameter logs
Dice Throw	1 kt	31	o No poles broken o Earth walls (unshored) collapsed	o Constructed same as at 53 psi

TABLE 8. PREVIOUS TEST RESULTS
LOG-COVERED TRENCH SHELTER (CONCLUDED)

Event	Equivalent HE Yield	Overpressure (psi)	Results	Comments
Dice Throw	8 kt	53	o Upper parts of earth walls in Russian Half were collapsed o No poles broken	o 1/2 scale model tested at 1 kt implies 8 kt yield o Constructed same as full scale at 53 psi
Dice Throw	8 kt	31	o Damage similar to 1/2 scale test at 53 psi	o 1/2 scale model tested at 1 kt implies 8 kt yield o Constructed same as full scale at 31 psi

TABLE 9. CONCLUSIONS OF PREVIOUS TESTS

Shelter	
Door-Covered Trench	If subjected to longer-duration overpressures and greater amplitudes of ground motions, affords inadequate blast protection at overpressure ranges considerably less than 15 psi.
Aboveground Door-Covered	Impractical for use as a blast-protective shelter against blast effects considerably less than those at the 15 psi overpressure range for even very small nuclear weapons.
Aboveground Ridge-Pole	Impractical because of blast wind scouring of soil.
Small Pole	Reliable up to 50 psi if in stable soil.
Log-Covered	Earth mounds unstable for long duration blast wind loads. Shelter walls should be shored.

SHELTER EVALUATION PROCEDURES

As specified by the sponsor, shelter acceptability requires that occupants not be mortally injured. The following approach was set for determining allowable overpressure levels for shelter acceptability for both structural integrity and blast pressure leakage:

- o Identify expected shelter structural failure mechanisms
- o Analyze each shelter to determine expected structural failure loads
- o Establish allowable leakage pressures for occupant safety
- o Develop a priority list for testing shelters
- o Measure shelter blast response and pressure leakage in scale modeled tests at the Fort Cronkhite shock tunnel
- o Certify occupant safety overpressure limits for each shelter.

Damage mechanisms which could mortally injure occupants were classified as exposure to overpressure, debris impact/burial, or occupant translation/impact. Because structural failure of the shelters creates any or all of the occupant damage categories, initial efforts to eliminate candidate shelters from certification testing were based on structural analyses of the shelters. Failure modes can differ for the various shelter descriptions. The more apparent failure modes for each of the shelters are listed in Table 10.

Tilt-Up Doors and Earth Evaluation

The tilt-up doors and earth shelter combines an expedient shelter with a permanent structure. Because the response of the permanent structure is uncertain, and could possibly cause debris or bury the expedient shelter, it was eliminated from further consideration.

Car-Over-Trench Evaluation

The car-over-trench expedient fallout shelter and the instructions for its construction appear in Reference 1. In analyzing its response to

TABLE 10. SHELTER FAILURE MODE POSSIBILITIES

Shelter Type	Failure Mode			
	Overturn/ Translation	Trench Collapse	Roof Collapse	Adjoining Structure Collapse
Car-Over-Trench	•	•		
Door-Covered Trench		•	•	
Aboveground Door-Covered	•		•	
Tilt-Up Doors and Earth		•	•	•
Crib-Walled	•		•	
Aboveground Ridge-Pole	•		•	
Small-Pole		•	•	
Log-Covered Trench		•	•	

nuclear weapons blast, it is apparent from Reference 8 that, although the sheet metal in the car body may be badly dented and windows may be broken at incident blast overpressure levels of 5 psi, the car will be structurally intact and able to protect the shelter trench at that overpressure, and probably much higher pressures. But, cars struck by long-duration 5 psi blast waves from the side would be overturned by the net unbalanced diffraction and drag pressures.

So, the critical mode of response of the car-over-trench shelter is overturning by an air blast wave incident on the side of the car. A general solution to this problem is available in graphic and dimensionless equation form, based on solution of the equations for blast diffraction and drag loading and rigid-body response. Two prediction equations resulted from this analysis, one for scaled total specific impulse $\bar{i}_t$ as a function of scaled incident blast overpressure $\bar{P}_s$ and specific impulse $\bar{i}_s$, and the other for scaled threshold specific impulse for overturning $\bar{i}_\theta$ as a function of scaled target geometry and inertial properties. The equations are:

$$\bar{i}_t = \frac{1.47\ \bar{P}_s\ \bar{i}_s}{(7 + \bar{P}_s)} + \frac{(1 + 3\bar{P}_s)\ \bar{P}_s}{(1 + 0.857\ \bar{P}_s)^{1/2}} \tag{1}$$

and

$$\bar{i}_\theta = \left[\frac{2}{3} + \frac{1}{6}\left(\frac{K}{b}\right)^2 + 2\left(\frac{H}{b}\right)^2\left(\frac{h_{cg}}{H}\right)^2\right] \cdot \left\{\left[\frac{1}{4} + \left(\frac{H}{b}\right)^2\left(\frac{h_{cg}}{H}\right)^2\right]^{1/2} - \left(\frac{H}{b}\right)\left(\frac{h_{cg}}{H}\right)\right\}^{1/2} \tag{2}$$

In these equations,

$$\bar{P}_s = P_s/p_o,\ \bar{i}_s = \frac{a_o C_D\ i_s}{p_o H},\ \bar{i}_t = \frac{i_t a_o}{p_o H},\ \bar{i}_\theta = \frac{i_\theta A\ h_{b\ell}}{m g^{1/2} b^{3/2}} \tag{3}$$

Individual terms are*:

a_o = speed of sound in air = 13,400 in./sec

p_o = ambient pressure = 14.7 psi

g = acceleration of gravity = 386 in./sec^2

m = mass of body (lb sec^2/in.)

C_D = drag coefficient (dimensionless)

H = height of body (in.)

$h_{b\ell}$ = height of center of pressure (centroid of presented area) (in.)

h_{cg} = height of center of gravity (in.)

A = presented area (in.^{2})

b = base width (in.)

P_s = incident blast wave overpressure (psi)

$\bar{i}_s$, $\bar{i}_t$, $\bar{i}_\theta$ = specific impulses (psi-sec).

Equations (1) and (2) are plotted for ranges of input parameters in Figures 10 and 11 respectively.

An assessment was made for the response of a typical American two-door sedan to the blast wave from an air burst at optimum height of a 1 MT yield nuclear weapon. The incident overpressures as given in Table 1 are repeated in Table 11 along with corresponding specific impulses.

A 1979 Chevrolet Monte Carlo two-door sedan was chosen as a typical car which might be used for this shelter. Its empty weight is about 3500 lb. Its geometry can be closely approximated by the simplified block sketches in Figure 12. This shelter requires covering the hood of the car with a layer of 8 inches of soil, removing the seats and covering the floor

*The equations apply for any consistent set of units. We have chosen pounds for force, inches for length, and seconds for time.

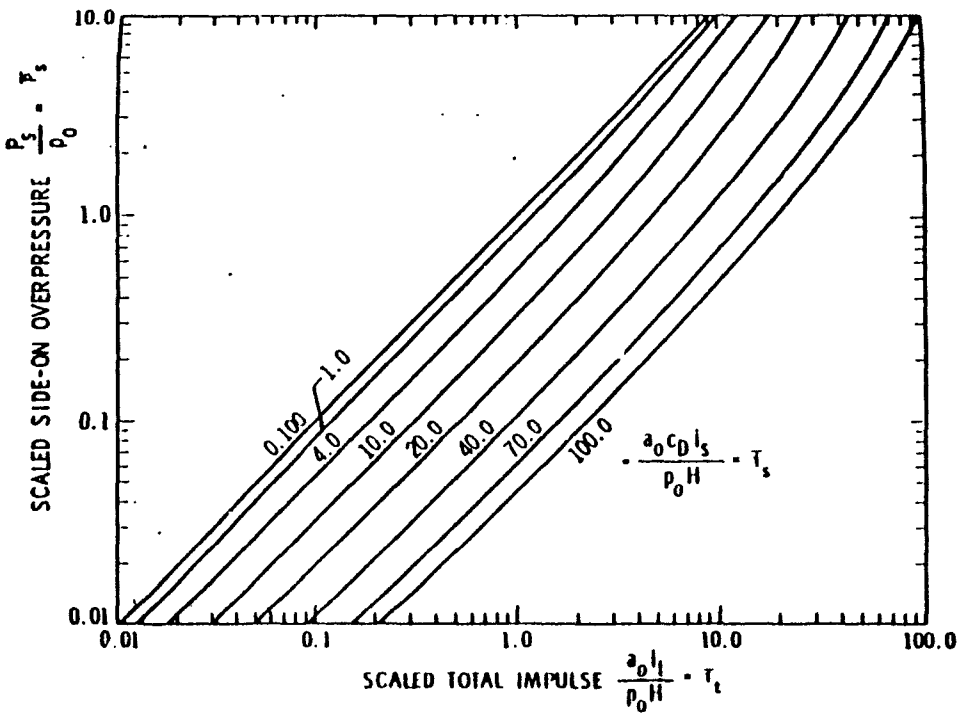

Figure 10. Specific Impulse Imparted to a Target Which Might Overturn

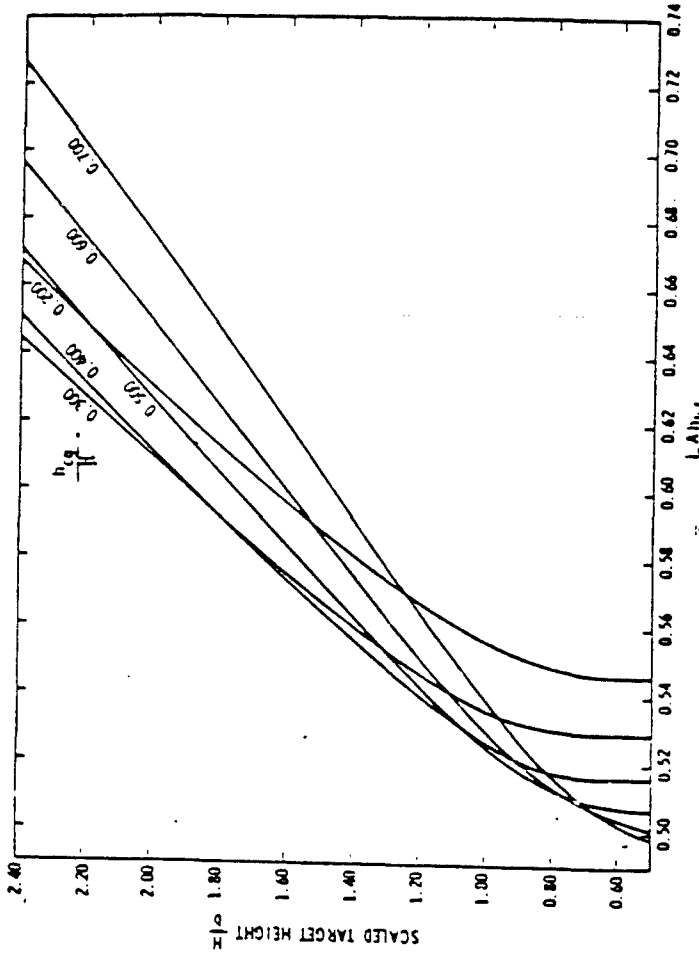

Figure 11. Impulse for Threshold of Overturning

TABLE 11. INCIDENT BLAST WAVE PARAMETERS FOR 1 MT BURST AT OPTIMUM HEIGHT OF BURST (HOB)

Ground Range R, ft	HOB, (ft)	P_s, psi	i_s, psi-sec
42,000	11,000	2	3.7
26,000	11,000	4	6.6
14,600	7,500	10	13.0
9,200	6,000	20	21.0
6,400	5,400	30	26.0
4,900	4,000	50	28.0

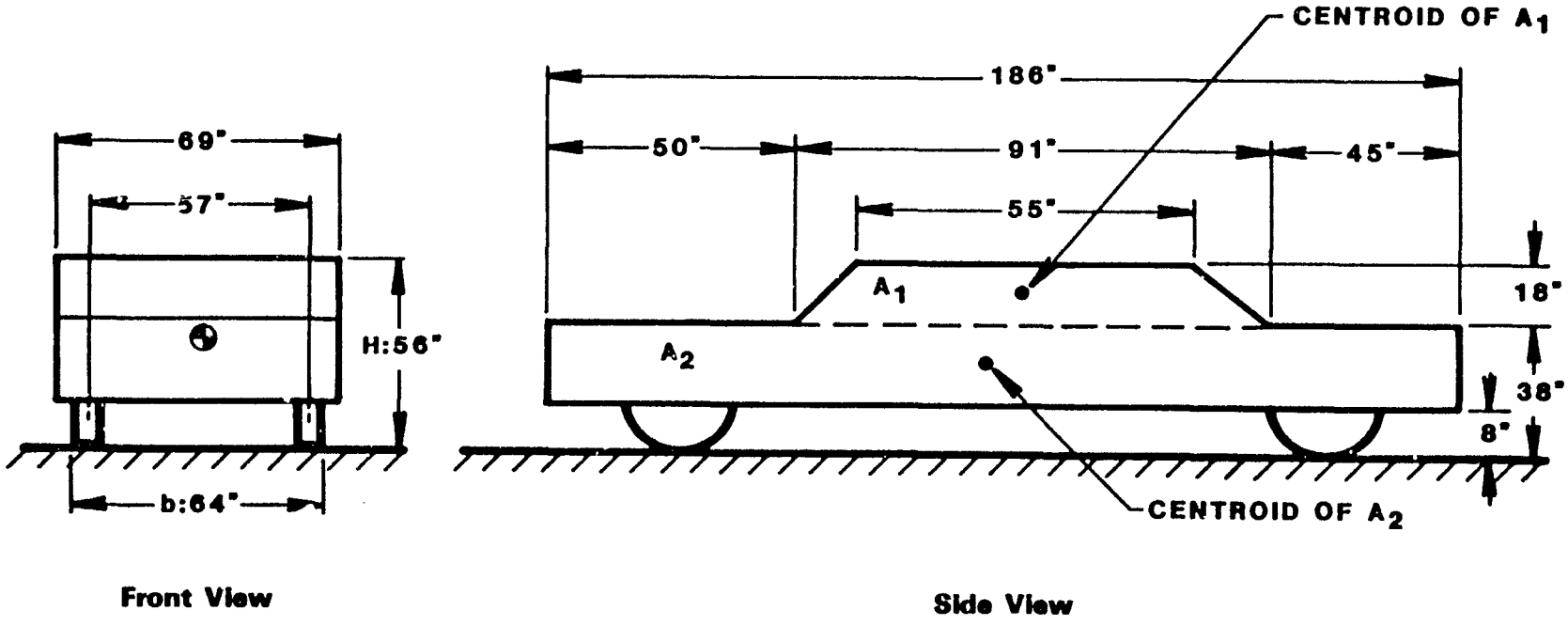

Figure 12. Block Representation of 1979 Two-Door Monte Carlo

with 12 inches of soil, and covering the trunk floor with 12 inches of soil. Assuming that uncompacted soil has a specific weight of 100 lb/ft^3 the calculated weight of soil to add to W_t, and mass m are 10,500 lb and 27.2 lb sec^2/in., respectively.

Based on dimensions given in Figure 12, the following values were determined:

Presented area	6894.0 in.^{2}
Center of pressure (height)	9.74 in.
$h_{b\ell}$	27.4 in.
H	56.0 in.
b	64.0 in.
C_d	1.2

From the given input, the specific impulse for threshold of overturning (i_θ) was found equal to 0.758 psi-sec.

For given P_s and $\bar{I}_s$, applied scaled specific impulse $\bar{I}_t$ can be calculated from Equation (1). This is shown in Table 12 for several blast loads from Table 11 as well as unscaled $\bar{I}_t$. By graphical interpolation, the threshold overpressure for overturning is:

$$P_s \approx 5.4 \text{ psi.}$$

These methods can easily be used to predict this threshold for other size cars.

Analysis of Remaining Shelters

The remaining six shelters were analyzed to determine overpressures at which shelter coverings or walls would collapse. Coverings included doors or small poles with earth overburden. Critical structural elements were identified for each shelter and idealized into a simple structural system. Physical properties of the simple systems were then transformed into single-degree-of-freedom (SDOF) models using well-established techniques (Reference 9). With an established failure criterion and described blast loadings, the SDOF models could then be used to predict expected failure overpressures through the following steps:

TABLE 12. APPLIED TOTAL SPECIFIC IMPULSE

P_s, psi	$\bar{P}_s$	i_s psi-sec	$\bar{i}_s$	$\bar{i}_t$	i_t, psi-sec	i_θ, psi-sec
2.0	0.14	3.7	72.3	2.3	0.14	0.76
4.0	0.27	6.6	129.0	7.3	0.45	0.76
10.0	0.68	13.0	253.0	34.0	2.1	0.76
5.4	(by graphical interpolation)				0.76	0.76

1. The real system was idealized using engineering judgment. The actual structural members of the various concepts were represented as either simply supported or fixed beams having uniform cross sections loaded by an evenly distributed soil overburden. For simplicity, the mass of the system is comprised of the soil and wood members and the strength of the system is derived from the wood members alone as illustrated in Figure 13. Because of the material properties of wood, there is no elastic-plastic or plastic response. For a fixed beam, when the material yields at the supports the system has failed. For a simply supported system, when the material yields at mid-span, the system has failed.
2. The idealized system was then converted to a SDOF model. This conversion was made using transformation factors based upon an assumed deformed shape of the actual structure and conservation of energy. Thus, a simple spring mass system was established. The deflection and velocity of this SDOF system is the same as that for some significant point on the idealized system; in this case, the mid-span.
3. Loading was idealized for this analysis. The loading was considered uniform over the idealized system at any instant in time; however, the magnitude of the load varied with time. The blast analysis indicated the load in one case (aboveground ridge-pole shelter) to have a sharp rise to some peak pressure, fall quickly to a drag phase pressure, and then reduce very slowly with time to atmospheric pressure. In other cases the loading was equal to the side-on pressure loading one would measure for a level terrain. The first load type has a bilinear pressure pulse, and the second type a triangular pressure history as shown in Figure 14. In each case loads from the blast pressures are added to the constant dead load of the soil overburden.
4. Initial conditions include consideration of the soil overburden. The system has an initial deflection due to this dead load. Initial velocity of the system is zero.

Real System

Idealized System Using Engineering Judgment

Single-Degree-of-Freedom System

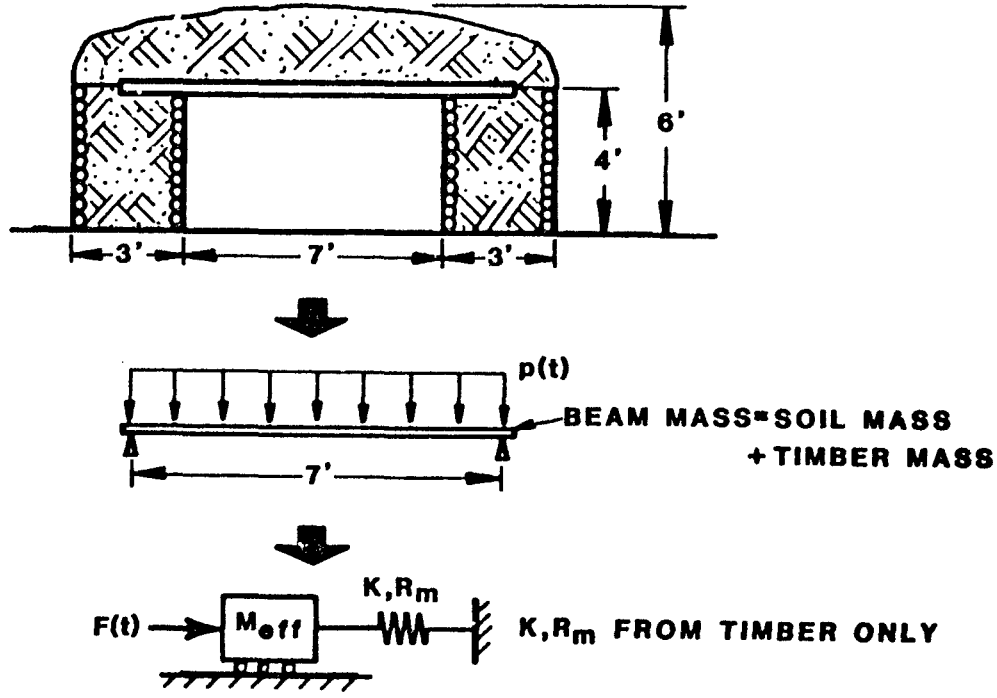

Figure 13. Structural Response Analysis

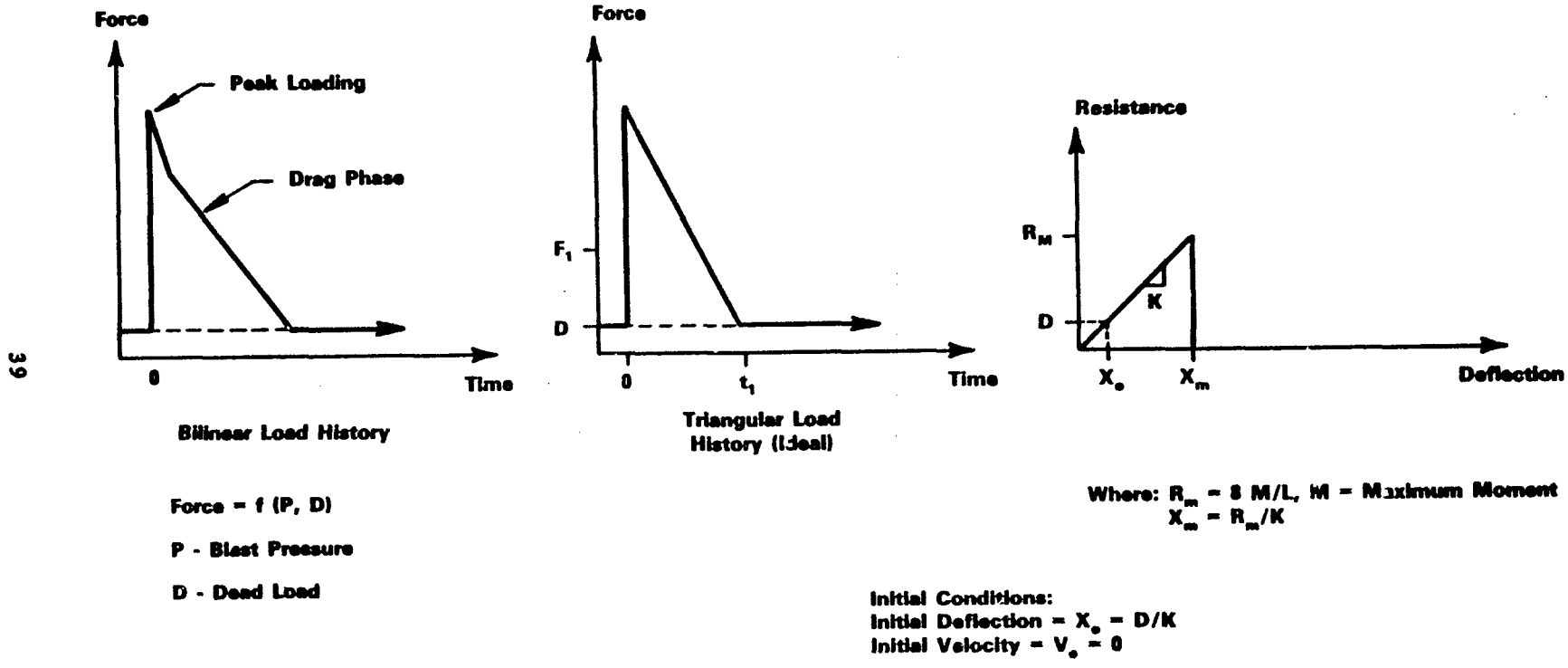

Figure 14. Load Profiles and Resistance-Deflection Function

5. At this point the response of a shelter covering system can be evaluated for a given load. Several blast loading conditions of increasing severity can be evaluated for a single covering system to determine when the structure would fail. This is somewhat tedious, and it is more convenient to back-calculate the load which would cause failure. This can be done if the blast loading is further idealized. For the bilinear forcing function, the drag phase can be considered static and suddenly applied. Energy methods can be used to predict the failure loading. The external work (total static force times displacement to failure) is equated to the total internal energy of the system (area under the resistance-deflection function). The initial deflection and overburden load are accounted for in the equation. Thus, an estimate of the side-on pressure which corresponds to the failure loading is determined.

6. Using the estimate from step 5, the forcing function was determined as discussed in step 3 which corresponds to the side-on, static pressure estimated in step 5. An SwRI computer code was used to determine the system deflection. Input to the code was a load history. The deflection was compared with the failure deflection to confirm the results of step 5 for the time-dependent load. Reiteration can be made if necessary to establish a failure related side-on pressure. A sample calculation illustrating the analysis technique is given in Appendix B.

The beam models of the shelter covering system discussed above were analyzed using the engineering theory for stresses in beams to determine if these members were susceptible to a shear failure prior to attaining their full bending capacity. Considering the static capacity of the beams, it was determined that each would fail in bending before failing in shear. This conclusion was extended to the dynamic loading case.

Table 13 summarizes analysis results. Both simple and fixed support conditions were considered for the door-covered trench and log-covered trench shelters. Each of the six shelters analyzed passed the two psi overpressure criterion for qualifying as a fallout protection shelter.

TABLE 13. SUMMARY OF STRUCTURAL FAILURE LOADS

Shelter Concept	Side-On Overpressure (psi)	Member Type	Boundary Conditions	Span (inches)
Door-Covered Trench	15.9	Door	FF*	36
	3.4	Door	SS**	60
Aboveground Door-Covered	16.2	Door	FF	36
Crib-Walled	7.2	Door	SS	84
Aboveground Ridge-Pole	4.8	Pole	SS	101
Small Pole	9.2	Pole	SS	74
Log-Covered Trench	45.6	Pole	FF	42
	14.5	Pole	SS	60

*FF = Fixed-fixed
**SS = Simply Supported

A solution technique was developed to determine the slope failure threshold for vertical excavations such as found in the covered-trench shelters. The method is essentially a Coulomb-wedge technique (Reference 10) for a uniform surcharge over a specified bearing area. Because the trench excavations are shallow, the soil weight in the failing wedge is neglected. The solution technique is presented graphically in Figure 15.

Threshold pressures for slope failure are given in Table 14 for the candidate trench shelters. These calculations were made based on the material properties for the soil used in the Fort Cronkhite tests, as given in Appendix C.

Human Tolerance

Literature concerning the harmful effects of blast on humans has been published since as early as 1768. However, knowledge of the mechanisms of blast damage to humans was extremely incomplete until World War I, when the physics of explosions was better understood. Since that time, numerous authors have contributed considerable time and effort in the study of blast damage mechanisms and blast pathology. Each situation has its own unique environment with trees, buildings, hills, and various other topographical conditions which may dissipate the energy of the blast wave or reflect it and amplify its effect on an individual. Because of these different variational factors involved in an explosion-human body receiver situation, only a simplified and limited set of blast damage criteria will be included here. The human body receiver will be considered standing in the free-field on flat and level ground when contacted by the blast wave. Excluding certain reflected wave situations, this is the most hazardous body exposure condition. Air blast effects can be divided into four categories: primary blast effects, tertiary blast effects, ear damage, and blast generated fragments (Reference 11). Only primary blast effects are considered in this analysis.

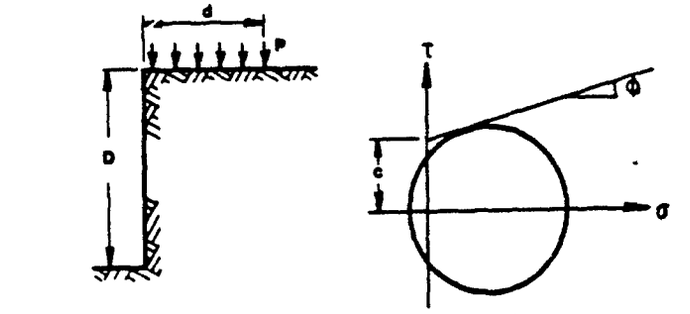

p — Structural Member Reaction Bearing Stress
d — Bearing Length
C — Soil Cohesion Intercept Stress (Material Property)
D — Excavation Depth
ϕ — Soil Friction Angle (Material Property)

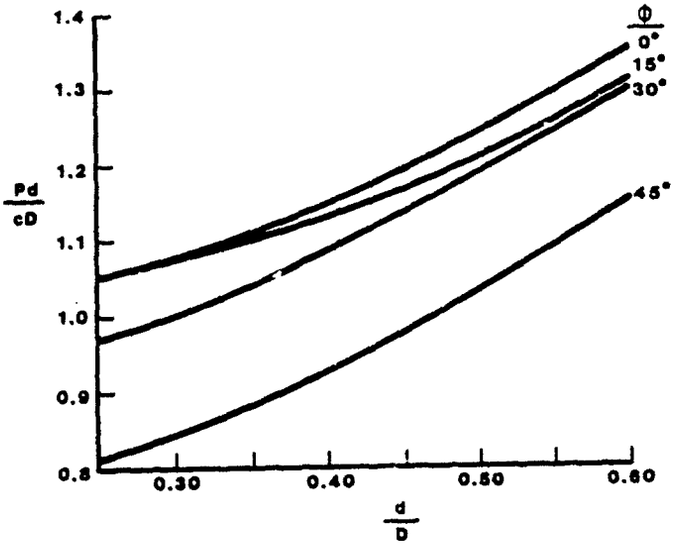

Figure 15. Threshold for Slope Failure

TABLE 14

THRESHOLD PRESSURES FOR SLOPE FAILURES

ϕ = 25.8 degrees

C = 4.5 psi

	SHELTER	
	Door-Covered Trench	Log-Covered Trench
Member Length L (in)	80	88
Bearing Length d (in)	22	23
Trench Depth D (in)	54	54
$\frac{Pd}{CD}$	1.15	1.16
Bearing Stress P (psi)	11.06	10.06
Overpressure $p = \frac{P(2d)}{L}$	6.1	5.5

Primary Blast Damage

Primary blast effects are associated with changes in environment pressure due to the occurrence of the air blast. Mammals are sensitive to the incident, reflected and dynamic overpressure, the rate of rise to peak overpressure after arrival of the blast wave, and the duration of the blast wave (Reference 11). Specific impulse of the blast wave also plays a major role (References 12 and 13). Other parameters which determine the extent of blast injury are the ambient atmospheric pressure, the size and type of animal, and possibly age. Parts of the body where there are the greatest differences in density of adjacent tissues are the most susceptible to primary blast damage (References 11, 14 and 15). Thus, the air-containing tissues of the lungs are more susceptible to primary blast than other vital organs (Reference 16).

Pulmonary injuries directly or indirectly cause many of the pathophysiological effects of blast injury (Reference 17). Injuries include pulmonary hemmorrhage and edema, rupture of the lungs, air-embolic insult to the heart and central nervous system, loss of respiratory reserve and multiple fibrotic foci, or fine scars, of the lungs. Other harmful effects are rupture of the eardrums and damage to the middle ear, damage to the larynx, trachea, abdominal cavity, spinal meninges, and radicles of the spinal nerves and various other portions of the body.

Bowen, et al., (Reference 15) and White, et al., (Reference 12), have developed pressure versus duration lethality curves for humans. Some of the major factors which determine the extent of damage from the blast wave are the characteristics of the blast wave, ambient atmospheric pressure, and the type of animal target, including its mass and geometric orientation relative to the blast wave and nearby objects. Although Richmond, et al., (Reference 13) and later White, et al., (Reference 12) both from the Lovelace Foundation, discuss the tendency of the lethality curves to approach isopressure lines for long duration blast waves, their lethality curves demonstrate dependence on pressure and duration alone. Since specific impulse is dependent on pressure as well as duration, pressure-impulse lethality or survivability curves appear to be more appropriate. The tendency for pressure-impulse lethality curves to approach asymptotic

limits is also very aesthetically appealing from a mathematical point of view. Also, since both pressure and specific impulse at a specified distance from most explosions can be calculated directly, it is especially appropriate that pressure-impulse lethality (or survivability) curves be developed. This has been done and is described in Reference 18. These curves and their use are reproduced here as Figure 16.

It should be noted that these curves represent percent survivability, and higher scaled pressure and scaled impulse combinations allow fewer survivors. Presenting the curves in this fashion is advantageous since they apply to all altitudes with different atmospheric pressure and all masses (or sizes) of human bodies. The value for body weight used in the scaling is determined by the demographic composition of the particular area under investigation. It is recommended that 11 lb be used for babies, 55 lb for small children, 121 lb for adult women, and 154 lb for adult males. It should be noticed that the smallest bodies in this case are the most susceptible to injury. For the blast pressures and impulses as previously specified, survival rates are shown on the flat horizontal portions of curves in Figure 16. Expected survival rates and overpressure levels are given in Table 15. The threshold for lung damage occurs at approximately 8 psi.

MODEL ANALYSIS

The Pi Theorem was used to develop dimensionless ratios for blast loads enveloping a shelter. The shelter may be above ground or buried. Basically, either logs or doors are laid in some configuration and covered with earth. By keeping a description of the shelter simple, a model analysis can be conducted which can be applied to any of the designs. Parameters important to the analysis are shown in Figure 17.

To scale the loading, three atmospheric conditions must be included in the model analysis. We elected to use atmospheric pressure P_o, atmospheric density ρ_o, and the ratio of specific heats for air γ_o. The loads of interest will include the peak free-field overpressure P, the maximum drag pressure q, and the duration of the loading T.

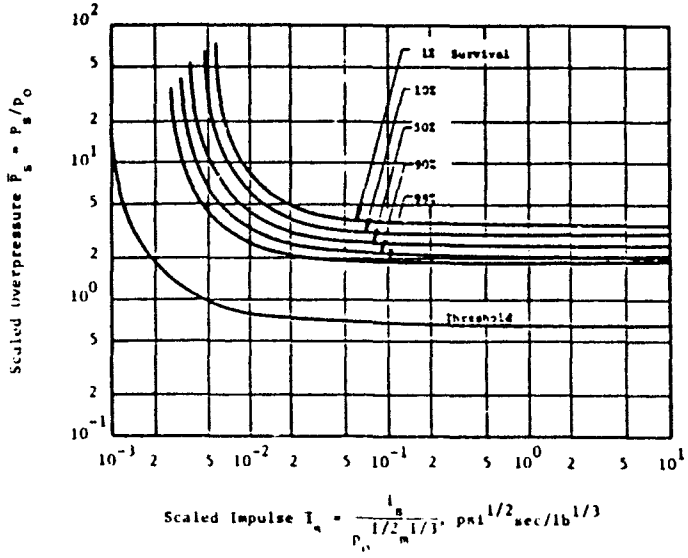

$\bar{P}_s$ = scaled incident peak overpressure

P_s = peak incident overpressure

p_o = ambient atmospheric pressure

$\bar{i}_s$ = scaled specific impulse

i_s = specific impulse

m = weight of human body

Figure 16. Survival Curves for Lung Damage to Man

TABLE 15

LUNG DAMAGE
SURVIVAL RATES AND OVERPRESSURES

SURVIVAL RATE (%)	OVERPRESSURE (psi)
100 (Threshold)	8
99	28
90	30
50	35
10	45
1	50

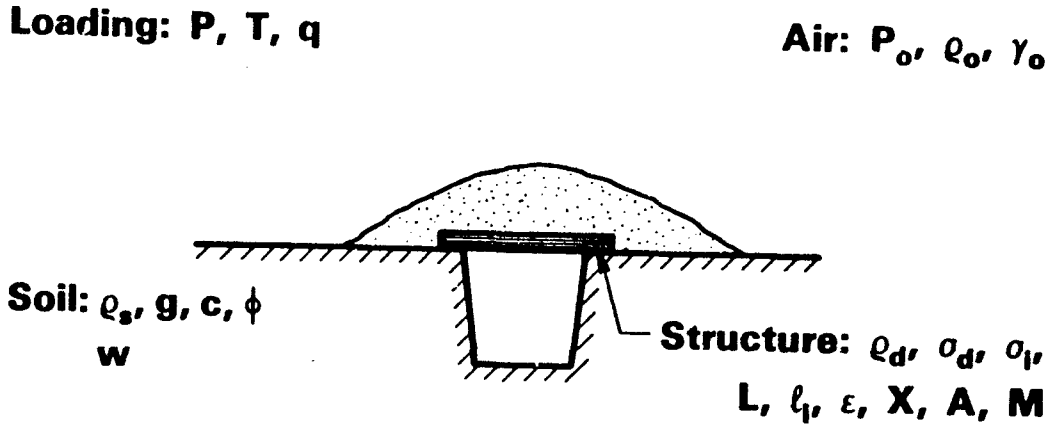

Figure 17. Physical Parameters

Soils contribute to the response of the shelter system so we will include soil mass density ρ_g, cohesion c, friction angle , and moisture content w in this analysis. In this manner, both soil strength and inertial effects have been considered in the analysis. One additional parameter, the acceleration of gravity g, is added should dead weight or gravitational effects become important. Inclusion of g in the analysis is subject to debate, because most investigators would agree that gravitational effects are secondary. Gravity is included in the analysis to see if it can be scaled, too, which would not become apparent without listing the acceleration of gravity. Although the car-over-trench shelter was not tested, it is included in the model analysis for completeness. To model rigid body translation or overturning, as when the car is parked over a trench, gravity must be included in that analysis.

To simulate a car parked over a trench the total mass M must be known. The parameter M can also represent the mass of a person which may be in a trench and thrown about. When a mass M and acceleration of gravity g are listed, both inertial and gravitational effects are being considered in modeling rigid body motion.

For the wood in the door or poles being used structurally in the trench design, the mass density ρ_d, characteristic strength such as ultimate strength σ_d and all other strengths relative to the characteristic strength σ_i must be simulated in any model. The parameter σ_i represents many stresses or strengths such as yield point relative to σ_d, material toughness relative to σ_d, and even strengths of second or third materials relative to the strength of the basic material σ_d. Essentially, σ_i can be considered a term representing any strength.

So far geometry has not been discussed in this model analysis. Many different parameters will be needed to completely define a trench, inforcement dimension, size of earth cover, etc.; however, geometry can be represented by a characteristic length L and ratios of the numerous other geometric lengths relative to L can be made using a parameter $_i$. Numerous $_i$ parameters are needed to interrelate the trench, door, poles, earth cover, person, and loading conditions.

The remaining parameters to be defined are the responses of interest. These include strain ε at various locations in the shelter, the displacement X of shelter walls, and acceleration A experienced by a person or object inside the shelter.

These 20 parameters are summarized in Table 16 together with their fundamental units of measure in an engineering system of force F, length L, and time T. From these 20 parameters a list of 17 dimensionless ratios, called pi terms, follows. The process for obtaining pi terms is purely algebraic. No new assumptions are made in going from a list of parameters to a list of dimensionless ratios provided the list is complete. Many textbooks exist which can present the formal mathematical procedures of obtaining pi terms.

One acceptable and complete set of dimensionless ratios is given in Table 17. What can and cannot be done with the Fort Cronkhite facility can be illustrated using the list in Table 17.

Two different systems, a model and prototype, are equivalent when the nondimensional ratios are the same in both. The individual parameters do not have to be the same, only the pi terms and the dimensionless ratios. To satisfy this specific requirement is often difficult. Facility limitations can make meeting scaling requirements especially difficult. The pi terms in Table 17 must be reviewed to determine what can and can't be accomplished in satisfying dimensionless ratios.

Because three fundamental units of measure have been used, three assumptions can be made concerning possible scale factors. Then all pi terms must be inspected to see if all terms are the same in both model and prototype systems.

One method of constructing a model is to build a geometrically smaller model with materials of the same strength and density in corresponding locations of model and prototype systems. If one defines a scale factor for length λ_L to mean length in the model L_m divided by length in the prototype L_p, then this definition means:

TABLE 16. LIST OF PARAMETERS

Parameter	Symbol	Fundamental Units of Measure
Peak Overpressure	P	F/L^2
Duration	T	T
Drag Pressure	q	F/L^2
Atmospheric Pressure	P_o	F/L2
Atmospheric Density	ρ_o	FT^2/L^4
Ratio of Specific Heats for Air	γ_o	—
Mass Density of Soil	ρ_s	FT^2/L^4
Acceleration of Gravity	g	L/T^2
Cohesion of Soil	c	F/L^2
Friction Angle of Soil	ϕ	—
Moisture Content of Soil	w	—
Total Mass of Car or Person	M	FT^2/L
Mass Density of Door or Poles	ρ_d	FT^2/L^4
Characteristic Strength of Door or Pole	σ_d	F/L^2
Other Strengths or Stresses	σ_i	—
Characteristic Length	L	L
Other Lengths Relative to L	ℓ_i	—
Strain Caused by Loading	ε	—
Displacement of Objects	X	L
Acceleration of Rigid Bodies	A	L/T^2

TABLE 17. LIST OF DIMENSIONLESS RATIOS

$\pi_1 = \frac{P}{\sigma_d}$	Constitutive Similarity	$\pi_{11} = \frac{T \sigma_d^{1/2}}{L \rho_d^{1/2}}$	Scaling of Time
$\pi_2 = \frac{q}{\sigma_d}$		$\pi_{12} = \frac{A \rho_d L}{\sigma_d}$	Scaling of Acceleration
$\pi_3 = \frac{P_o}{\sigma_d}$		$\pi_{13} = \frac{g \rho_d L}{\sigma_d}$	
$\pi_4 = \sigma_i$		$\pi_{14} = \varepsilon$	Scaling Strain
$\pi_5 = \frac{c}{\sigma_d}$			
$\pi_6 = \frac{X}{L}$	Geometric Similarity	$\pi_{15} = \gamma_o$	Scaling Ratio of Specific Heats
$\pi_7 = \ell_i$		$\pi_{16} = \phi$	Scaling Friction Angle
$\pi_8 = \frac{\rho_o}{\rho_d}$	Similar Densities	$\pi_{17} = w$	Scaling Water Content
$\pi_9 = \frac{\rho_s}{\rho_d}$			
$\pi_{10} = \frac{M}{\rho_d L^3}$	Lumped Mass Relative to Distributed Mass		

$$\lambda_L \equiv \frac{L_m}{L_p}$$

Similarly, a scale factor for density λ_{ρ_d} can be defined to mean:

$$\lambda_{\rho_d} \equiv \frac{\rho_{d_m}}{\rho_{d_p}}$$

and a scale factor for strength λ_{σ_d} can be defined as:

$$\lambda_{\sigma_d} \equiv \frac{\sigma_{d_m}}{\sigma_{d_p}}$$

When the same materials are used in corresponding locations as in a replica model

$$\lambda_{\rho_d} = \lambda_{\sigma_d} = 1.0$$

and of the three scale factors, only λ_L has a value other than 1.0

$$\lambda_L = \lambda \ .$$

One does not want too small a model; yet, the model must be small enough so as not to choke flow in the test facility. Replica modeling can be demonstrated considering an example value for λ of 1/6. Under these conditions a 1/6-scale replica model would satisfy all pi terms if parameters were scaled as in Table 18.

While scaling all parameters as in Table 18 theoretically meets the requirements presented by the terms in Table 17, in reality these requirements cannot be met. The acceleration of gravity g is the same in model and prototype. However, Table 18 indicates that the acceleration of gravity should be greater in the model than in the prototype. Because this requirement will not be met, gravitational effects are not scaled in this model. If gravitational effects can be considered to be secondary, the model will still be appropriate. For failure of a door or structure

TABLE 18. EXAMPLE SCALE FACTORS FOR A REPLICA MODEL

Parameters	Symbols	Scale Factor	Scale Factor In 1/6-Scale Model
Length	L, $\bar{X}$	λ	1/6
Pressure	P, q, P_o	1.0	1.0
Stresses	σ_d, c	1.0	1.0
Densities	ρ_s, ρ_s, ρ_o	1.0	1.0
Strain	ε	1.0	1.0
Friction Angle	ϕ	1.0	1.0
Water Content	w	1.0	1.0
Ratio of Specific Heats	γ_o	1.0	1.0
Lumped Mass	M	λ^3	1/216
Time	T	λ	1/6
Accelerations	A, g	$1/\lambda$	6.0

fabricated from poles, gravitational effects are insignificant. For rigid-body sliding or overturning of a vehicle over the trench, gravity provides a righting force which cannot be ignored. Hence, in vehicle-over-trench designs, a replica model is inappropriate.

Another problem arises caused by facility limitations. The Fort Cronkhite facility can only generate shock waves of 8 psi maximum overpressure with a 120 ms duration down the tunnel. While many candidate designs could fail at overpressures less than approximately 8 psi, the 120 ms duration will be too short. A duration of 120 ms in the 1/6-scale model corresponds to 0.720 sec duration in the prototype. Large megaton nuclear weapons have durations of several seconds associated with most conditions to be tested. This facility limitation means that durations will be too short in all replica model tests. Fortunately, the structural response of most shelter designs falls in the quasi-static loading realm. Provided the response of a model also falls in this domain, duration of loading does not have to be rigorously scaled. If peak deflections in the shelter and strains occur before a time which is less than 1/4 the duration of the loading, the response can be considered as being in the quasi-static loading realm. Provided the response of both systems is in the quasi-static loading realm, the Fort Cronkhite facility can be used for replica model tests. Replica modeling means that Fort Cronkhite will be facility limited to overpressures which are approximately 8 psi or less.

A replica model does have advantages. The major advantage is that the same materials are used in corresponding locations. It is easy to make smaller poles or a small door and mound earth of the same material as in the prototype to heights which are much less than in the prototype. For a 1/6-scale model test only 1/216 the volume or mass of material is used as in a prototype test.

Because a desire exists for testing up to prototype overpressures of 50 psi, another approach is to ask what might be done by testing at reduced pressures. In other words if:

$$\lambda_p \equiv \frac{P_m}{P_p} = \beta$$

Three assumptions are still allowed so a smaller model would still mean:

$$\lambda_L = \lambda$$

The third assumption would be to keep the acceleration of gravity the same in model and prototype so that dead weight effects could be simulated. This requirement would mean:

$$\lambda_g = 1.0$$

For this model all parameters would scale as in Table 19.

The parameter β can take on any value less than 1.0. Unfortunately, problems will arise unless the test tunnel can be evacuated. The model law says that atmospheric pressure must also be scaled by a factor β. Alone, the parameter P_c is not that important; however, P_o does determine how q and P relate to one another. Figure 18 is a plot of q/P versus P/P_o. Notice that for small values (P/P_o less than 1.0), doubling P increases q by a factor of four. However, this increase does not hold true for P/Po ratios greater than 1.0. Eventually, a change in P causes no change at all in q relative to P when P/p_o becomes very large. The reason that one would test at a reduced pressure at all is that high prototype pressures might be simulated in exchange for the extra difficulty. Whenever overpressures become very high, both the drag load q and overpressure P must be modeled if the entire loading history applied to a shelter roof is to be scaled.

Were the test facility able to be evacuated to 1/6 of an atmosphere, very high pressures could be modeled in the Fort Cronkhite tunnel. If P_o is reduced, the ratio P/P_o stays the same in Figure 18, and thus the ratio q/P stays the same in model and prototype. For a 1/6-scale geometric model, the densities of wood and soil would have to be the same in model and prototype, but the strength of soil and wood would be reduced by a factor of 6. Such a modification would be possible, but cannot be considered unless the Fort Cronkhite facility is modified. Because of the results in Figure 18 and the importance of pi terms such as P_o/σ_d, P/σ_d,

TABLE 19. SCALE FACTORS WITH MODEL TESTS AT REDUCED PRESSURE

Parameters	Symbols	Scale Factor
Length	L, X	λ
Pressure	P, q, P_o	β
Stresses	σ_d, c	β
Densities	ρ_s, ρ_d, ρ_o	β/λ
Strain	ε	1.0
Friction Angle	ϕ	1.0
Water Content	w	1.0
Ratio of Specific Heats	γ_o	1.0
Lumped Mass	M	$\beta\lambda^2$
Time	T	$\lambda^{1/2}$
Accelerations	A, g	1.0

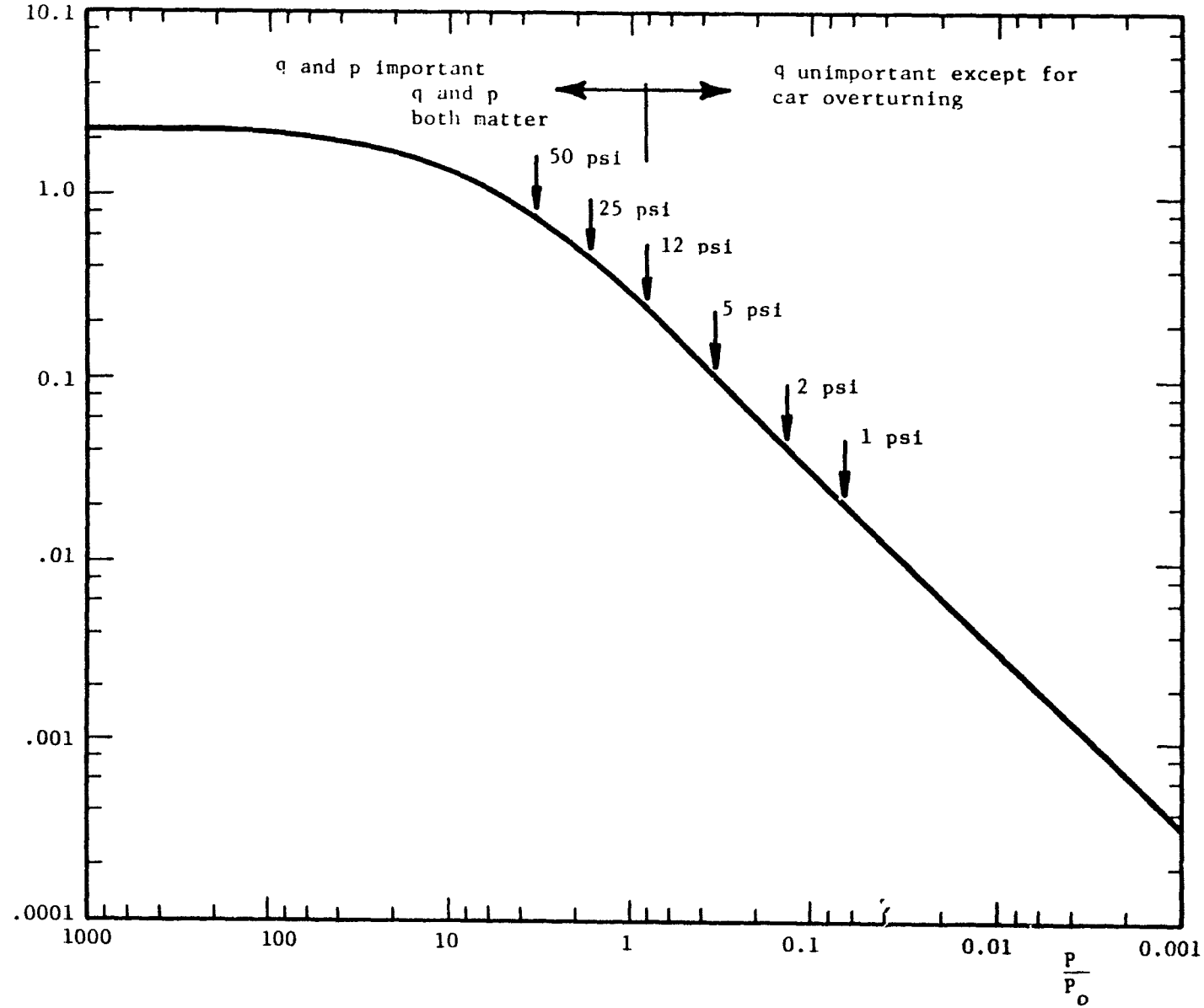

Figure 18. Relationship for Dynamic Pressure, Overpressure and Initial Pressure

and q/σ_d, no high overpressure tests above approximately 8 psi loadings are currently possible in the Fort Cronkhite facility without undergoing major facility modification.

One final method for obtaining long durations so problems such as blowing away earth cover can be simulated is to change gases in the tunnel. Whenever air is used in a 1/6-scale replica model, the maximum prototype duration which can be simulated is 0.720 seconds. If a denser gas such as freon replaces air in the tunnel, this prototype duration in the same 1/6-scale model can be extended to 2.173 seconds. For the same initial ambient pressure of 14.7 psi in a freon tunnel, the ratio q/P_s can be kept in the same proportions even though P_s might not be the same in a freon tunnel as in an air-filled tunnel. A change in P_s would be countered with a change in the strength σ_s of the shelter. This approach for scaling durations leads to a change in the materials from which a shelter is built. In other structural response studies, dissimilar material models (models built from other materials) have been fabricated.

Delving further into the possibility of using dissimilar material models seemed pointless at this stage because the Fort Cronhkhite test facility cannot take other gases. Until the Fort Cronkhite facility is modified to allow lower ambient pressures and/or substitution of other gases in the tunnel, use of it as a test facility is limited to replica models. A wider range in facility capabilities is required before alternative modeling approaches become possible.

TEST DESIGN

One of the serious limitations of the Fort Cronkhite facility for simulating megaton yield weapons' blast is that the blast durations are much too short, even for small scale testing. Maximum duration attainable is only about 120 ms (0.120 sec). But, if this duration is still long relative to critial response times of the model shelters, then loading is quasi-static, and this limitation is of little concern.

To determine the loading realm and select model sizes, response times were estimated for the shelters. Fundamental vibration frequencies were calculated for the main strength structural members for each shelter except the car-over-trench shelter. Wooden dowels were chosen to represent logs in the pole shelters. Material properties used to determine pole shelter natural frequencies were:

Compressive Strength $\sigma_p = 8{,}700$ psi

Young's Modulus $E_p = 741{,}000$ psi

Main structural members in the pole shelters are generally four inches in diameter. Selecting 3/8-inch dowels to model the poles resulted in a scale factor of:

$$\lambda_{poles} = \frac{0.375}{4.0} = \frac{1}{10.7}$$

Several types and sizes of plywood were tested along with solid door sections to select modeling materials and sizes. Average bending strengths are summarized in Table 20. Utile plywood, 3/16-inch thick, was selected to model doors serving as structural members. Using 3/16-inch plywood to model the nominal 1-3/8 inch thick doors resulted in a scale factor of:

$$\lambda_{doors} = \frac{\frac{3}{16}}{1\frac{3}{8}} = \frac{1}{7.33}$$

TABLE 20. DOOR MATERIAL BENDING STRENGTHS

Material	Thickness (in.)	Average Bending Strength (psi)
Solid Door	1-13/32	11,384
Utile	1/4	8,694
Utile	3/16	12,619
Okoume	1/4	7,581
Okoume	3/16	8,736
Utile/Epoxy Coated	1/4	12,936
Utile/Epoxy Coated	1/36	12,320
Okoume/Epoxy Coated	1/4	8,085
Okoume/Epoxy Coated	5/32	8,601

Fundamental periods were calculated for each of the shelters and summarized in Table 21. With the scale factors chosen, overpressure loadings could be considered quasi-static, meaning the load duration was several times longer than the shelter response period to assure maximum response was attained. A ratio T/τ_m greater than 4 was considered in the quasi-static response realm.

Test Bed for Excavations

A major consideration in test planning was the arrangement of model-scale test structures within the expansion chamber of the Fort Cronkhite Facility, and the effects of this arrangement on blast loads on the structures. Essentially, all of the expedient shelters involve some sort of trenching, so much of the shelters are below grade. To simulate such shelters within the test facility a soil-filled test section was installed inside the shock tunnel to allow preparation or insertion of model-scale shelters below grade. Nominal length and height dimensions of the test section are given in Figure 19. Laterally, the test section spanned the entire width of the tunnel (12 feet). To allow smooth shock wave loading approaching the models, a ramp was installed upstream at the front of the test bed. Downstream of the models, the test bed or false floor was continued to prevent premature expansion of the incident shock wave. A down ramp was also installed on the downstream side to terminate the test bed. By providing a 1-foot high elevated floor over a 28-foot length of the tunnel floor, several models could be tested at one time. An estimate of the flow over the models was made to approximate the worst case shock loading that would occur.

The blockage factor due to the elevated floor is small and the elevated floor provides enough depth for sublevel structures to be incorporated into the earth. With a 1-foot elevated surface, side-on shock pressure at the floor is increased by 5 percent over the pressure that would be obtained were the tunnel to be used in the usual fashion.

TABLE 21. SHELTER FUNDAMENTAL PERIODS

Shelter	τ, sec (full-scale)	Approximate Scale	τ, sec (scaled)	T/τm*	Quasi-Static
Door-Covered Trench	0.0380	1/7.33	0.00518	23.1	Yes
Aboveground Door-Covered	0.030	1/7.33	0.00409	29.3	Yes
Crib-Walled	0.18	1/10.7	0.0168	7.1	Yes
Aboveground Ridge-Pole	0.25	1/10.7	0.0234	5.1	Yes
Small Pole	0.17	1/10.7	0.0159	7.5	Yes
Log-Covered Trench	0.024	1/10.7	0.00224	53.6	Yes

* T = 0.12 sec
τm = natural period of model

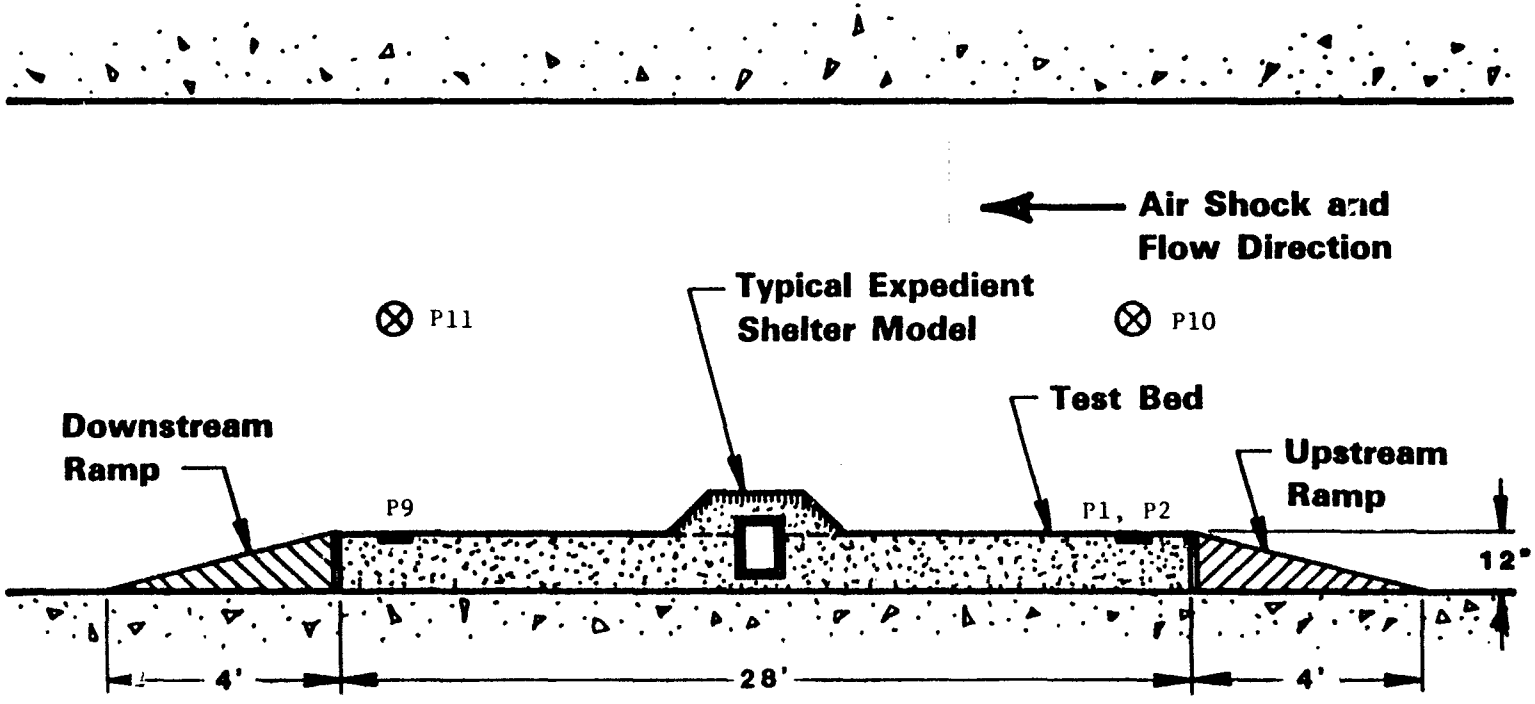

Figure 19. Elevated Soil Test Section

The shock Mach number which would be obtained for 10 psi overpressure driven loading is predicted to be 1.29 and, correspondingly, the particle velocity resulting is 473 ft/sec (q = 2.7 psi). Temperature after the shock front would be approximately 165°F and the density would be 1.49 times ambient. The flow Reynolds number would be 3.6×10^6 per foot. The boundary layer that develops behind the shock front would grow to a depth of approximately five inches at the front of the elevated surface. The momentum thickness associated with these conditions would be approximately one-half inch. It is anticipated that the viscous flow related parameters realistically simulate full-scale parameters that would be encountered in a nuclear blast.

By considering the interference drag that results between the models after the passage of the shock front, the spacing between models was determined. The spacing between models in tandem is that spacing necessary to eliminate interference drag. A similar approach was used to evaluate the spacing needed to eliminate interference drag in the tunnel axis direction. This method of determining spacing requirements follows procedures used to space obstacles in a conventional wind tunnel. By this technique, it was determined that eight models may be tested during one test run using a 28-foot long elevated test surface.

Axial spacing, based on this procedure, requires that the test models be six feet apart on centers, with the first pair of models being four feet behind the transition from a 15-degree ramp up to the test surface. The fourth set of models would be, for a 25-foot test surface, three feet forward on centers from a 15-degree ramp down to the shock tunnel floor. Recommended lateral spacing was based on having models with the lowest profile located toward the front edge of the elevated test bed. The last set of two models could be any of the models in pairs or in duplicate. The trench shelters would be three feet from a side wall to the edge of the model. The small-pole or aboveground door-covered shelters would be 1-1/2 feet from a side wall and the crib-walled and aboveground ridge-pole shelters would be two feet from a side wall to the edge of the model.

Shock diffraction interference with these arrangements would not be significantly different or altered from that found on an isolated model.

Statistical Design Considerations

One of the program objectives is to be able to use the results of the test program to "certify" that a given shelter design provides acceptable protection for a certain range of overpressure loads. In order to accomplish this objective, the terms "acceptable" and "certify" must be quantified.

The term acceptable is taken to mean that the shelter does not suffer severe structural damage that would be harmful to human inhabitants. These acceptability criteria can be stated quantitatively in terms of permanent structural rotation and deformation measures and internal pressure levels.

The definition selected for the term certify influences how the test program should be structured. Among several options possible are:

(1) Use test results to certify that there is a 90-percent confidence that shelter type A provides acceptable protection at least P_s percent of the time when exposed to a load of X psi.

(2) Use test results to certify that there is a 90-percent confidence that the response of shelter type A will be less than threshold value R (psi, degrees of rotation, etc.) when exposed to a load of X psi.

It is important to note that in the first option, the confidence interval is around P_s, which is a percentage or a probability number. In the second option, the confidence interval is around R, which is a structural response parameter. Each option is described in more detail in the following paragraphs along with some illustrations to help clarify the concepts. Both options were pursued in the test program.

Option (1) - Confidence Interval on P_s

Option (1) requires a binomial type of experiment that can be described as follows. Let a trial be defined as the application of a blast load of a given size to a shelter of type A. The "experiment" then consists of n repeated trials using the same blast load and the same shelter type. The outcome of each trial must be defined such that only one

of two possible choices can occur. In this instance, label the outcomes as survival and failure, where survival indicates that the shelter provides adequate protection and failure indicates that it does not. P_s, then, is defined to be the probability of shelter survival on any given trial.

The true value of P_s for a given shelter and applied load is unknown. One purpose of the test program is to estimate the true value of P_s by a statistic $\hat{P}_s$, which is calculated from the experimental results, and to quantify how much confidence can be placed in the estimate.

$$\hat{P}_s = \frac{\text{Total number of successes}}{\text{Total number of trials}} = \frac{s}{n}$$

When calculated in this fashion, P_s will be an unbiased estimate of the real probability of survival, P_s.

Figure 20 illustrates the type of certification that can be obtained from binomial experiments like the one described above. The solid curve represents the expected value of P_s for a given applied blast load. In order to generate this curve, repeated tests must be conducted for each of several applied blast loads. The tests results are then used to calculate P_s for these load values. The dashed band represents the confidence interval around P_s. The size of this confidence region is influenced primarily by the number of trials (n) conducted with a given blast load, and by the confidence level desired (e.g., 50, 90, 95 percent confidence). The curve of interest is really the one defining the lower bound of the confidence region. Using the sketch shown in Figure 20, we see as an example that there is more than 90-percent confidence that the probability of survival will be at least 0.5 for applied blast loads less than 7 psi. Such a result applies only to a given shelter type in one particular orientation to the blast wavefront.

Figure 21 illustrates the strong influence that the number of tests exerts on the size of the confidence region. If eight tests are conducted for a particular applied blast load, the probability of shelter survival can only be predicted within $\pm$ 0.3 with 90-percent confidence. Approximately 70 tests are required to reduce this error to $\pm$ 0.1 for a particular blast load. Certain critical conditions must be satisfied in order to be able to describe the test program as a series of binomial experiments. First, it was noted earlier that only two possible outcomes are allowed for

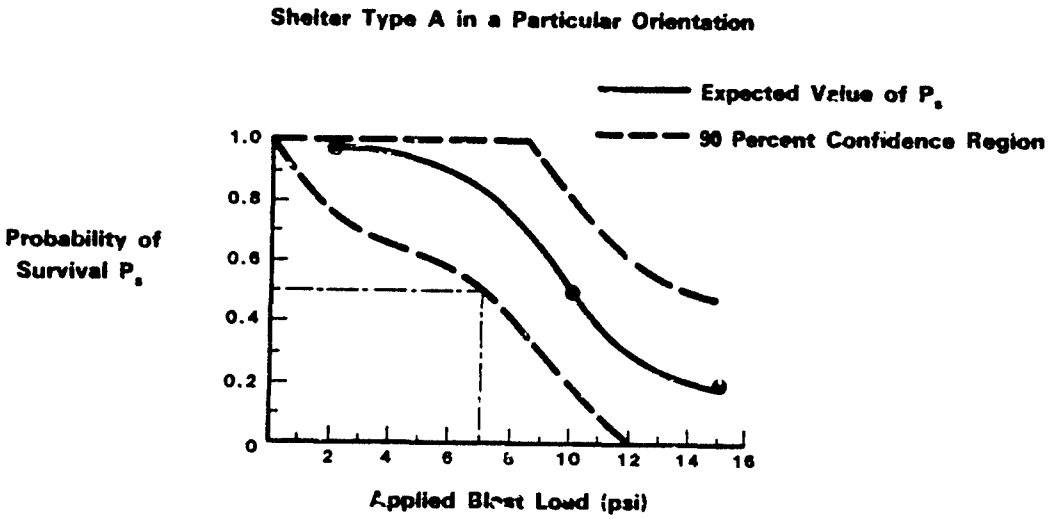

Figure 20. Confidence Region for P_s

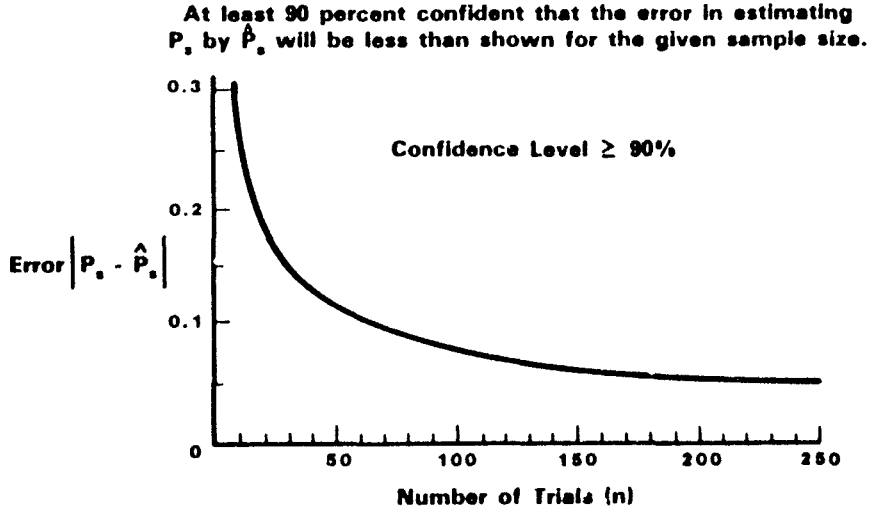

Figure 21. Number of Binomial Trials Required

each trial: survival or failure. This means that the test engineer must be able to make a clear and concise definition of survival that can be applied rigidly to each test. There can be no gray areas resulting in partial successes.

The second assumption is that the trials are independent. Violations of this assumption could occur:

(1) if the shelter models are placed in the shock tunnel in such a way that the blast wave reaching a model is influenced by reflections and turbulence from nearby models, or

(2) if debris from one test model flies down the test chamber and causes damage to another test model, or

(3) if shelter models that are used more than once suffer some type of undetected cumulative damage effects (e.g., residual stresses) from trial to trial.

Care must be taken in test setup and design to avoid these conditions.

The third assumption for a binomial experiment is that the true value of P_s remains constant from trial to trial. The main factors that influence the validity of this assumption are the reproducibility of the applied blast load for each trial, and the similarity (i.e., consistency) of the shelter models of a given type. If care is exercised in model building, this latter error factor can be reduced to negligible proportions. The former error source is, however, a problem for this test program. The pressure trace is not uniform throughout the test section of the shock tunnel. It oscillates rapidly through a series of peaks as a function of time, and it also degrades with distance in the downstream direction. Consequently, it is not possible to produce exactly the same pressure loading at any two shelter positions in the test chamber, and it is difficult to reproduce the same loads from test to test. All of this translates into between-test variability in the true value of P_s, a condition in direct violation of one of the key assumptions.

Option (2) - Confidence Interval on R

Option (2) requires that a regression analysis be performed to arrive at a predictive equation for the shelter response parameter of interest.

This response parameter, R, might be the amount of permanent beam displacement or rotation observed, the peak pressure experienced inside the shelter, or some other similar type of quantitative measure of a shelter's response to an applied external blast load.

The regression equation, in its simplest form, will be

$$R = \alpha + \beta L + \varepsilon$$

where α and β are unknown constants estimated from the test data, L is the load (psi) applied to produce response R, and ε is an error term which reflects the fact that observed responses are subject to variability and cannot be expressed exactly as a weighted multiple of L.

The true value of R for a given L cannot be computed because the true values of constants α and β are unknown. Consequently, the test program is used to collect data from which statistical estimates α, β and R can be made, and to quantify how much confidence can be placed in these estimates.

Figure 22 illustrates the type of certification that can be obtained using the regression analysis approach. The solid line represents the expected value of the response parameter, R, for a given value of the external load, L. This line is generated by computing a least-squares fit to the raw data collected in the test program. Note that in this approach, repeated response measurements for the same applied load are not required, whereas they were in the binomial experiment.

The spread of the observed data about the least-squares regression line is used to define a confidence region about the line. The curve of interest in Figure 22 is really the one defining the upper bound of the confidence region. Using Figure 22 as an example, we see that there is more than 90-percent confidence that the peak internal pressure will be less than 2.75 psi for an applied blast load of 9.7 psi. Such a result would apply only to a given shelter type in one particular orientation to the blast wavefront.

There are two types of confidence intervals that can be determined:

(1) A confidence interval on the <u>average</u> response that will be obtained in repeated testing with an applied load L_o.

(2) A confidence band on the <u>observed</u> response that will be obtained

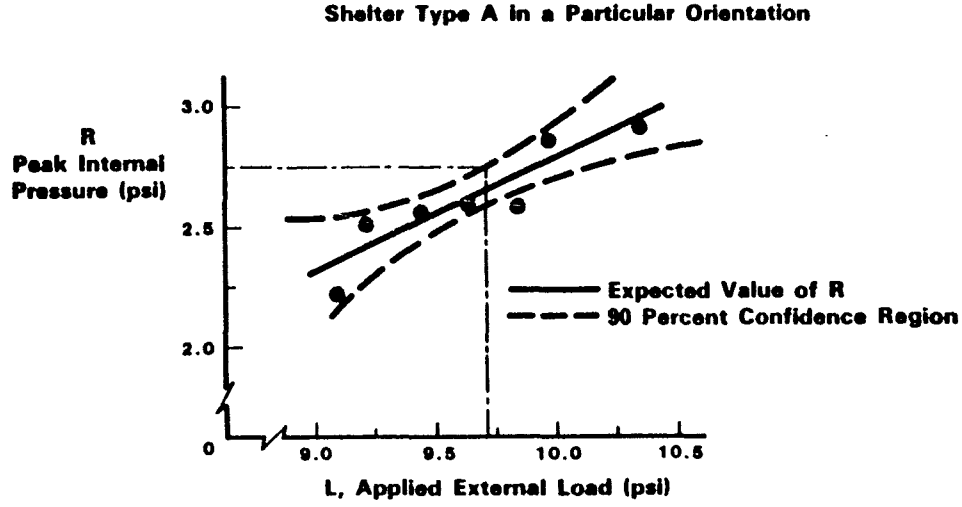

Figure 22. Confidence Region for R

on any one test conducted at some future time using an applied load L_o.

The second type of interval will be wider than the first type, but it is the one most applicable to the objectives of this research. Neither of the intervals will have a uniform width. As indicated in Figure 22, the confidence interval will be narrowest in the region close to the average value of L used in the tests. The interval on R widens as L moves away from this mean.

It can be shown by examining the theory behind the generation of the confidence intervals that two additional factors influence the width of the intervals. One factor is the number of trials. The other factor is the variability of the test data about the least-squares regression line. This means that the test engineer can improve the confidence band in either of two ways. One obvious way is to increase the number of tests. The second option is to improve the quality of the tests; i.e., reduce data scatter through careful model building, improved accuracy of data collection devices, more precision in blast wave generation, etc. In the binomial approach described earlier, there was only one effective way to reduce the width of confidence intervals—run more tests.

There are some critical conditions that must be satisfied before the regression approach to certification can be a viable one. First, the error terms in the regression model must be independent and must be characterized by approximately normal distributions having zero mean and constant variance. There are statistical techniques for checking the validity of this condition after the data have been collected, but not before. If we are careful to include all important predictor variables in the regression model, then the remaining error sources will probably satisfy the above conditions reasonably well.

Another condition is that the regression model must be correctly specified. This means that (1) all important parameters for predicting the shelter response must be included, and (2) the form of the equation must match the shape of the data trend. Applied blast load L is probably the most important predictor variable. Blast wave orientation is another important predictor, but it can be deleted by running all the tests with one shelter orientation. Matching the form of the equation to the shape of

the curve can be accomplished by making mathematical transformations as required on the predictor variables. This process can be simplified by restricting the range of test values for L so that data trends become more linear.

The final condition for proper use of the regression approach is that predictor variable L be nonrandom and measured without error. This may be a problem. The pressure trace at the shelter will be a series of many pressure peaks arriving in a short period of time as opposed to a constant applied pressure. If the shelter responds to each of these pressure peaks, then the above condition may be violated since the exact form of the pressure trace cannot be predicted or repeated. The more probable case, however, is that the shelter cannot respond separately to each of the individual pressure peaks because their duration is so short. Instead, the shelter will react as if it saw a single pulse representing some average form of the multiple peaks. If this is the case, then the above condition for the regression analysis will be more realistic.

TEST PROCEDURE

All 12 experiments in this program followed a similar test procedure regardless of which model shelters were being tested and which pressure level was used. As indicated previously, eight response shelters were installed in the test bed in each experiment along with two rigid models. The normal test sequence was begun by measuring carefully and marking on the soil test bed the location of each model shelter. Then, each model shelter was assembled or installed in place following the instructions provided in Reference 1 for five types of shelters and in Reference 2 for one type of shelter.

While all the model shelters were being installed, the pressure measurement system was set up and checked for proper end-to-end operation. Amplifier gain and tape recorder voltage levels were set to accommodate the peak pressure expected. After the model shelters were completed and the measurement system configured properly, the exit from the shock tunnel was closed and Primacord explosive placed in the compression tube. The back door to the compression tube was then closed, and the area around the shock

tunnel was secured. After a short countdown sequence the explosive array was detonated, and the pressure data were recorded.

The tunnel exits and back door were then opened to allow natural ventilation of the explosion gases before test personnel would return to the test section of the tunnel to record the condition of the test shelters. In the meantime, the pressure data were played back into a transient recorder for quick-look analysis using Polaroid prints of the pressure-time histories. After it was safe to return inside the shock tunnel, SwRI personnel recorded the condition of each model shelter. The tested shelters were then carefully disassembled to determine their internal condition and then finally removed altogether from the test bed. The test bed was then readied for the next set of shelters to be tested.

Model Shelter Fabrication and Assembly

Six different fallout shelters were tested in this project to determine their structural blast resistance. As indicated in previous discussions, two other shelters were originally identified for evaluation but were eliminated from testing. The eight shelters were numbered for identification and the six that were tested are listed in Table 22 along with the scale factor used to size their components.

The models of the six expedient shelters were prefabricated as much as possible at SwRI prior to departure to the Fort Cronkhite Shock Tunnel. In some cases, such as shelter 7, it was possible to assemble the complete wooden structure at SwRI. In other cases wooden subassemblies were put together before departure and later assembled at the test site. Finally, for some shelters (for example, shelter 2), only the model components for the logs and doors could be prepared at SwRI, and the complete assembly was effected at the test site. For those shelters which used soil trenches, wooden molds were fabricated at SwRI and used to form the trenches in the soil test bed.

The door-covered trench shelter, 2, was one of the below ground designs for which a mold was made and used to form the trench. The procedure for making the trench was begun by digging an oversized hole in the test bed, filling, and tamping the soil at the bottom of the hole to

TABLE 22. MODEL EXPEDIENT FALLOUT SHELTERS TESTED

Shelter No.	Shelter Name	Scale Factor
2	Door-covered trench	1 : 7.33
3	Aboveground door-covered	1 : 7.33
5	Crib-walled	1 : 10.7
6	Aboveground ridge-pole	1 : 10.7
7	Small pole	1 : 10.7
8	Log-covered trench	1 : 10.7

obtain the required depth for the trench. The mold was then placed in the hole and backfilled and hand-tamped in layers with a two-by-four board. The soil used to backfill and to cover the shelters was sifted using a sieve made from 1/4-inch wire mesh. Water was then added to obtain a moisture content of about 10 percent, a level which provided the best soil workability in making the trenches with the mold. Figure 23 shows a completed trench for a No. 2 shelter. After all the trenches for these shelters were completed, their assembly followed strictly the plan illustrated in Reference 1. The earth-filled rolls were made using Saran Wrap® for the plastic material specified in the shelter plan. The same type of wrap was used to rainproof the roof soil cover. Figure 24 provides an example of a completed No. 2 shelter just prior to testing.

The aboveground door-covered shelter, 3, required a much shallower trench than shelter 2. However, earth rolls are specified for the above-ground walls. Therefore, the wooden mold for these shelters was used not only to make the trench, but also as the form against which the earth-filled rolls were placed. The earth rolls were made using plastic wrap also. Figure 25 shows a partially completed shelter 3 ready to have the five doors placed in their final position as the roof of the shelter. With the doors in place, plastic wrap was placed over the doors and the entire roof covered with soil as specified in the plan for this shelter. Figure 26 is a photograph of the completed model shelter.

Shelter 5, the crib-walled aboveground shelter, was to a great extent prefabricated at SwRI. The five required cribs for each of the five models made were all completed prior to arriving at the test site. In addition, the roof poles were precut in sets for each model shelter. Note that a significantly larger number of poles were required to make the roof than is indicated in Reference 1. The cribs were assembled and filled with soil as specified in the shelter plan using plastic wrap to line each crib. Figure 27 shows a model of shelter 5 during assembly. The earth cover was then placed on the roof as specified. Figure 28 shows the completed model shelter 5 ready for testing.

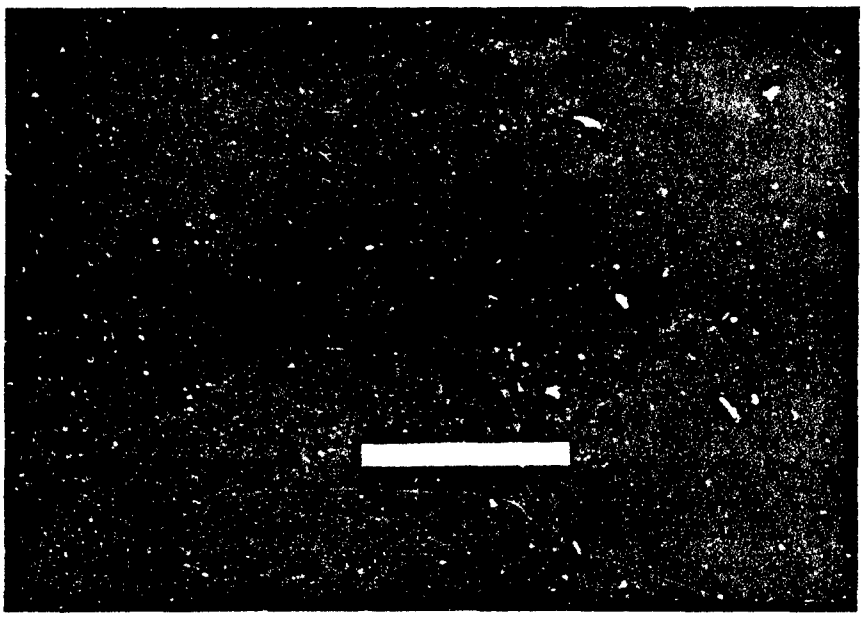

Figure 23. Soil Trench for Door-Covered Trench Shelter (2)

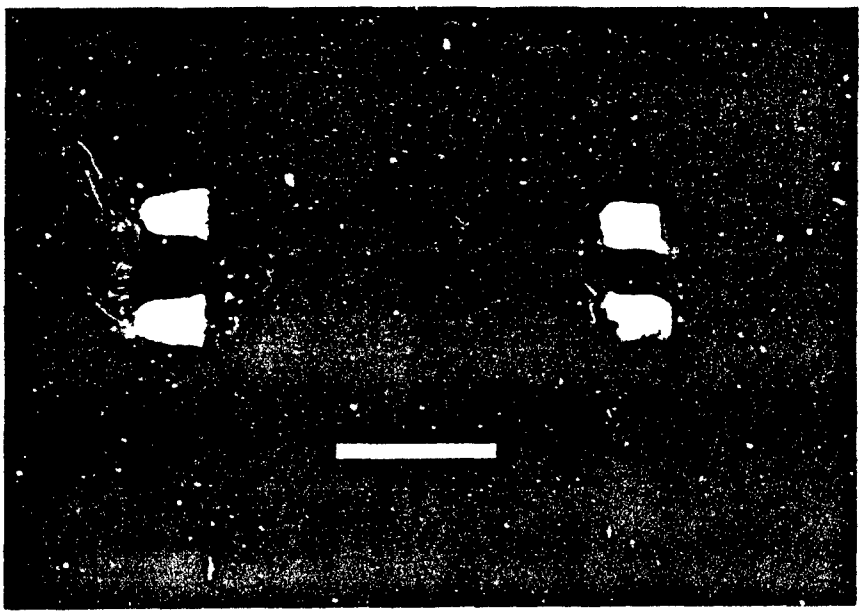

Figure 24. Completed Model of Door-Covered Trench Shelter (2)

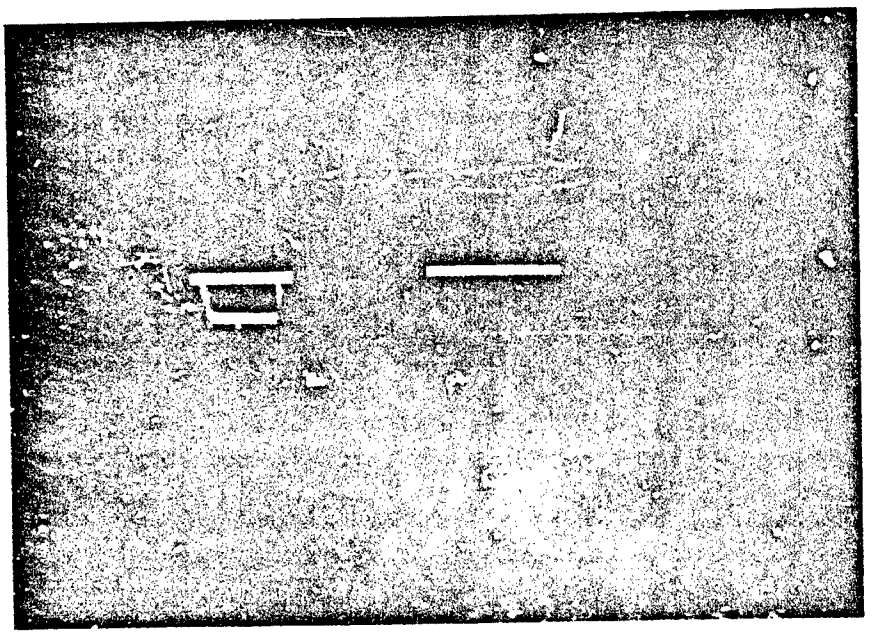

Figure 25. Trench and Earth Roll Walls For Aboveground Door-Covered Shelter (3)

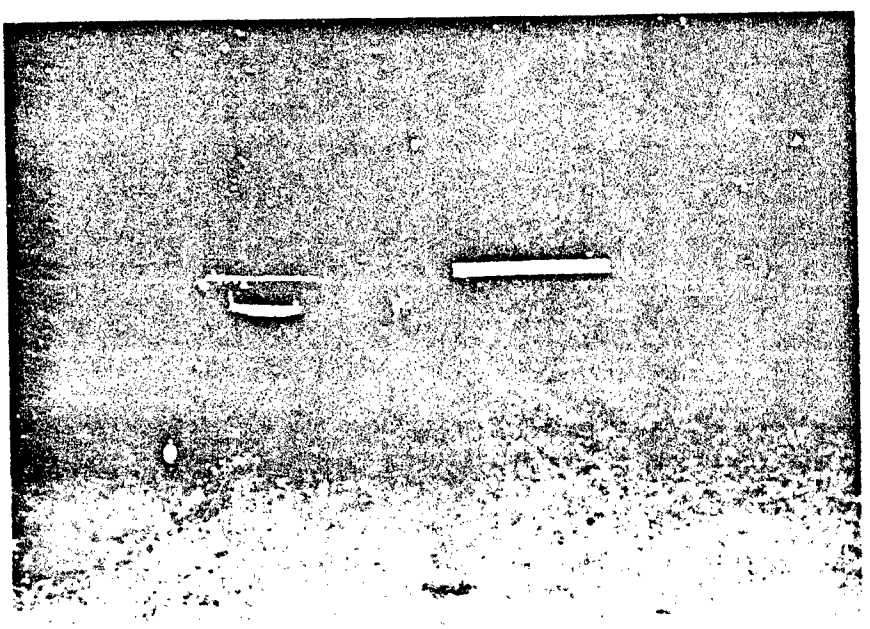

Figure 26. Completed Model of Aboveground Door-Covered Shelter (3)

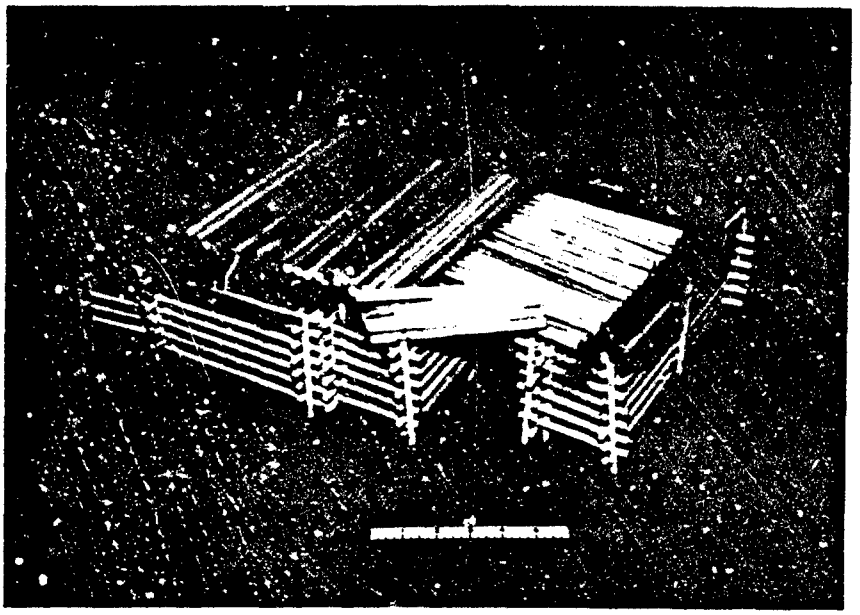

Figure 27. Assembled Cribs and Roof For Shelter No. 5

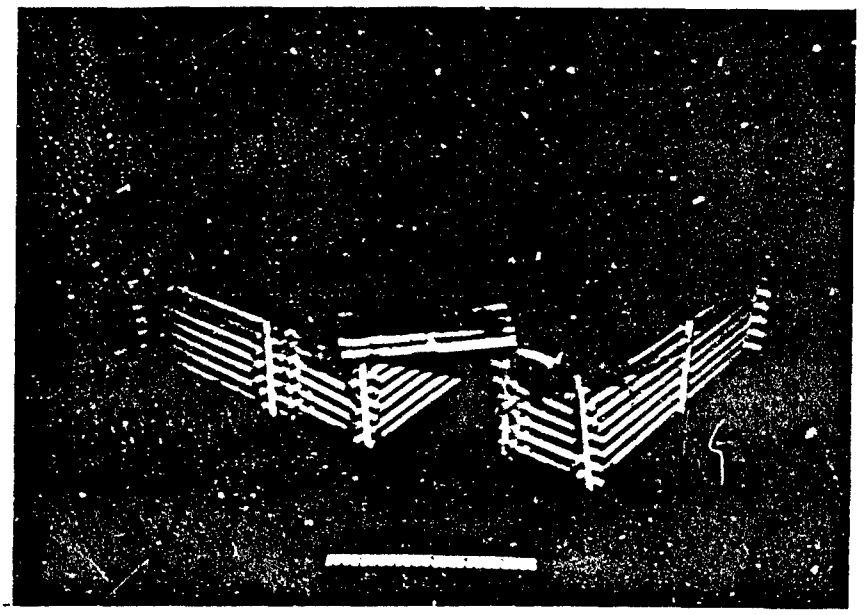

Figure 28. Completed Model of Crib-Walled Shelter (5)

The aboveground ridge-pole shelter, 6, was partially preassembled at SwRI to minimize assembly time at the test site. All of the model logs not preassembled for each of six model shelters were also cut to size at SwRI. Figure 29 shows the complete structural assembly for one of these model shelters. Plastic wrap was used over the poles to hold the first soil layer as well as in between the soil layers as the waterproofing layer. Figure 30 depicts a completed model shelter 6 before performance of an experiment.

Shelter 7, the small-pole shelter, was the only shelter evaluated in this program that is detailed in Reference 2. Five complete models of this shelter were completely fabricated and assembled prior to departure from SwRI to the Fort Cronkhite Shock Tunnel. Each of these model shelters was installed in the test bed by first digging an oversized hole of the specified depth, placing the assembled shelter in the hole, and then backfilling and tamping the soil all around the shelter to obtain the results shown in Figure 31. Soil was then piled over the roof poles as specified in the shelter building instructions using plastic wrap for the rainproofing material in between the earth cover. A completed model shelter 7 is shown in Figure 32.

The log-covered trench shelters, 8, were assembled at the test site in basically the same manner as the door-covered trench shelter. A trench, as shown in Figure 33, was made using a wooden mold. The roof logs over the trench, entry passage, and ventilation passage were then placed and soil-covered as outlined in the building instructions. A completed model shelter 8 is pictured in Figure 34.

Twelve blast tests were conducted in the Fort Cronkhite facility against the modeled expedient blast/fallout shelters. Responses of 96 individual models were observed with two rigid models per test. Shelter test locations are shown in Figure 35. The two rigid models geometrically represented shelters 5 and 8 and were used to measure internal blast pressure leakage into these shelters. The rigid model of the crib-walled shelter, 5, was fabricated from solid sections of wood with provisions for mounting pressure transducers on the roof and two walls. Figure 36 shows the completed rigid model R5. The rigid model of the log-covered trench shelter, R8, was constructed from aluminum plate as shown in Figure 37.

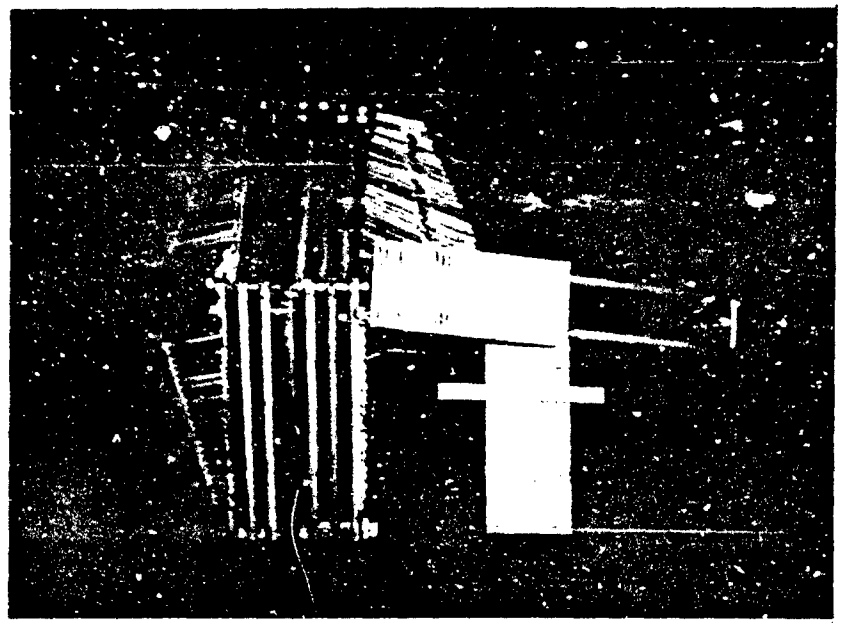

Figure 29. Plan View of Wooden Assembly for Aboveground Ridge-Pole Shelter (6)

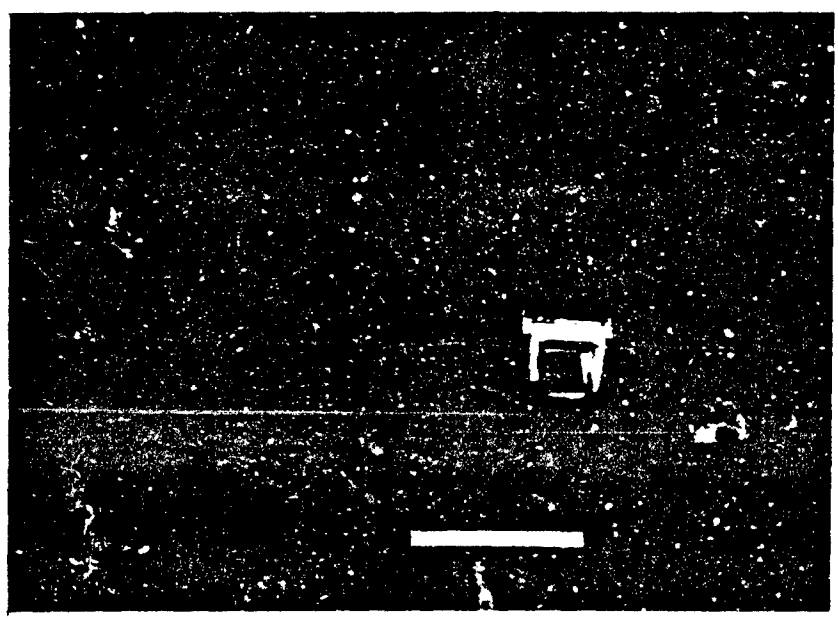

Figure 30. Completed Model of Aboveground Ridge-Pole Shelter (6)

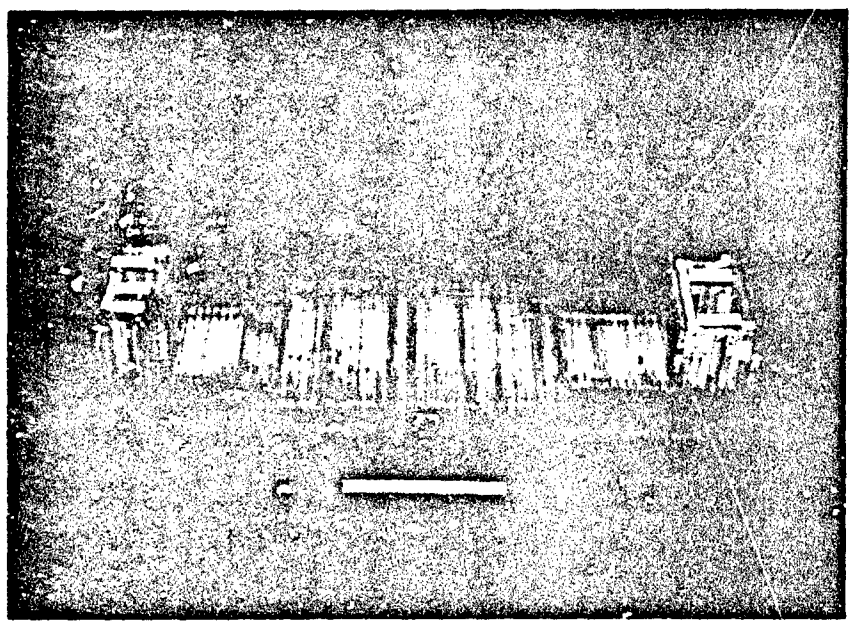

Figure 31. Assembled Small Pole Shelter (7) Buried in Soil Bed

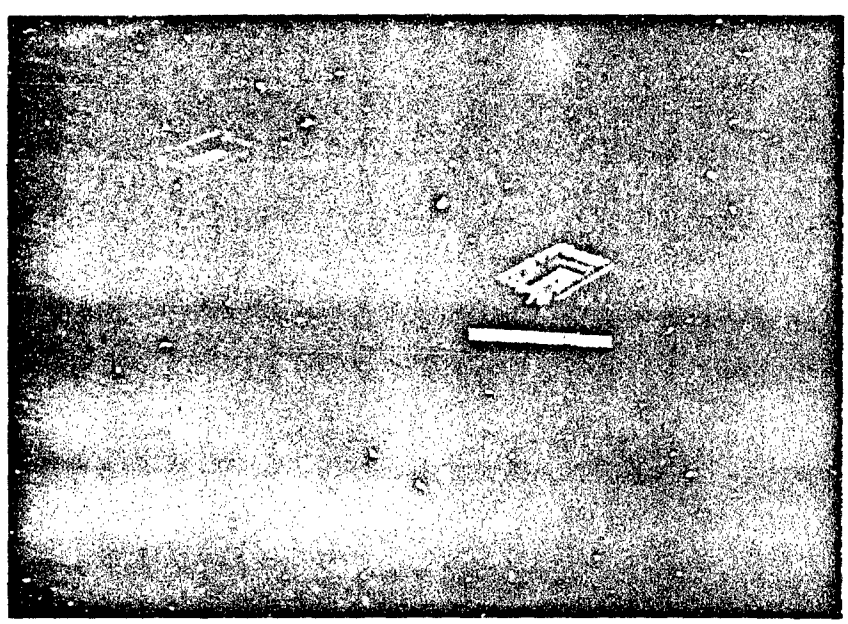

Figure 32. Completed Model of Small Pole Shelter (7)

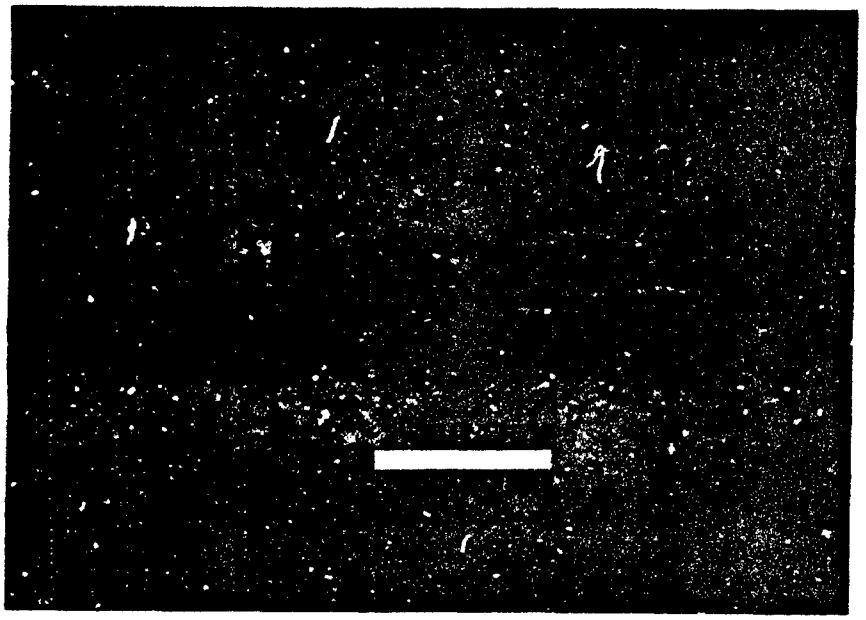

Figure 33. Soil Trench For Log-Covered Trench Shelter (8)

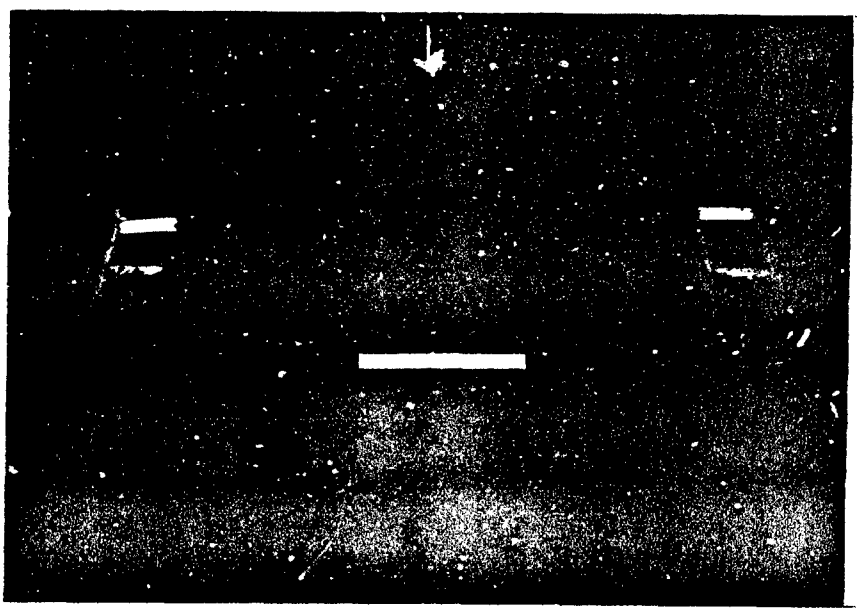

Figure 34. Completed Model of Log-Covered Trench Shelter (8)

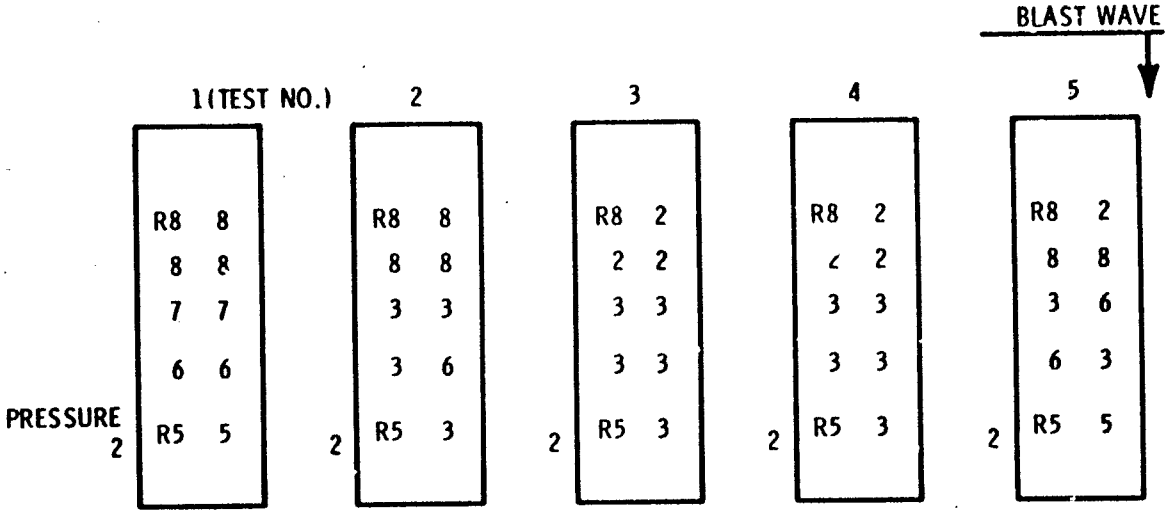

Figure 35. Test Matrix-Shelter Locations

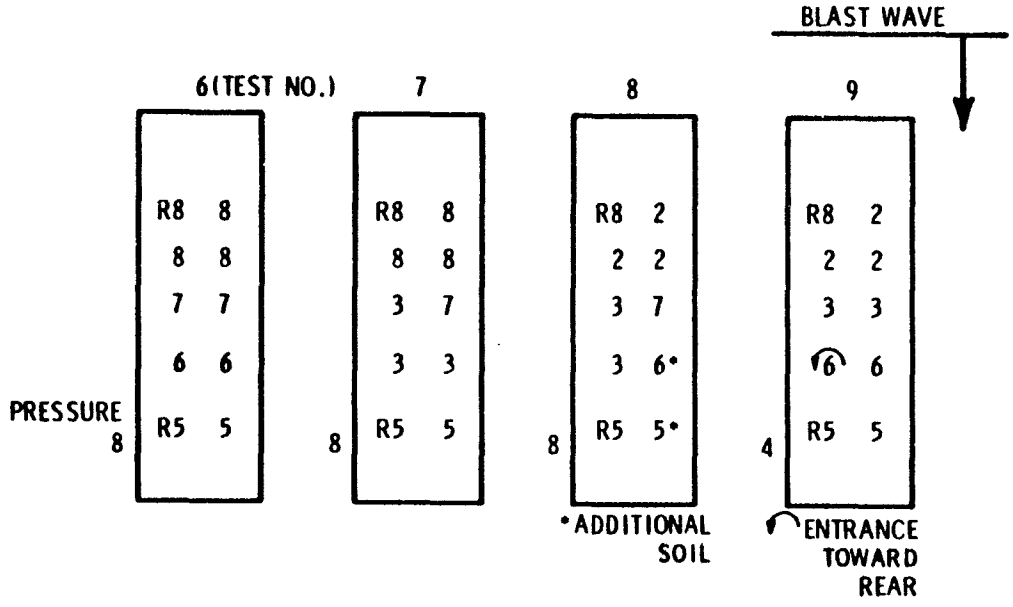

Figure 35(cont'd). Test Matrix-Shelter Locations

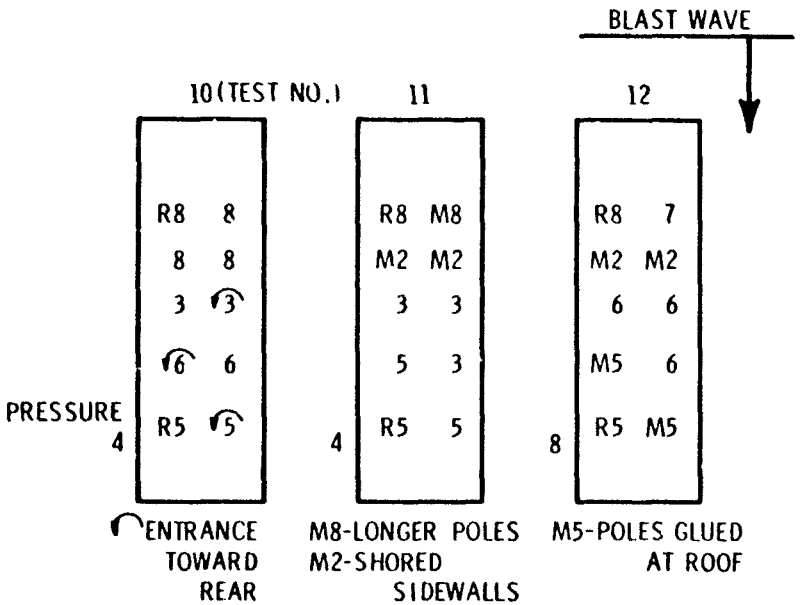

Figure 35(cont'd). Test Matrix-Shelter Locations

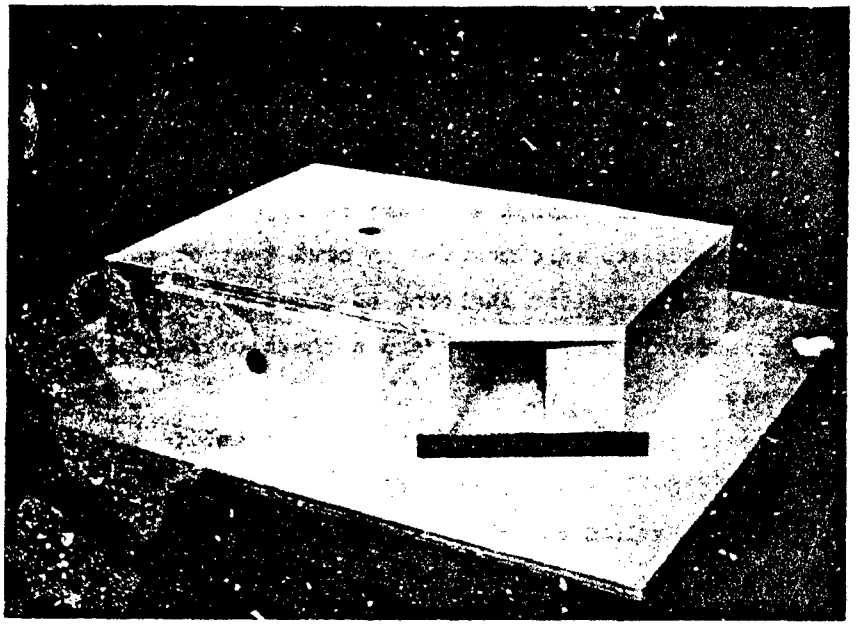

Figure 36. Rigid Model of Crib-Walled Shelter (5)

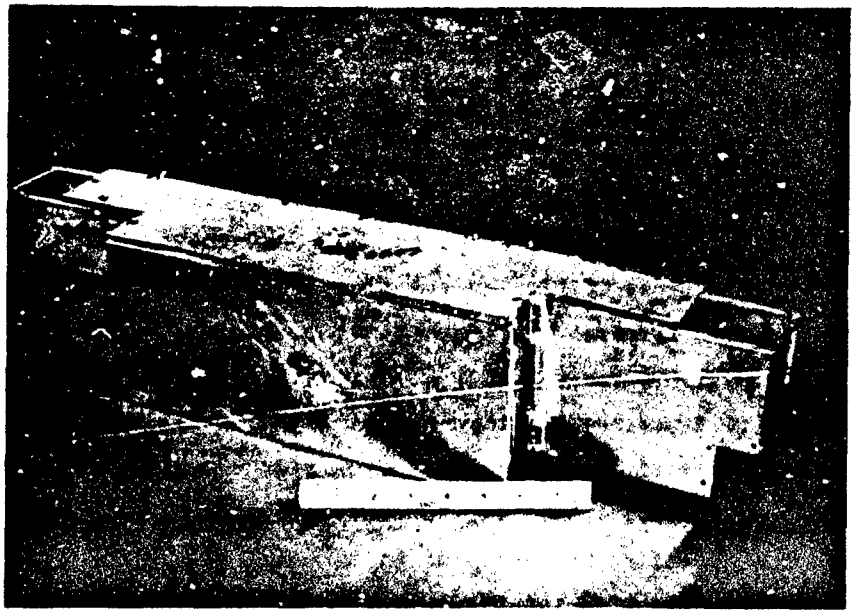

Figure 37. Rigid Model of Log-Covered Trench Shelter (8)

Pressure Measurements System

Pressures were sensed and recorded on each test. In all twelve tests, five transducers were mounted to sense the blast overpressure on the test bed and on one wall of the tunnel as shown in Figure 19. In addition, up to seven other transducers were mounted in each test on the rigid and reponse models of the expedient shelters to sense internal blast pressures. Two types of transducers were used to sense these pressures, piezoresistive and piezoelectric.

The piezoresistive pressure transducers were Kulite Model HEM-375 with a pressure range of 0-25 psig. This sealed miniature transducer is an all metal, electron beam welded assembly featuring a metal diaphragm as a force collector with piezoresistive strain gages bonded inorganically. Nominal sensitivity for one of these sensors was 2.5 mv/psi at an excitation voltage of 10 VDC. These transducers feature a high resonant frequency of approximately 50 kHz, good linearity, and static pressure response. Excitation voltage, bridge balance, and amplification for these pressure transducers was provided by Vishay Model 2310 signal conditioning amplifiers with the frequency response set at dc to 25 kHz (-5%).

The piezoelectric transducers used were all manufactured by PCB Piezotronics. Two of them were supplied, installed, and conditioned by Scientific Services, Inc. (SSI). These two Model 102A02 transducers were mounted at two locations on the tunnel wall, one near the front of the test bed and the other near the back. Their output was recorded by SwRI together with the output of the Model 102A05 and 102A15 supplied and installed by SwRI on the test bed and in the model shelters. All three types of PCB transducers utilize an acceleration-compensated, quartz sensing element coupled to a miniature source follower within the body of the transducer. The source follower converts the high impedance charge output into a low impedance, voltage output signal. The sensors have a rise-time capability of 1 microsecond. Each piezoelectric transducer was connected to a PCB Model 494A06 signal conditioner and amplifier. The amplifier has a specified frequency of 0.08 to 180,000 Hz (-3db) and a coupling time constant of 2 seconds.

All of the pressure transducers supplied by SwRI were installed in protective steel canisters which simplified handling and installation in the soil test bed. For those transducers used to sense the surface overpressure, the steel canister was buried so that the transducer was flush with the ground surface. Figure 38(a) shows a completely assembled transducer canister ready for burial. Figure 38(b) shows the canister installed in the ground with the transducer centered on a bolted, circular transducer holder. In a similar manner, the transducer canisters were mounted within the shelters to sense the internal pressures. Figure 38(c) shows typical installations in a below-ground small-pole shelter and an aboveground crib-walled shelter.

The amplified signals from both the piezoresistive and piezoelectric pressure transducers were recorded on magnetic tape with an Ampex Model 2230 tape recorder with Wideband II, FM electronics. At a record speed of 30 inches/second, the specified data bandwidth capability was 0-100 kHz (+1, -2db). Figure 39 illustrates the measurement system used in the twelve experiments.

The pressure data were played back at the test site after each experiment using a Biomation Model 1015 four-channel transient recorder. The data traces were recorded on Polaroid film for quick-look analysis using a Tektronix Model 602 display unit. Upon return to SwRI from the Fort Cronkhite facility the test data were played back and digitized using the system shown in Figure 40. Up to four channels of data were played back at one time through the analog filters into a Biomation Model 1015 four-channel transient recorder. This recorder digitizes the incoming analog signals at sample intervals of 0.01 milliseconds or greater. Since this unit has four separate analog-to-digital (A/D) converters, the samples for each of the four data channels are time correlated. The maximum number of samples which can be taken is 1024 per channel. The A/D units are 10-bit units, which means the analog signals are digitized with a resolution of one part in 1024 of the full-scale voltage setting. Once the test data are properly formatted in digital form, a DEC 11/23 computer extracts the data from the transient recorder memory through the Computer Automated Measurement and Control (CAMAC) data buss and stores them on an 8-inch flexible diskette. A graphics terminal is used to display each data

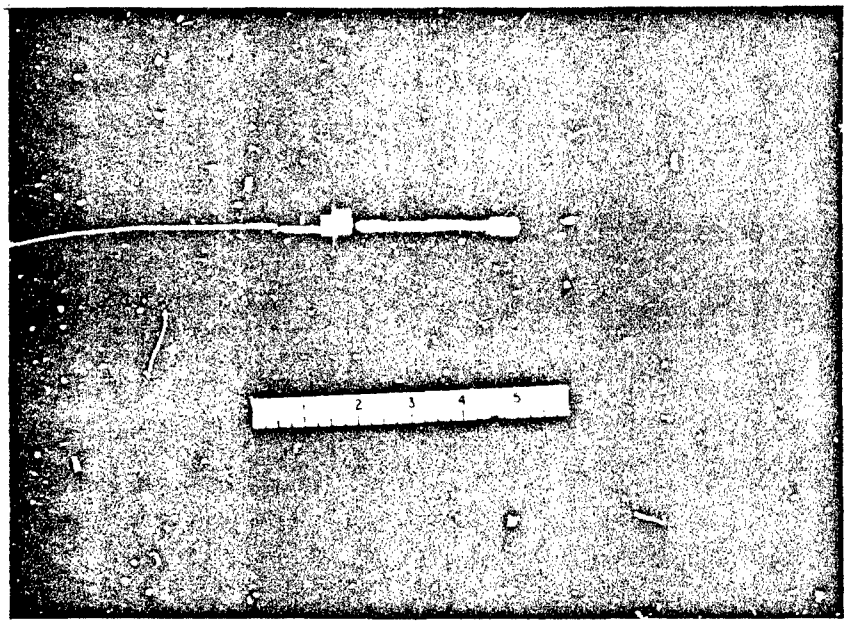

Figure 38a. Assembled Pressure Transducer Canister

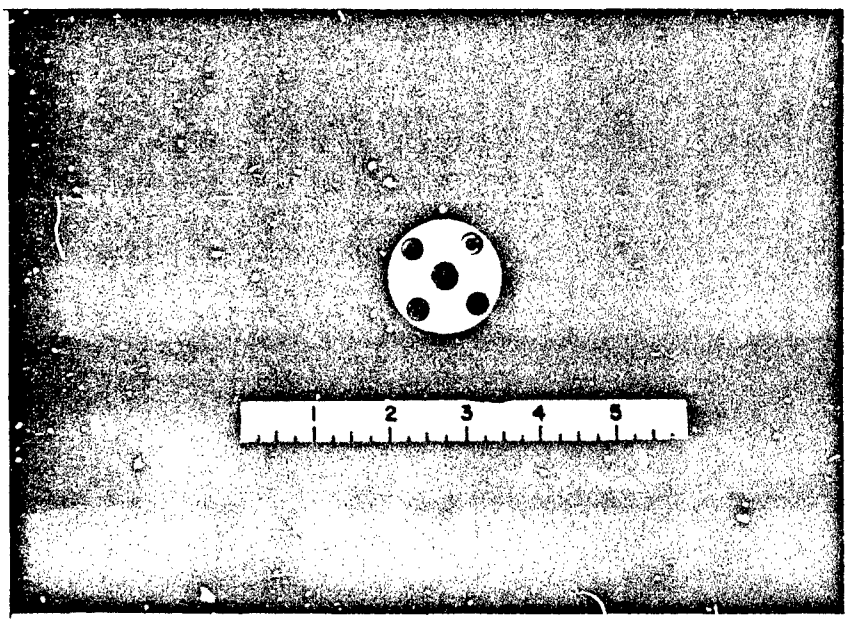

Figure 38b. Transducer Canister Installed in Soil Bed

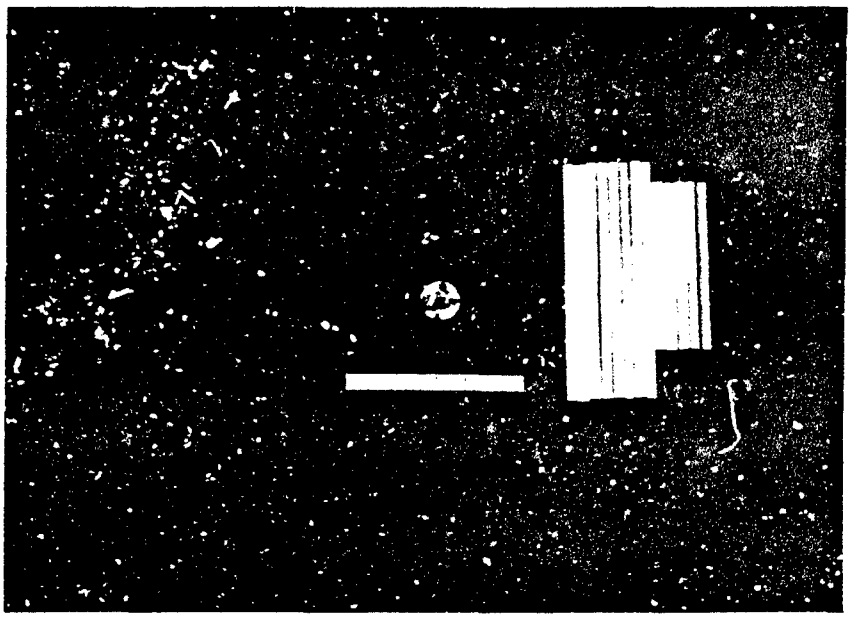

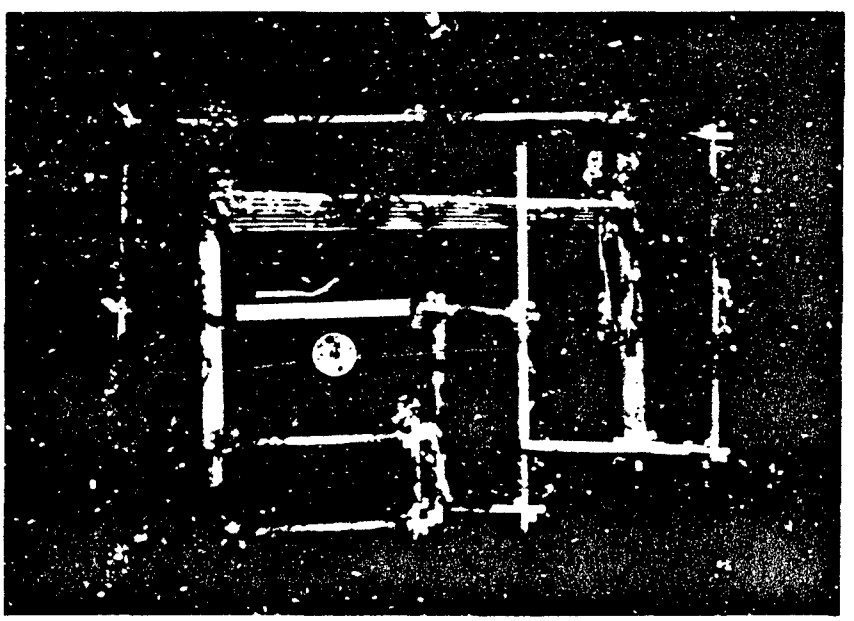

Figure 38c. Typical Pressure Transducer Installations in Shelters

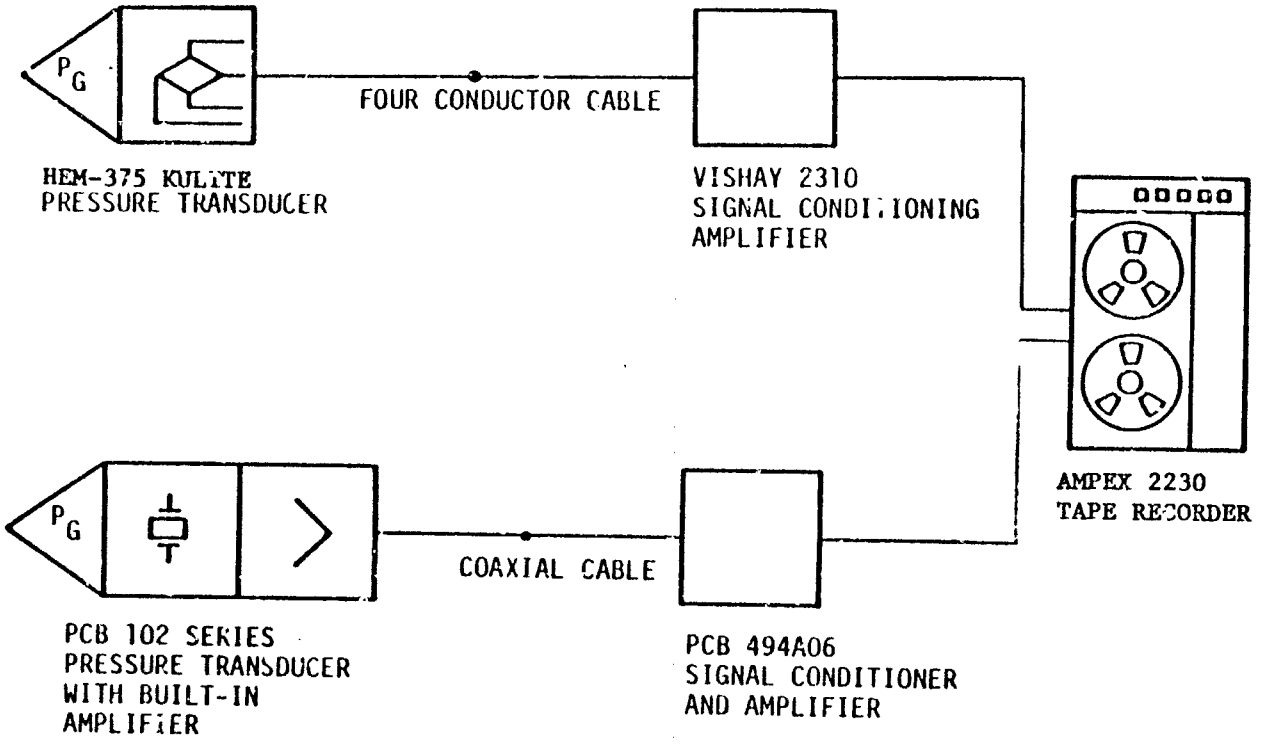

Figure 39. Blast Pressure Measurement System

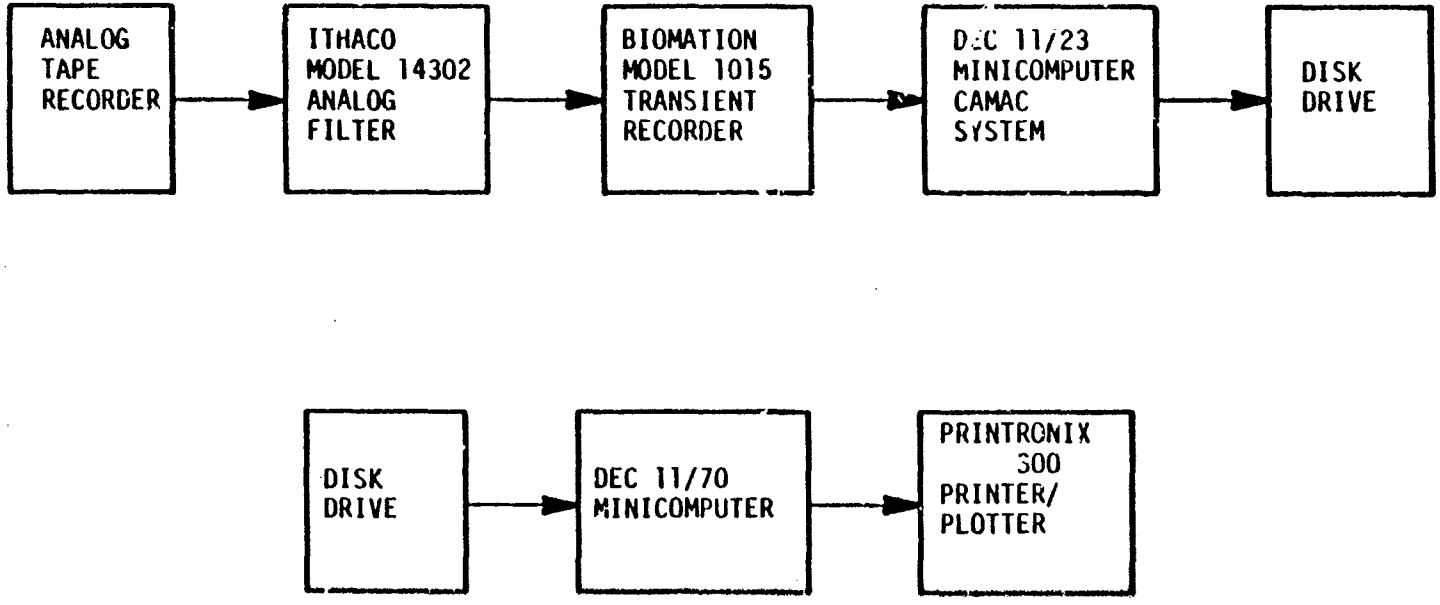

Figure 40. Test Data Playback System

trace for verification. The data stored on the diskettes were then read into a DEC 11/70 minicomputer, and engineering plots were prepared using a Printronix 300 printer/plotter.

TEST RESULTS

Surface Pressure Data

Up to 12 pressure measurements were made in each experiment. Five of these measurements were of surface overpressures, two on one wall of the tunnel and three on the soil bed surface. The rest of the transducers used in each test were installed on both the response models and the rigid models of the expedient shelters. Three different overpressure levels were used on the 12 tests. These were achieved by varying the number of Primacord strands detonated in the compression tube.

To achieve the lowest pressure level, two strands were used. The intermediate pressure load was achieved using four strands. For the highest pressure level, six strands were used. Analysis of the data traces for all three overpressure levels indicated a similar loading function in all cases. The five pressure transducers used for surface measurements were P1 and P2 located on the soil surface at the front of the test bed, P10 located on the wall at the front of the test section, P9 located on the soil surface at the rear of the test bed, and P11 located on the wall at the rear of the test section as shown in Figure 19. Figures 41, 42, and 43 show 250 millisecond long examples of the data recorded by P1 and P2 for the three nominal overpressure levels used. These measurements made on the surface of the test just upstream of the first row of test shelters indicate oscillating high-frequency pressure pulses superimposed on much lower frequency, higher amplitude pressure traces. These types of pressure records are quite similar to those recorded previously by various investigators using the Fort Cronkhite Shock Tunnel.

The peak overpressure for each of the five surface pressure transducers was obtained by eye-fitting the long duration pressure pulse through the high-frequency pressure oscillations. Table 23 summarizes the five

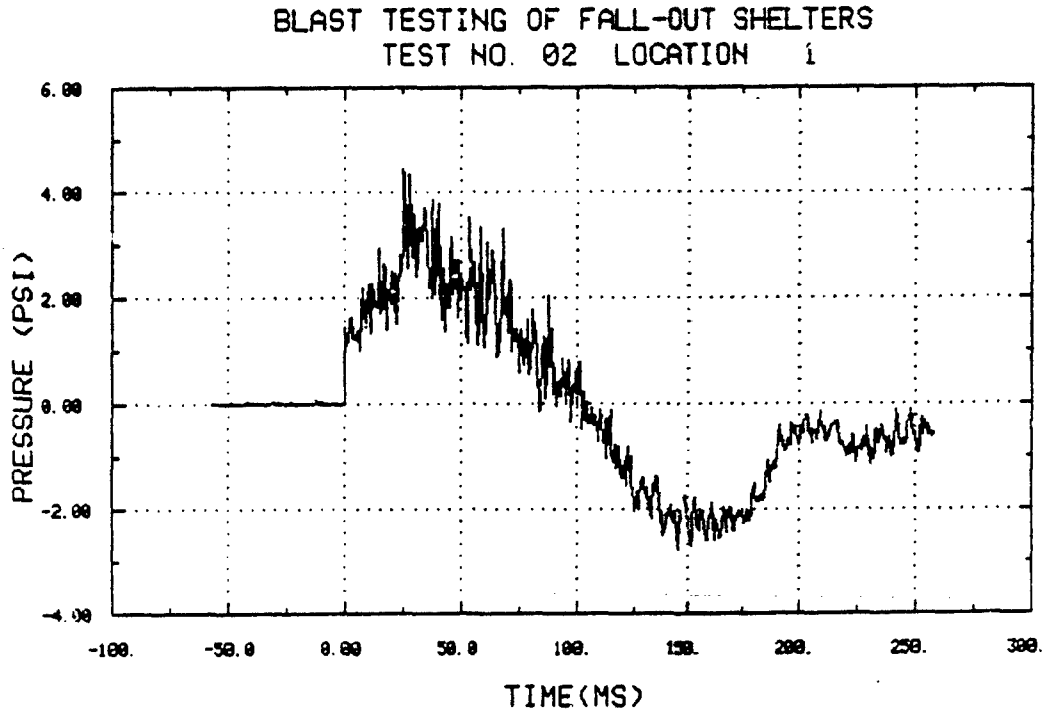

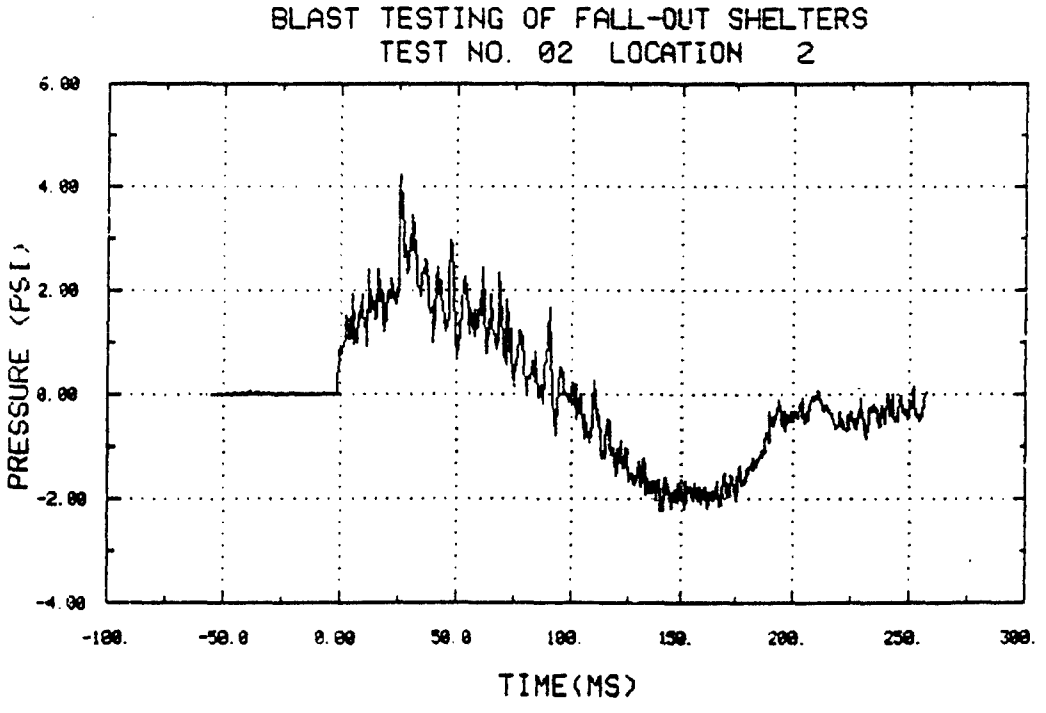

Figure 41. Test Bed Surface Overpressure for Low Pressure Test

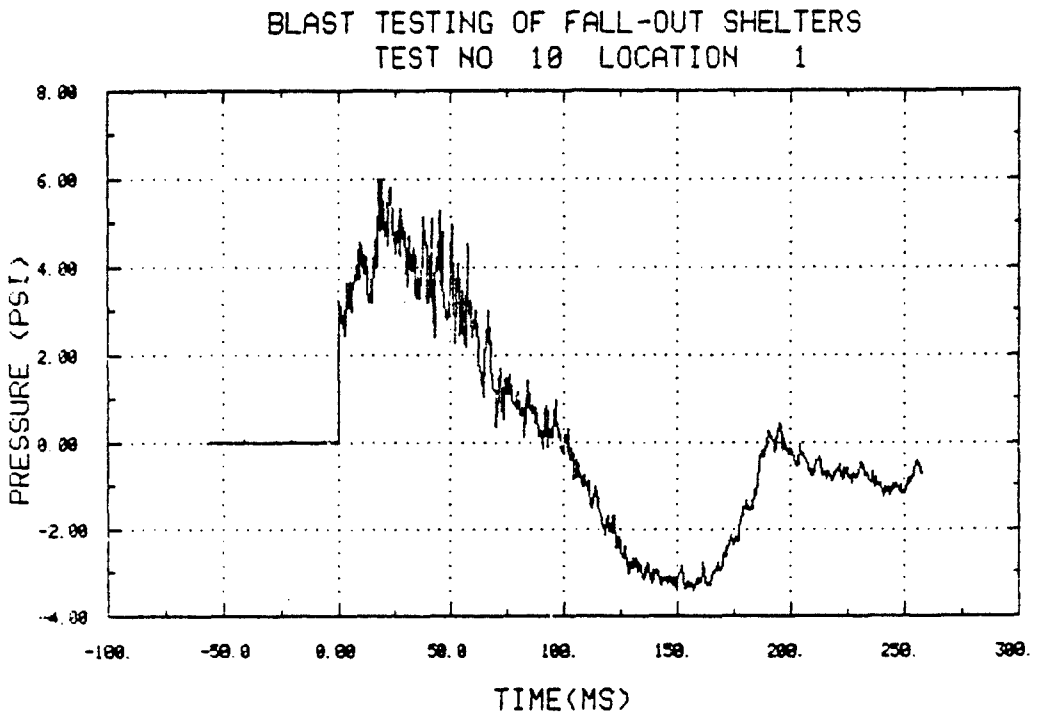

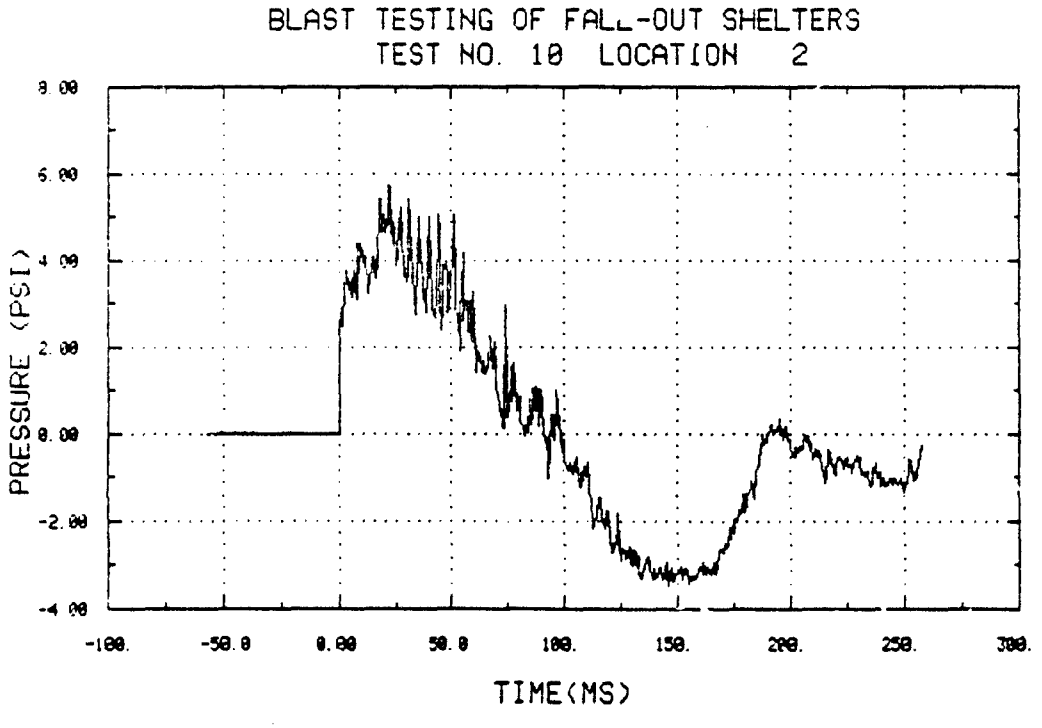

Figure 42. Test Bed Surface Overpressure for Intermediate Pressure Test

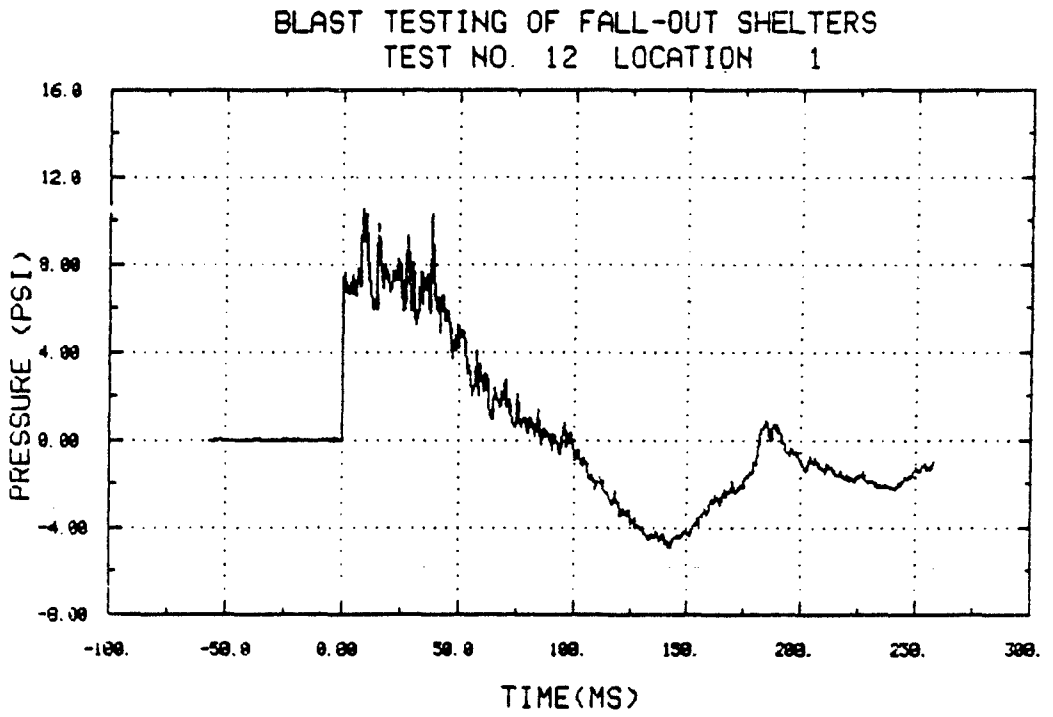

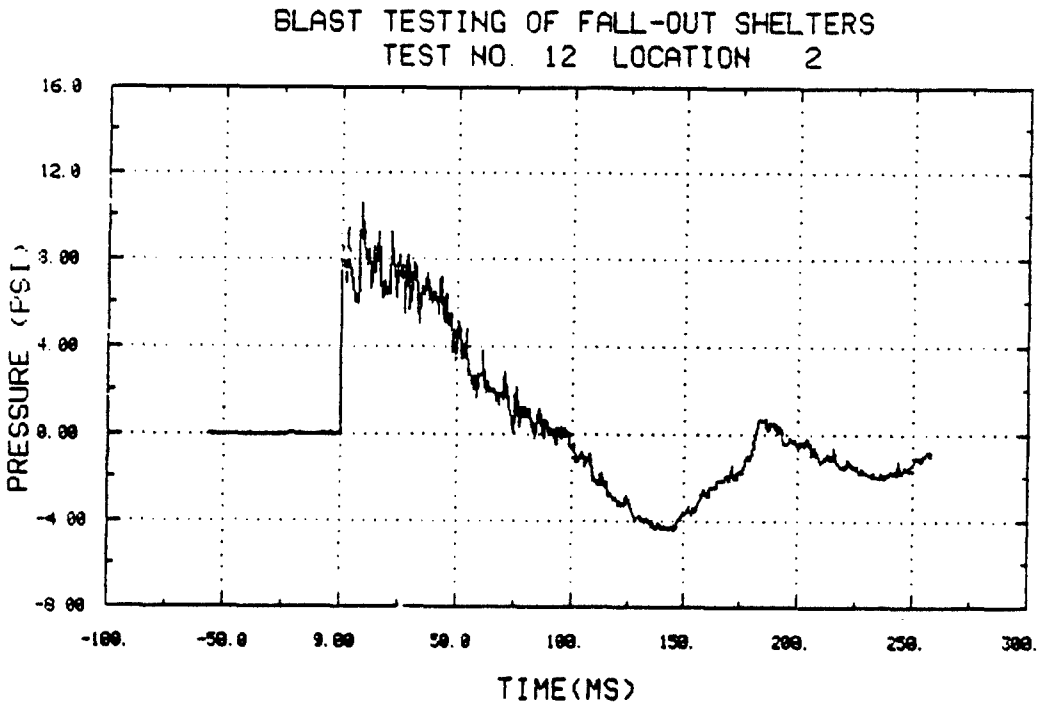

Figure 43. Test Bed Surface Overpressure for High Pressure Test

surface overpressure measurements obtained on each test. An average peak pressure was also computed for each test and is listed in Table 23. By averaging the average pressures in Table 23 for each pressure level, the three nominal test conditions used were 2.8 psig, 4.6 psig, and 8.8 psig.

Internal Shelter Pressures

Measurement of the internal shelter pressures were made with transducers mounted on both the rigid and the response models. On every test, two transducers were mounted on each of the two rigid shelters, R5 and R8. In addition, up to three response models were instrumented in every test. The transducers used in the response models were rotated among the test items from test to test to obtain representative data from within each type of response model for as many pressure levels as was possible. In most cases, the peak pressure measured inside each shelter was essentially the same as measured by the surface mounted transducers. Also, in most cases the time-history recorded for the internal transducers was similar to that of the exterior ones with the exception that the high-frequency oscillations were acoustically filtered. In some instances the rise time of the pressure pulse is definitely slower within a shelter and the peak pressure somewhat attenuated as compared to the external overpressure.

Figures 44 through 51 are examples of pressure-time records obtained from transducers sensing the internal pressure in each of the response and rigid models. The data traces in Figures 44 through 47 are for tests in which the nominal surface overpressure measured was a nominal 4.6 psig. These records from shelters 2, 3, 8, and R8 can be compared to those in Figure 42 to see how the internal geometry of each shelter affects the pressure buildup within the shelter. The data traces in Figures 48 through 51 are for an 8.8 psig nominal overpressure test. These data traces from shelters 5, R5, 6, and 7 can be compared to those in Figure 43 to see the similarities and differences between the internal and external overpressures measured.

For example, the internal pressure in shelter 2, Figure 44, is quite similar to the external overpressures shown in Figure 42. On the other hand, the internal pressure in shelter 3, Figure 45, shows a much slower

TABLE 23. PEAK SURFACE OVERPRESSURE (PSIG)

Test No.	P1	P2	P9	P10	P11	P(avg)
01	3.4	3.3	3.0	2.5	2.6	2.96
02	3.0	2.8	2.8	3.0	2.5	2.82
03	3.3	2.8	3.0	3.0	-	3.03
04	3.3	2.6	2.8	2.7	2.8	2.84
05	3.0	2.5	2.5	2.4	2.3	2.54
06	9.0	8.5	8.1	8.7	8.9	8.64
07	9.8	9.2	8.8	9.5	8.7	9.20
08	9.1	8.9	8.0	9.0	9.1	8.82
09	4.7	4.7	4.3	4.9	4.1	4.54
10	5.0	4.8	4.2	4.9	4.7	4.72
11	4.8	4.8	4.2	4.8	4.0	4.52
12	8.6	8.6	8.3	8.6	-	8.53

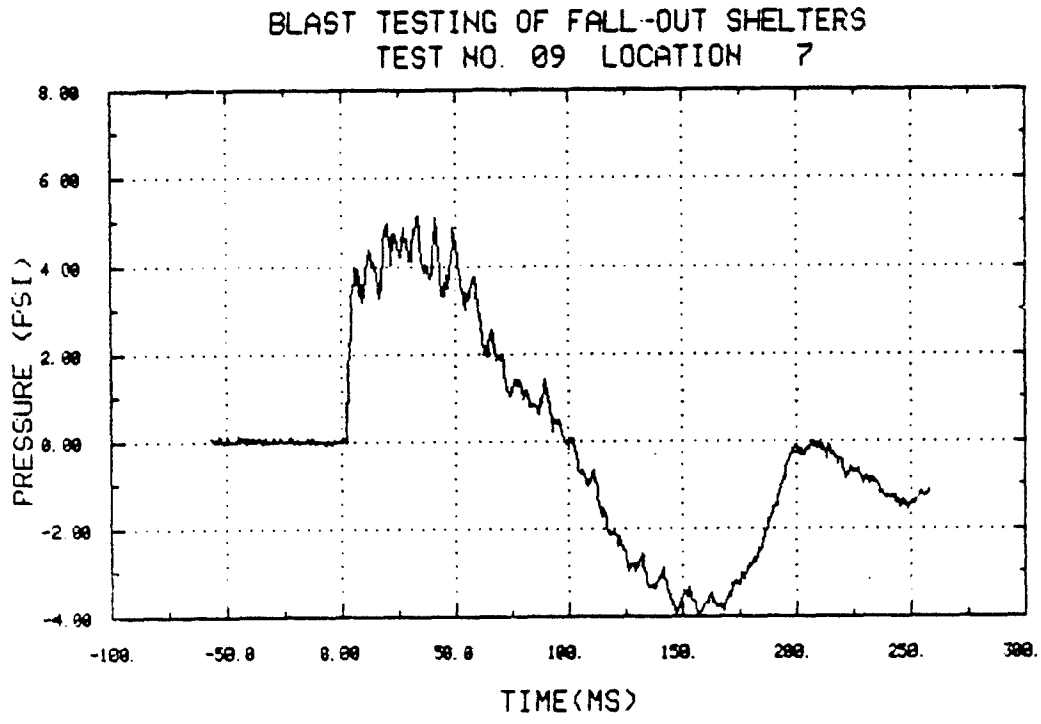

Figure 44. Internal Pressure in Door-Covered Trench Shelter (2)

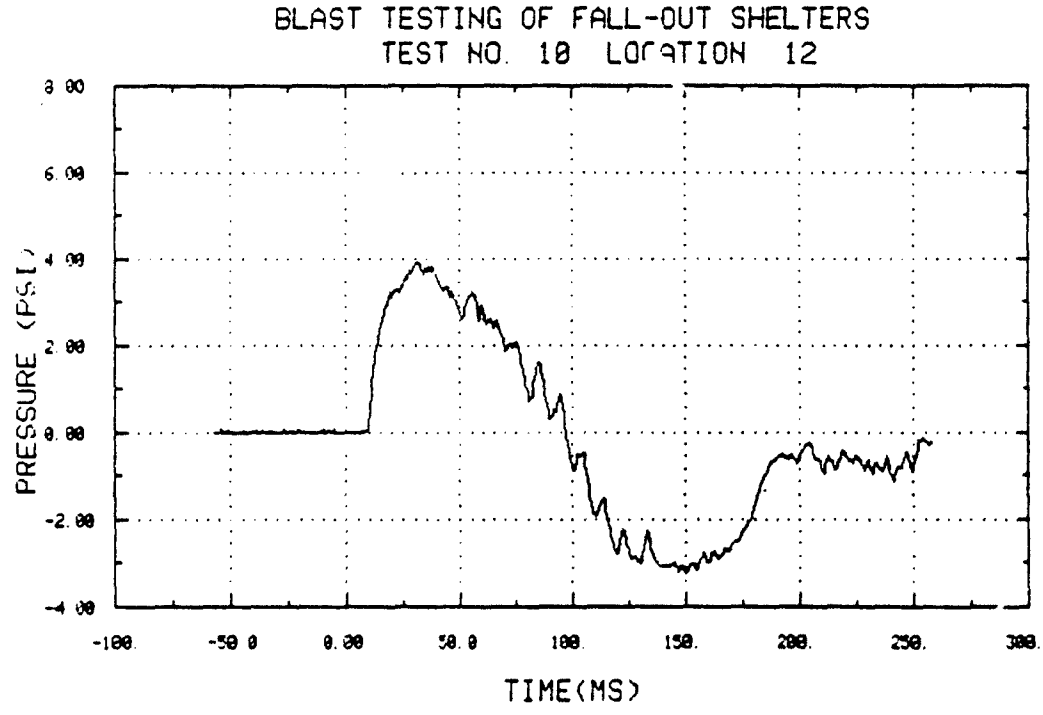

Figure 45. Internal Pressure in Aboveground Door-Covered Shelter (3)

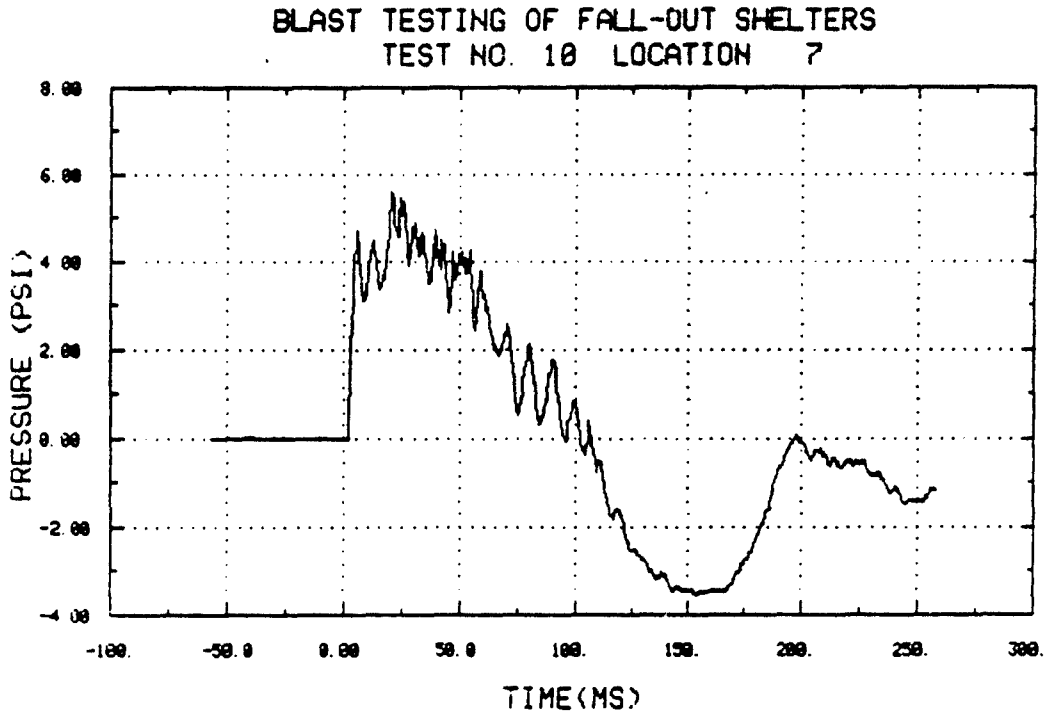

Figure 46. Internal Pressure in Log-Covered Trench Shelter (8)

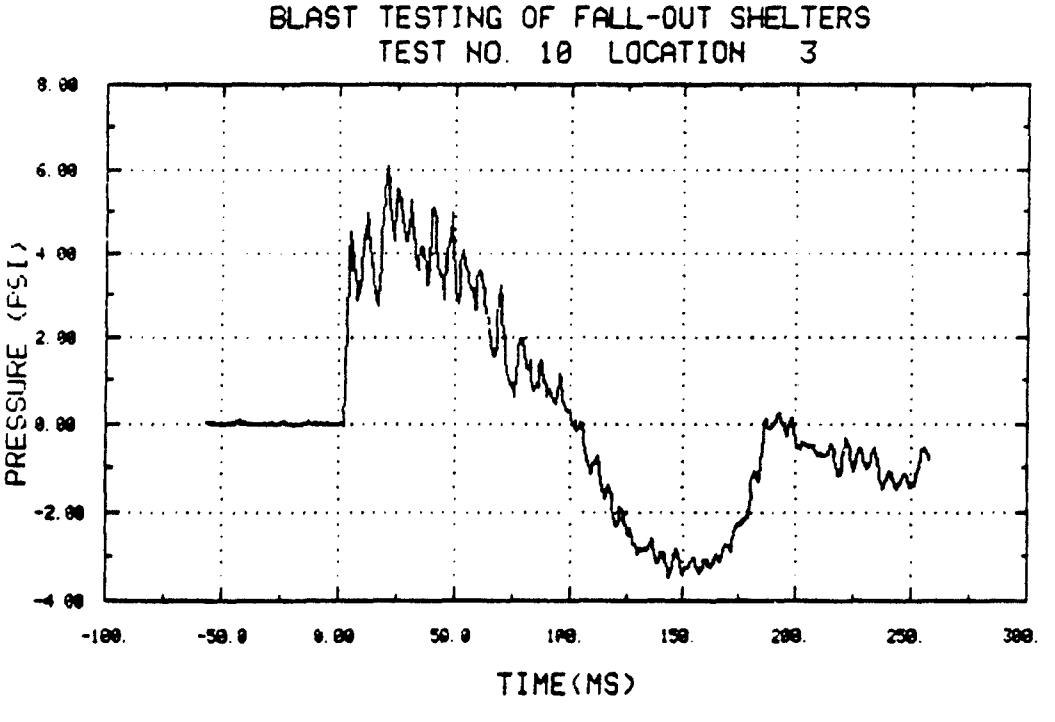

Figure 47. Internal Pressure in Rigid Model of Log-Covered Trench (R8)

rise time and considerably fewer high-frequency oscillations than the external overpressure records. These differences resulted primarily from the entrance to shelter 3 being mostly closed off by model sandbags as instructed in the building plans in Reference 1. In Figures 46 and 47, one can observe the similarities between the pressure records from shelters 8 and R8, as well as with the external overpressure records in Figure 42.

In Figures 48 and 49 the same kind of similarities can be observed for shelters 5 and R5 when compared to each other and to the external overpressure records in Figure 43. For shelter 6, the rise time in Figure 50 is somewhat slower than that in Figure 43 due to the relatively long entranceway for this shelter. An even slower rise time can be observed in Figure 51 for the pressure measured in shelter 7 which has even longer entrances leading into the shelter space.

Shelter Structural Evaluation

Each of the 96 response model shelters was inspected thoroughly after being tested and an evaluation made as to the possible survival of the occupants. The criteria for survival were based primarily on whether the occupants would have been able to survive any structural or soil failures observed in the shelter after it was tested. In some cases it was obvious that unless the soil cover was replaced over the shelter after the blast loading, little or no fallout protection would have been available to the occupants. However, this was not used as part of the survival criteria. (Similarly, as stated previously, the pressure inside most shelters during the tests was essentially the external overpressure. Therefore, for some tests there probably would have been some ear damage to the shelter occupants, and to a much lesser extent, lung damage. However, these considerations also were not included in determining the blast survivability of the shelters.) Table 24 summarizes the survival assessment of the model shelters. In most cases a yes or no rating was assigned. However, in a few cases a marginal category also was used for shelters whose structural condition was such that the interior space appeared marginally safe for immediate survival but perhaps not for long-term survival of its occupants.

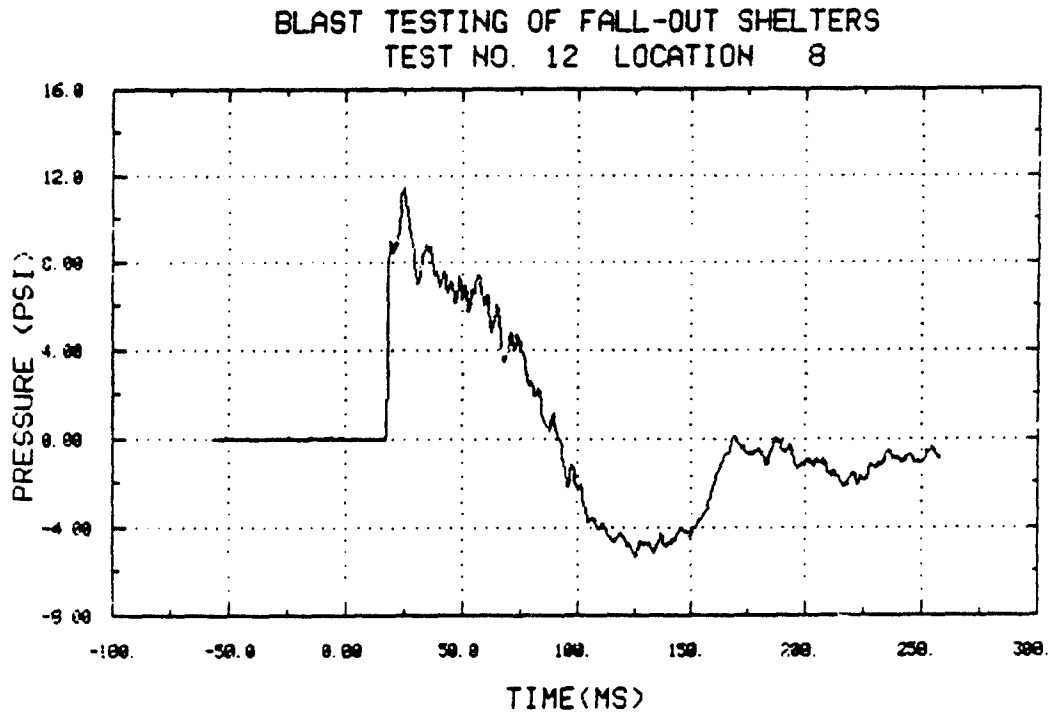

Figure 48. Internal Pressure in Crib-Walled Aboveground Shelter (5)

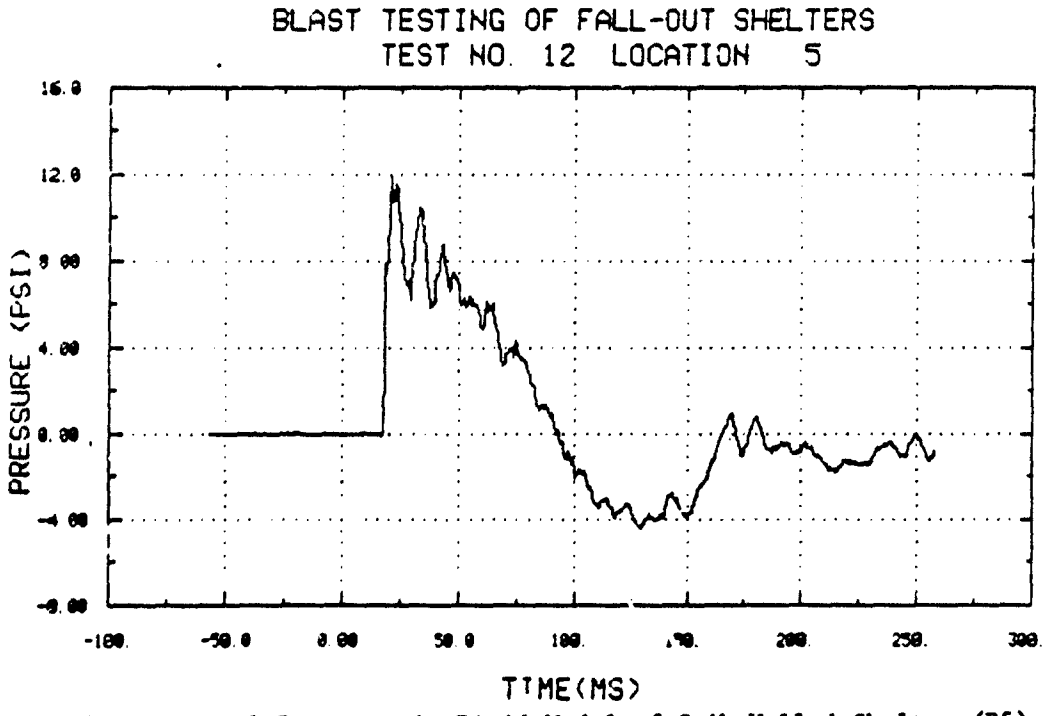

Figure 49. Internal Pressure in Rigid Model of Crib-Walled Shelter (R5)

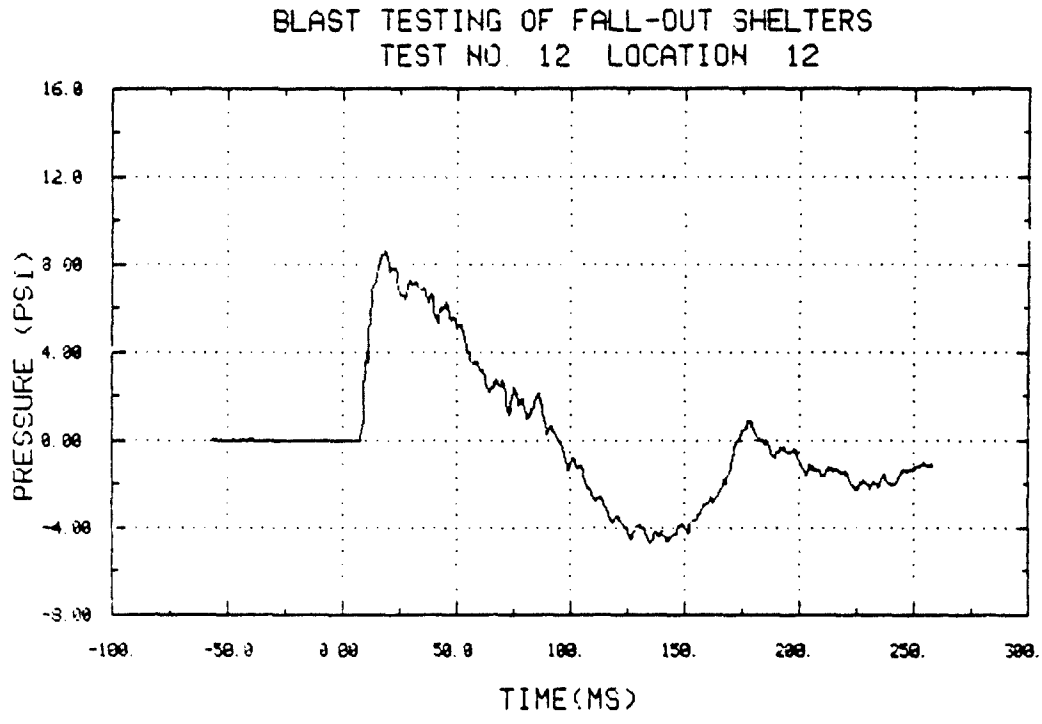

Figure 50. Internal Pressure in Aboveground Ridge-Pole Shelter (6)

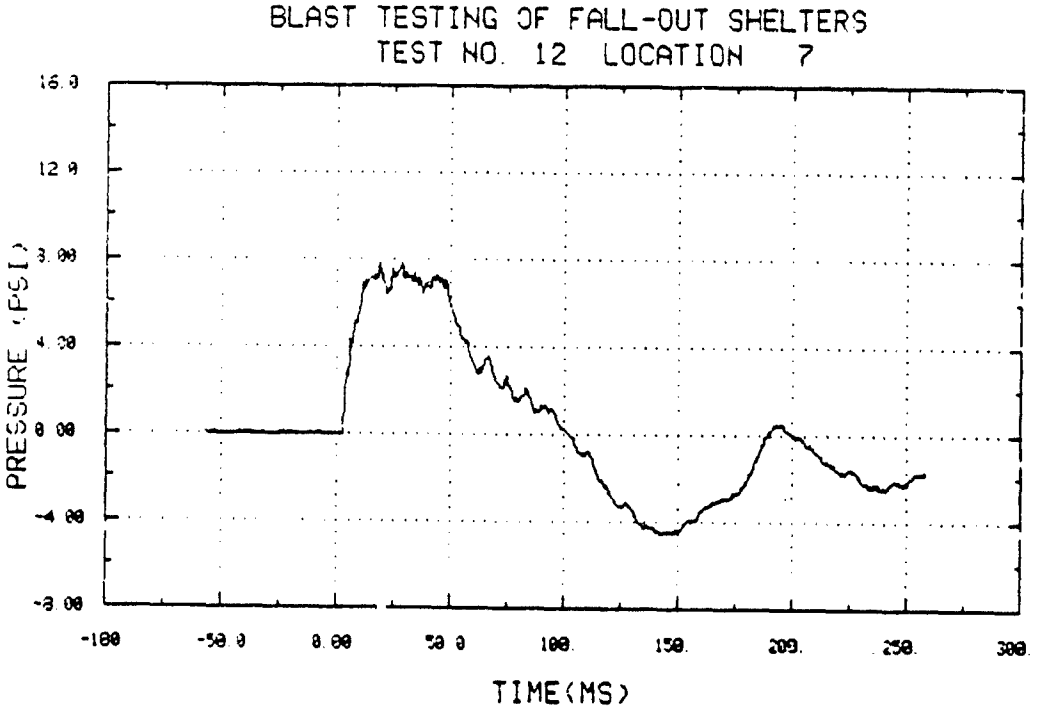

Figure 51. Internal Pressure in Small Pole Shelter (7)

TABLE 24. MODEL SHELTER BLAST SURVIVAL EVALUATION

Shelter	Nominal 2.8 psig			Nominal 4.6 psig			Nominal 8.8 psig		
	Yes	Marginal	No	Yes	Marginal	No	Yes	Marginal	No
2	3	0	4	0	2*	3	1*	1*	3
3	16	0	0	1	1	5	0	0	5
5	2	0	0	1	0	3	0	1+	4++
6	5	0	0	4	0	0	5	1	0
7	2	0	0	-	-	-	5	0	0
8	1	1	6	0	0	4	0	0	6

* Doors added to shore trench sidewalls
\+ Roof poles attached to crib walls and additional soil around cribs.
++ Roof poles attached to crib walls in one test.

As indicated in Table 24, almost half of the No. 2 shelters survived in the low overpressure (2.8 psig nominal) tests. Failures for this door-covered trench shelter occurred primarily from soil trench wall collapse. The top picture in Figure 52 shows a plan view of shelter 2 after a low pressure test. The bottom photo shows the failed trench walls. Figure 53 is an example of a door-covered trench that survived the low overpressure loading. None of these shelters survived the intermediate (4.6 psig nominal) and high (8.8 psig nominal) test overpressures without modifications. In Figure 54, an example of the almost total trench collapse is given for an intermediate pressure test. In the last two tests, doors were added to this shelter to shore the trench walls and determine if shelter survival would be increased. The model doors were braced as shown in Figure 55. The bottom picture in the same figure shows the uncovered trench after an intermediate pressure test. In this particular case the structural integrity of the shelter was rated as marginal because of the two large chunks of soil found inside from the one corner that had not been shored.

Shelter 3, the aboveground door-covered shelter, survived quite well in the low pressure tests. Typically, this shelter showed minimum interior damage, minor top soil erosion, and slight movement of the entryway sandbags at the 2.8 psig nominal overpressure. Figure 56 shows the exterior and interior condition of these shelters after a low pressure test. However, in the intermediate and high pressure tests this shelter did not survive in most instances. Failures were primarily due to the earth rolls being squeezed down and together. In some cases the trench space was filled completely with the earth rolls or loose soil. In some instances the soil cover was also eroded severely, and the door over the entranceway was blown away. Figures 57 and 58 are examples of failed shelters at the intermediate and high overpressures. In one of the intermediate pressure tests a model shelter 3 was rotated 180° so that the entrance was pointing downstream away from the blast wave. However, no significant difference in its condition after the test was observed. As was the case for most of these structures at the intermediate pressure level, it did not survive the blast loading.

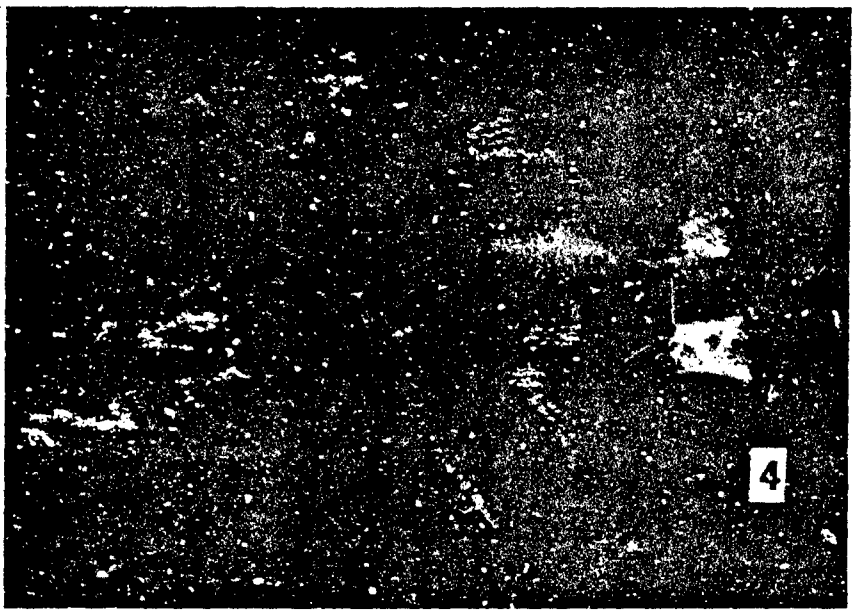

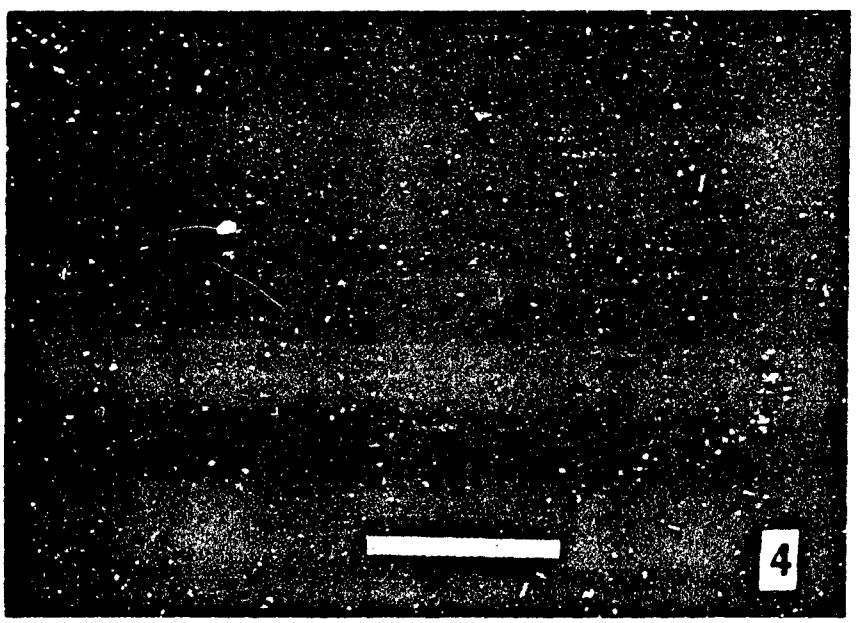

Figure 52. Typical Damage to a Non-Surviving Door-Covered Trench Shelter (2) in Low Pressure Test

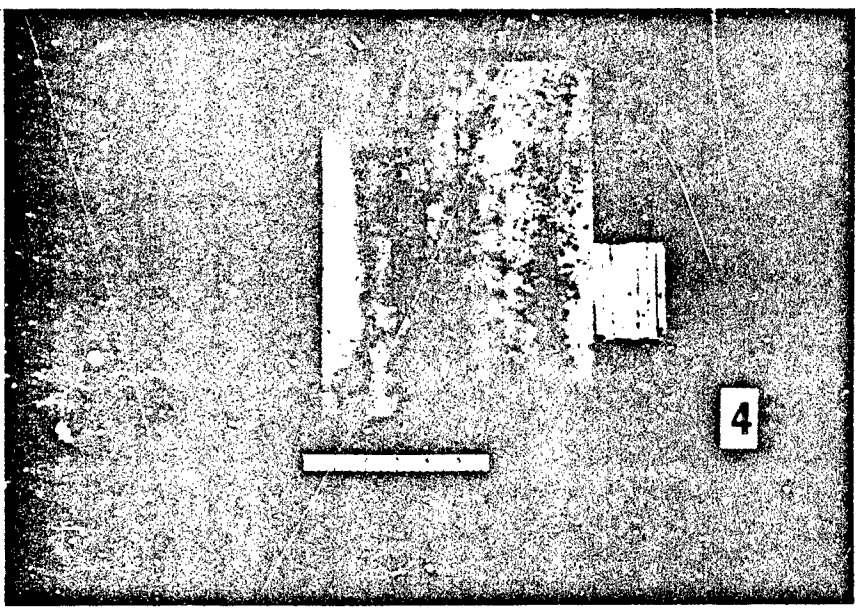

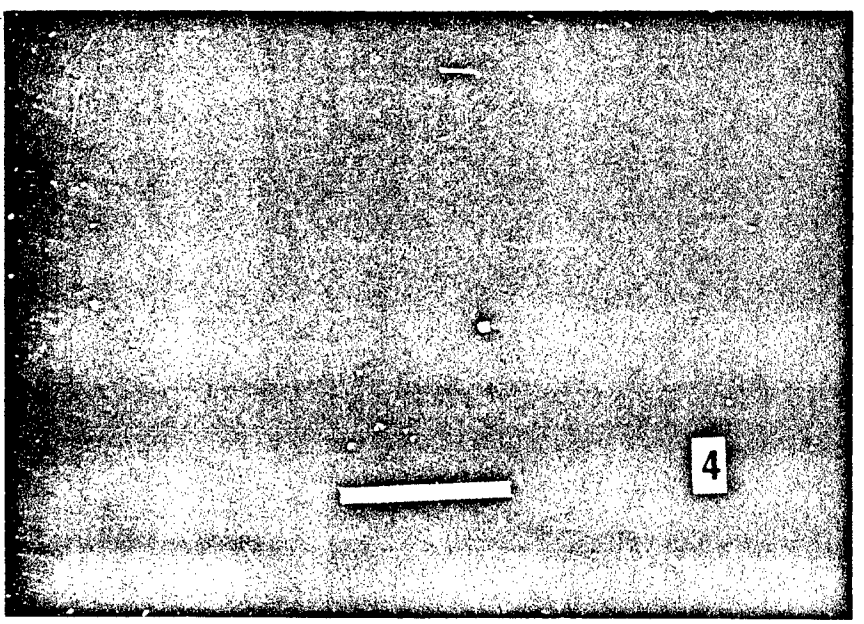

Figure 53. Typical Condition of a Surviving Door-Covered Trench Shelter (2) in Low Pressure Test

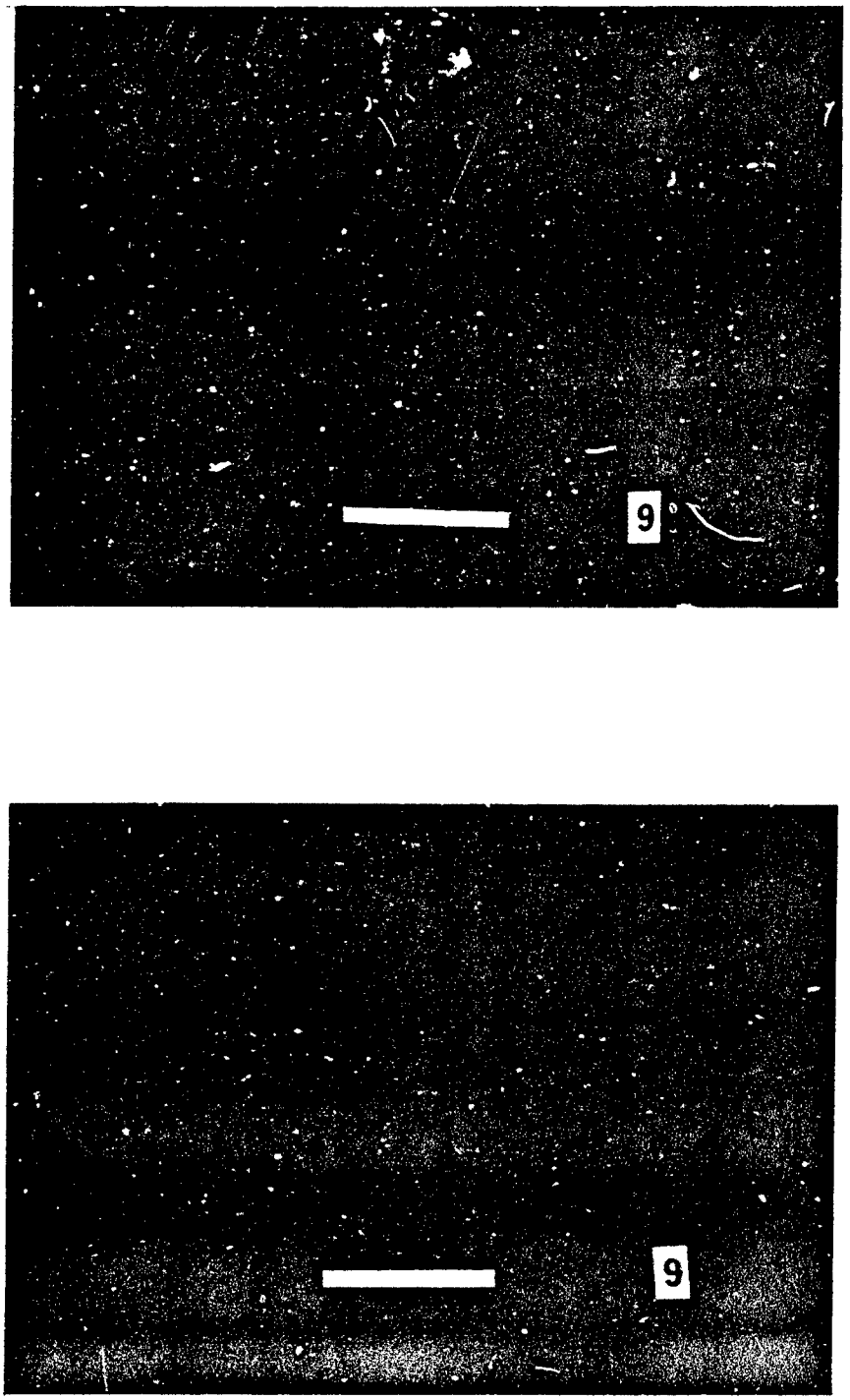

Figure 54. Typical Damage to a Door-Covered Trench Shelter (2) in Intermediate Pressure Test

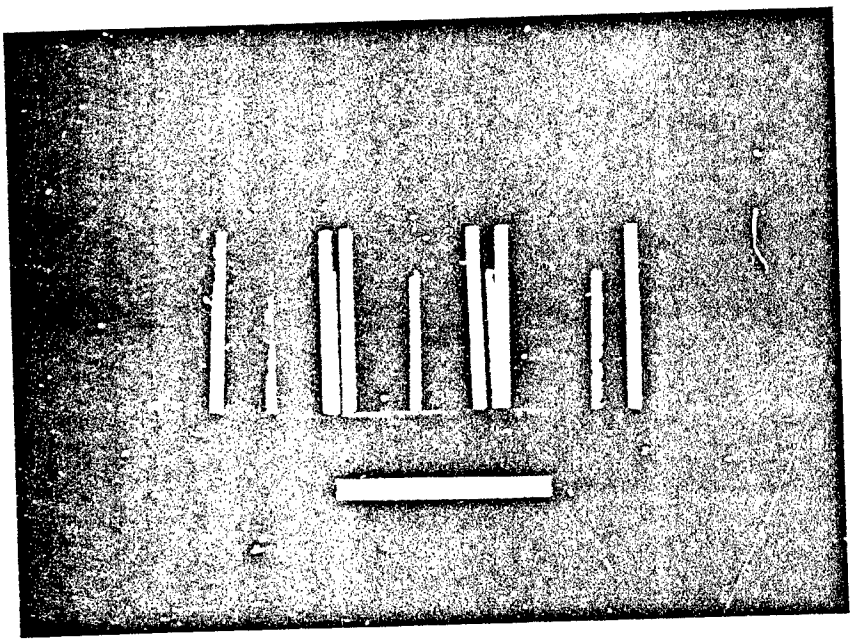

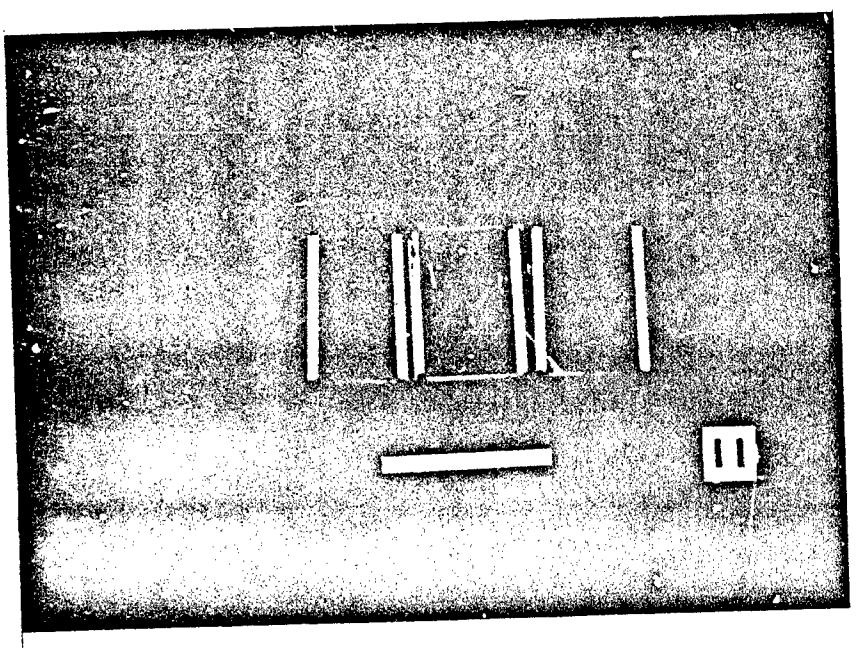

Figure 55. Modified Door-Covered Trench (2) Before and After Intermediate Pressure Test

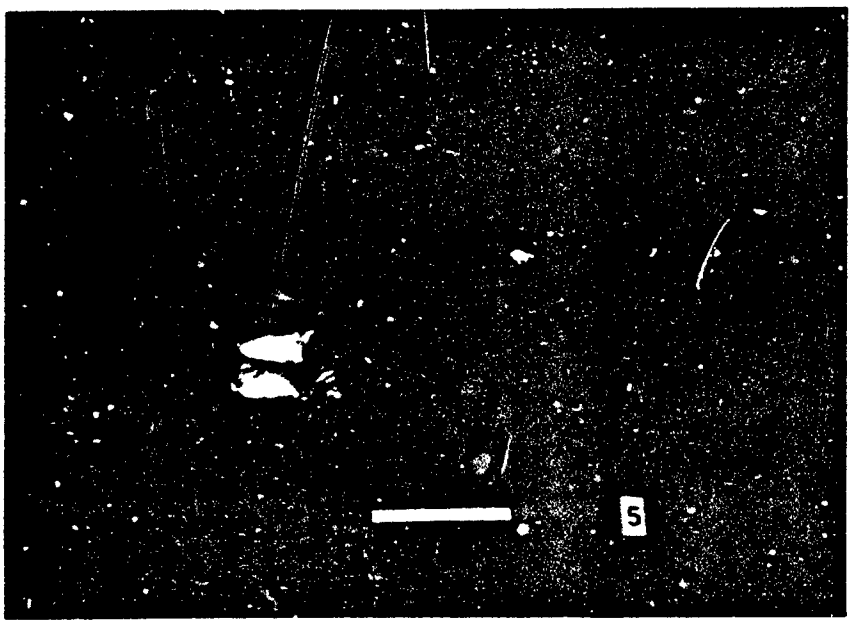

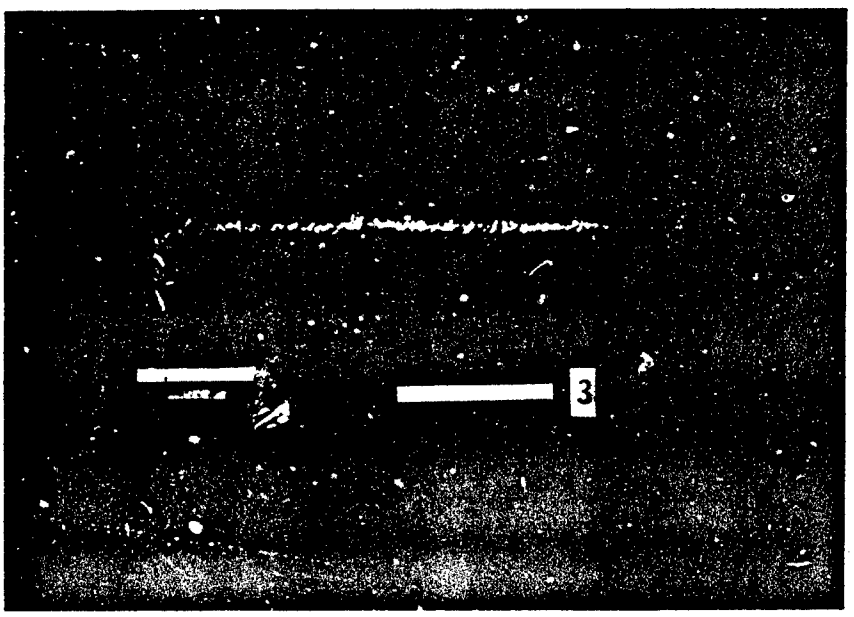

Figure 56. Exterior and Interior Condition of an Above-ground Door-Covered (3) After a Low Pressure Test

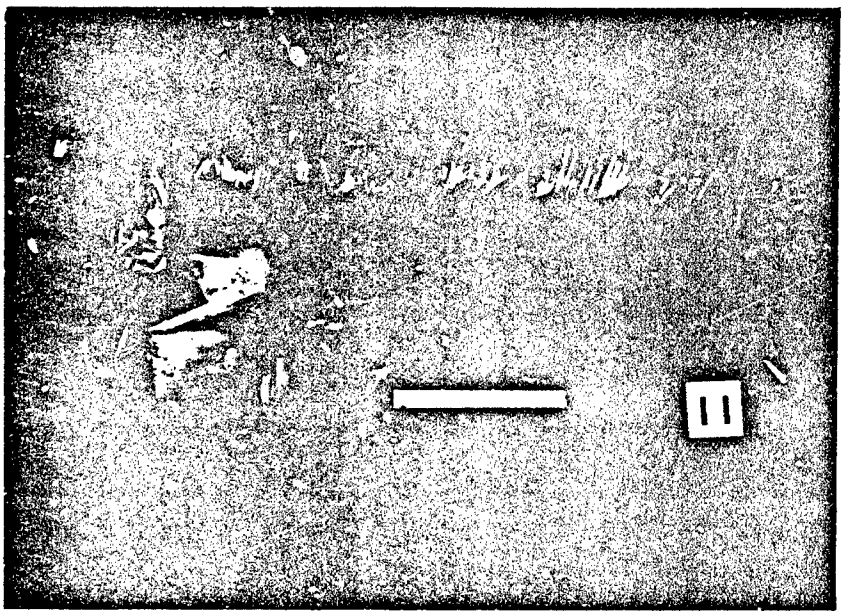

Figure 57. Damage to an Aboveground Door-Covered Shelter (3) in Intermediate Pressure Test

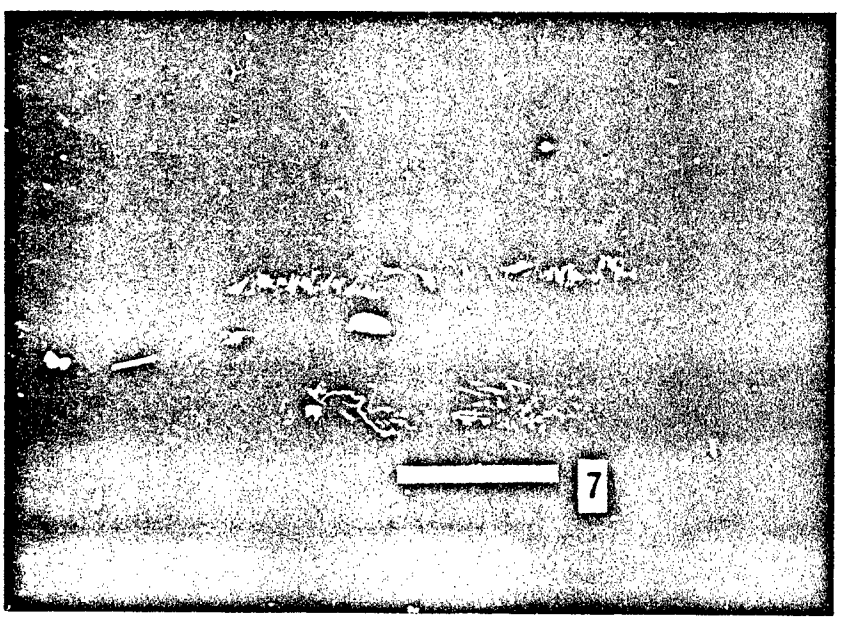

Figure 58. Damage to an Aboveground Door-Covered Shelter (3) in High Pressure Test

The aboveground crib-walled shelter, shelter 5, survived very well in the low pressure tests, but did poorly at the higher pressures. Most failures of these shelters occurred due to the roof poles and soil falling into the shelter, and in some cases for the high pressure loads due to the entire shelter being translated by the blast wave. In the low pressure tests, some of the soil cover was blown away as indicated in Figure 59, but the rest of the shelter remained intact. On the other hand, in the intermediate pressure tests, most of the soil cover was either blown away or fell into the interior of the shelter along with many of the roof poles as shown in Figure 60. Similar though more severe roof response was observed on the high pressure tests as indicated in Figure 61. In addition, the entire shelter was translated back about a shelter length and in some instances rotated slightly. Two modifications were tried on the last high pressure test. The roof poles of the two crib-walled shelters used in this test were glued along the edge of the cribs and to each other to represent their being tied down along the perimeter of the shelter. One of these shelters also was covered with additional soil around the cribs and the roof so that the entryway was the only part of the wooden framework that was visible from outside. In both cases most of the soil cover was blown away, but the roof poles remained in place as shown in Figure 62. However, the one model with the additional soil was translated back about three inches and consequently a marginal survival rating was assigned. The other model shelter 5 was translated back about 1.5 feet and rotated slightly. With such gross rigid body motion, a no-survival rating was assigned. It is very probable that with the attached roof poles modification this shelter would have survived at the 4.6 psig overpressure level. Even at 8.8 psig this shelter can probably survive if it can be anchored to avoid rigid body translations. For example, the entire shelter could be built in a shallow trench and with additional soil all around would be kept from moving during blast loading.

Shelter 6, the aboveground ridge-pole shelter, did very well structurally at all three pressure levels used on these tests. The main difference at each pressure level was the amount of earth cover blown away. In the low pressure tests, only the upper part of the top layer of soil cover was blown away. In the intermediate pressure tests parts of both

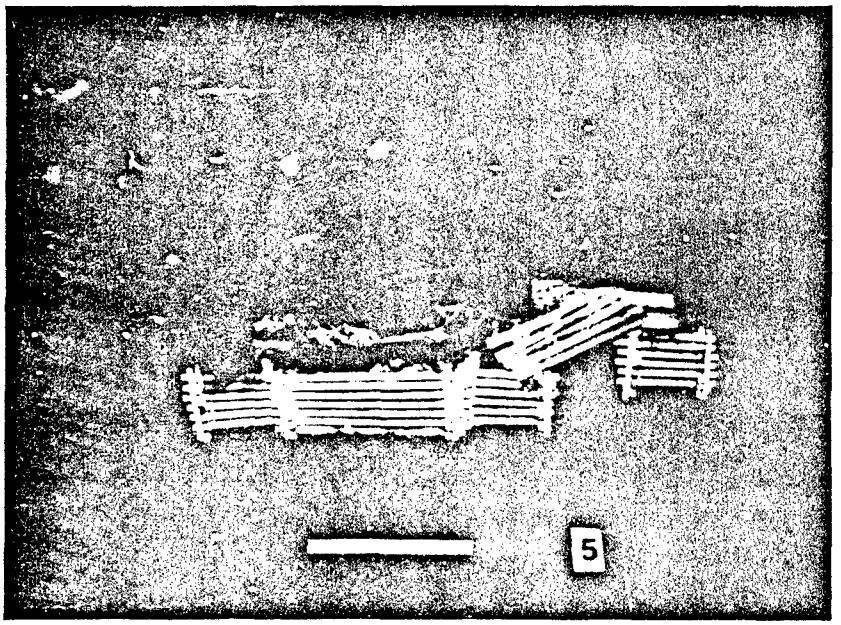

Figure 59. Crib-Walled Shelter (5) After Low Pressure Test

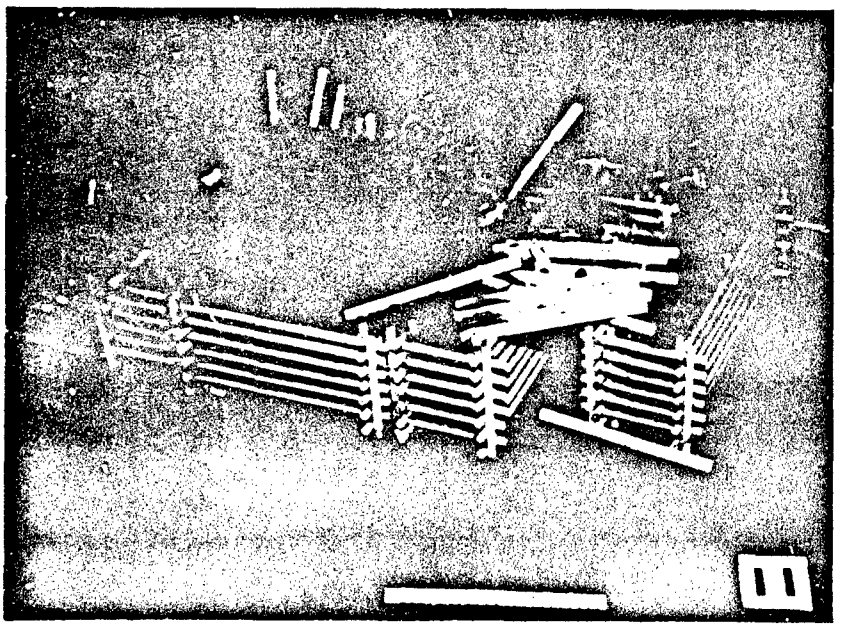

Figure 60. Crib-Walled Shelter (5) After Intermediate Pressure Test

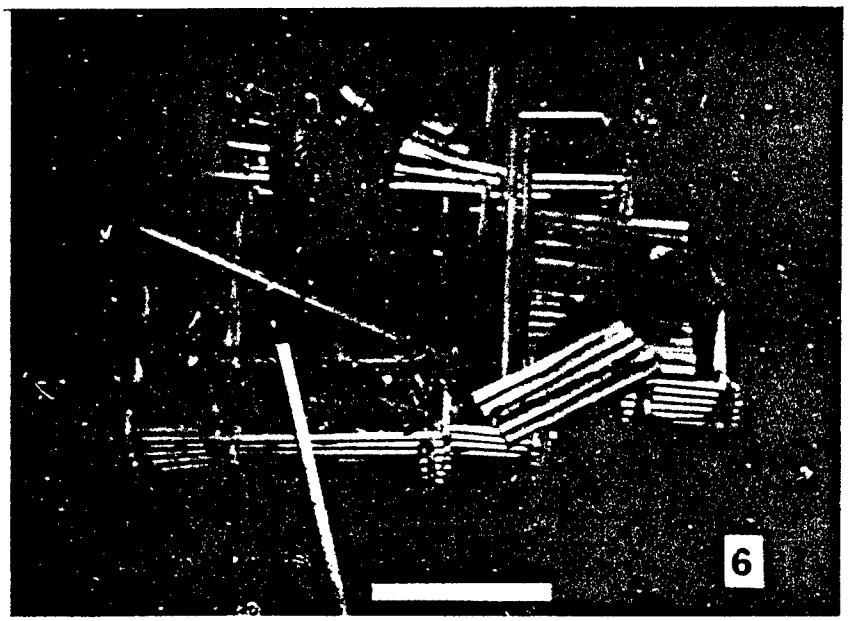

Figure 61. Crib-Walled Shelter (5) After High Pressure Test

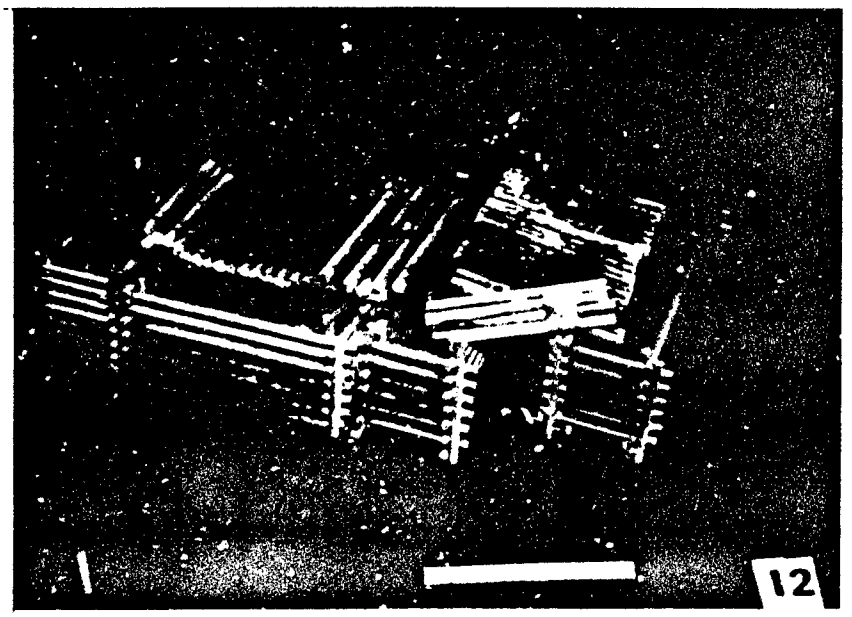

Figure 62. Modified Crib-Walled Shelter (5) After High Pressure Test

layers of soil were eroded exposing the top upper portion of the pole frame as shown in Figure 63. In the high pressure tests most of the soil cover was blown away exposing the ridge-pole frame as shown in Figure 64.

The small-pole shelter, shelter 7, provided the best blast protection in these tests. Not only did it survive structurally at the low and high overpressure loads, but it also kept most of its soil cover, even in the high pressure tests. Furthermore, as indicated earlier in the report, the internal geometry of this shelter also provided some attenuation to the blast pressure leakage so that internal pressures were usually lower in amplitude and had slower rise times than the external overpressures. Figure 65 shows one of these shelters before and after a low pressure test. Similarly, Figure 66 shows a No. 7 shelter before and after a high pressure test. In these high pressure tests some soil cover was blown away and into the entrance and vent openings. There was also some evidence of the floor soil being loosened slightly. In one case, a floor cross-frame pole was also loosened from the horizontal pole. Because this shelter always survived in the high pressure tests, it was not tested at the intermediate pressure level.

Shelter 8, the log-covered trench shelter, provided the least blast protection with only one shelter surviving in the entire test program. Generally, these shelters failed due to major collapse of the trench walls. Normally, the roof poles were pushed down into the soil in varying degrees as a function of the overpressure level. Upon removal of the soil cover and roof poles, the collapsed trenches were partially or completely filled with soil. The one small-pole shelter that survived is shown in Figure 67. The top picture shows the model shelter immediately after the low pressure test. The soil cover and poles were then removed to allow inspection of the trench. This is shown in the bottom picture. A typical failed shelter after an intermediate pressure test is shown in Figure 68. One modification was attempted on this shelter on an intermediate pressure test. This modification consisted of using considerably longer poles over the trench to increase the soil bearing surface. The result was a failure

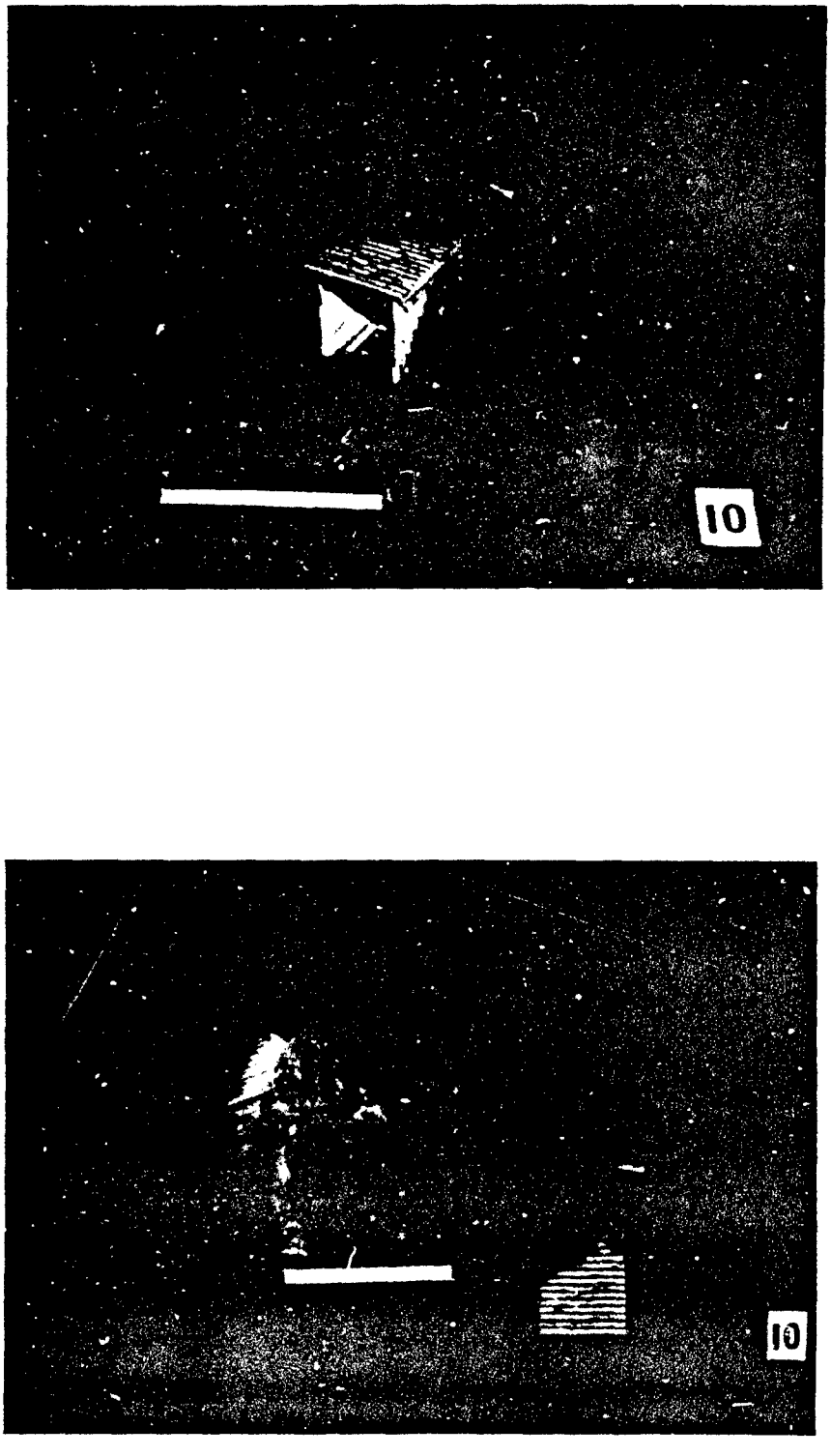

Figure 63. Ridge-Pole Shelter (6) After Intermediate Pressure Test

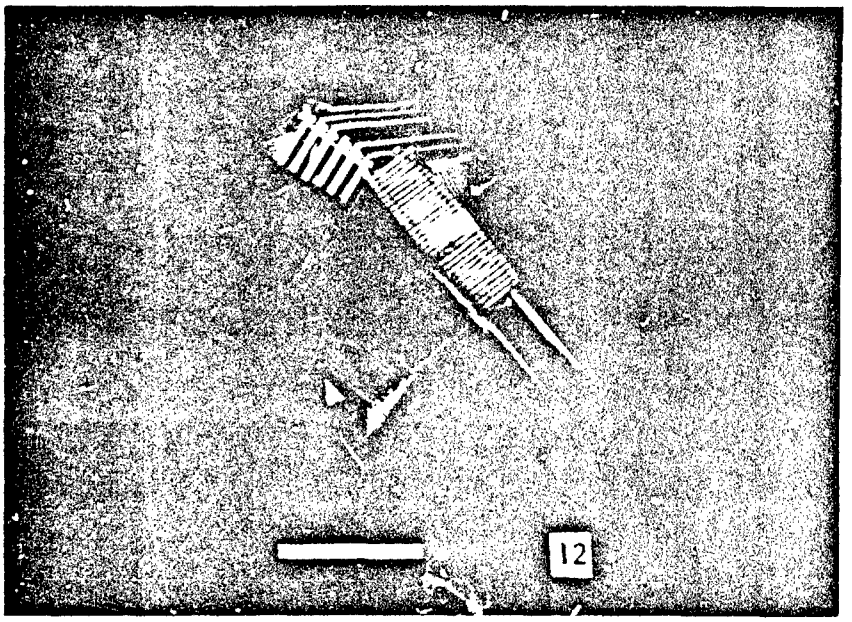

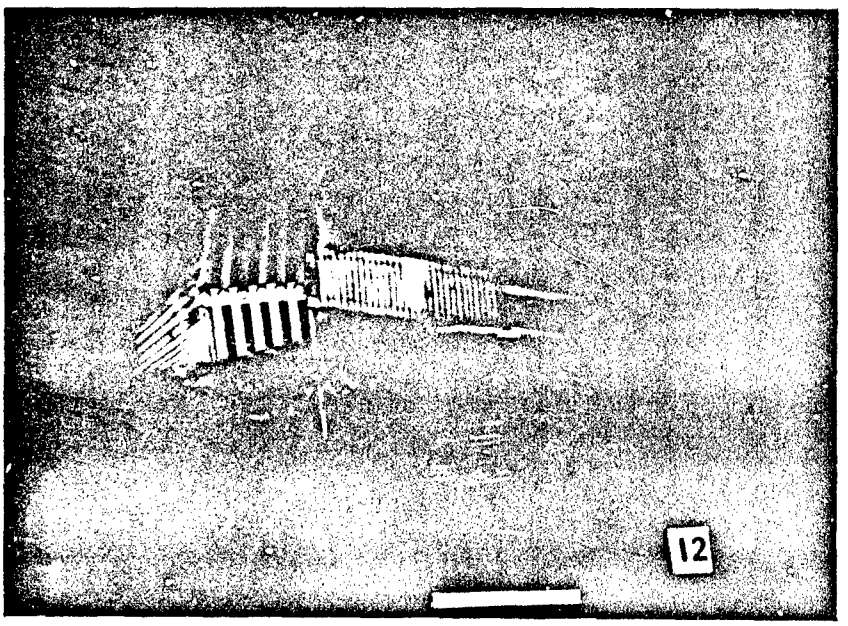

Figure 64. Ridge-Pole Shelter (6) After High Pressure Test

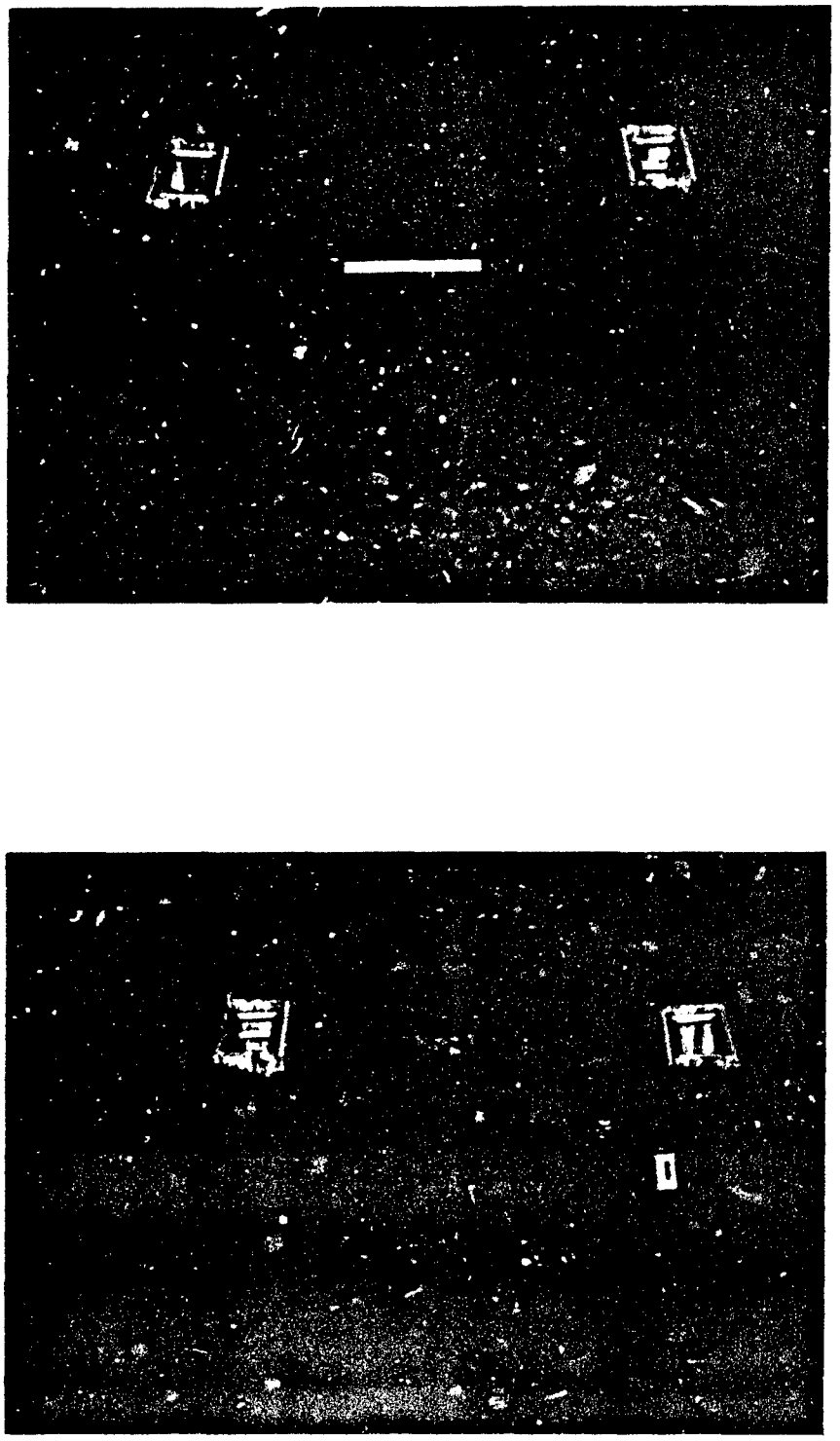

Figure 65. Small Pole Shelter (7) Before and After Low Pressure Test

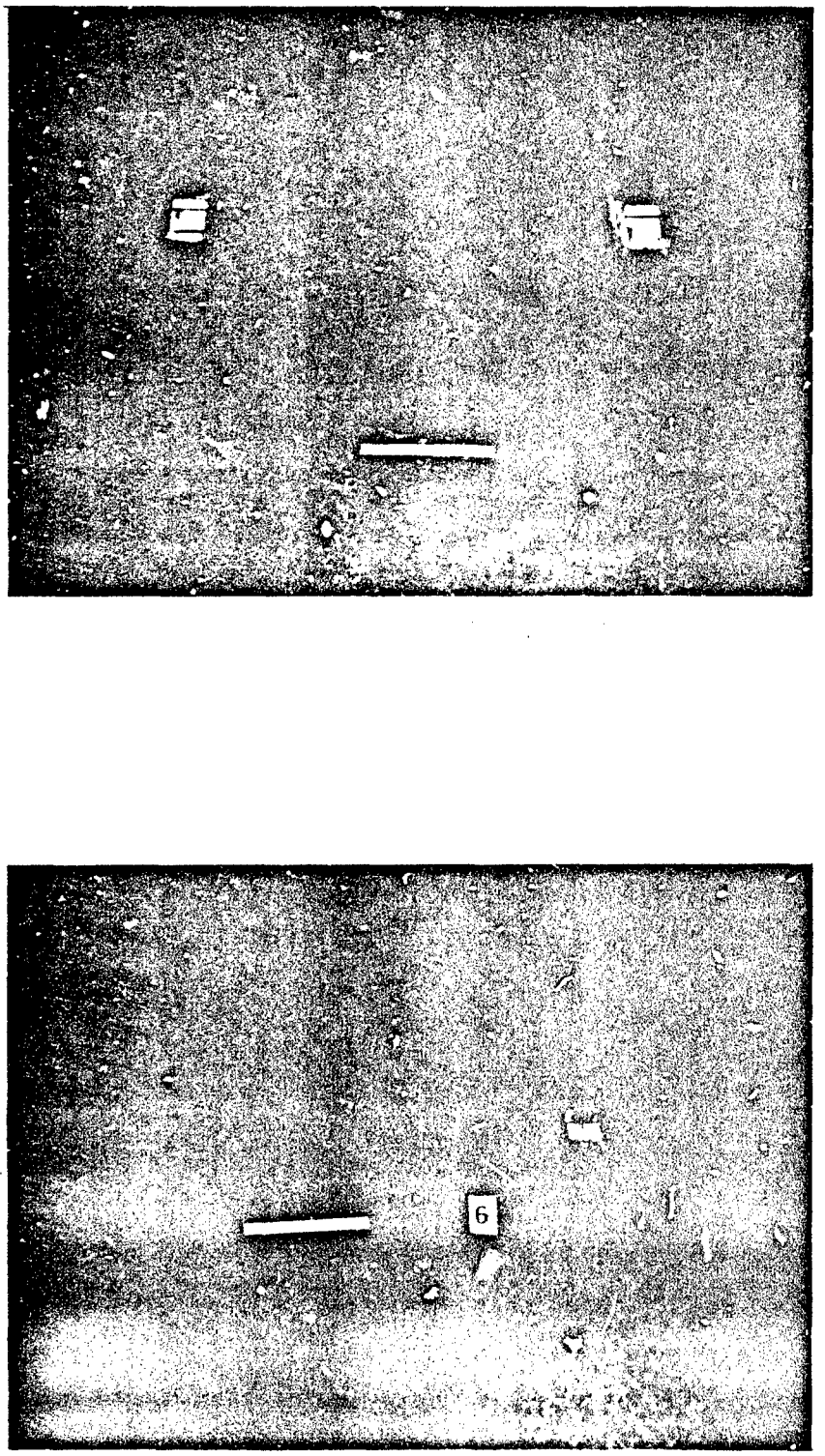

Figure 66. Small Pole Shelter (7) Before and After High Pressure Test

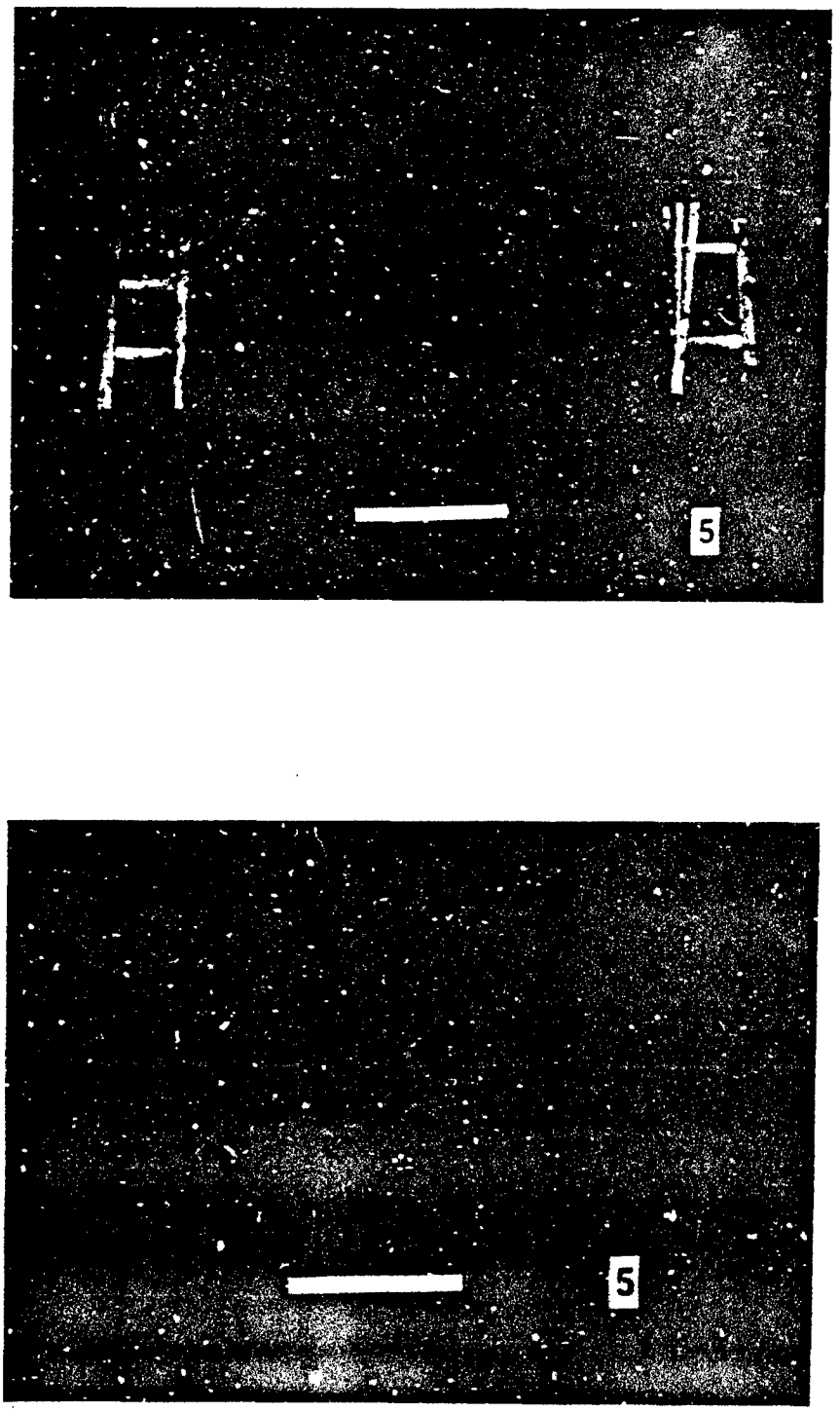

Figure 67. Low Pressure Survival of Log-Covered Trench Shelter (8)

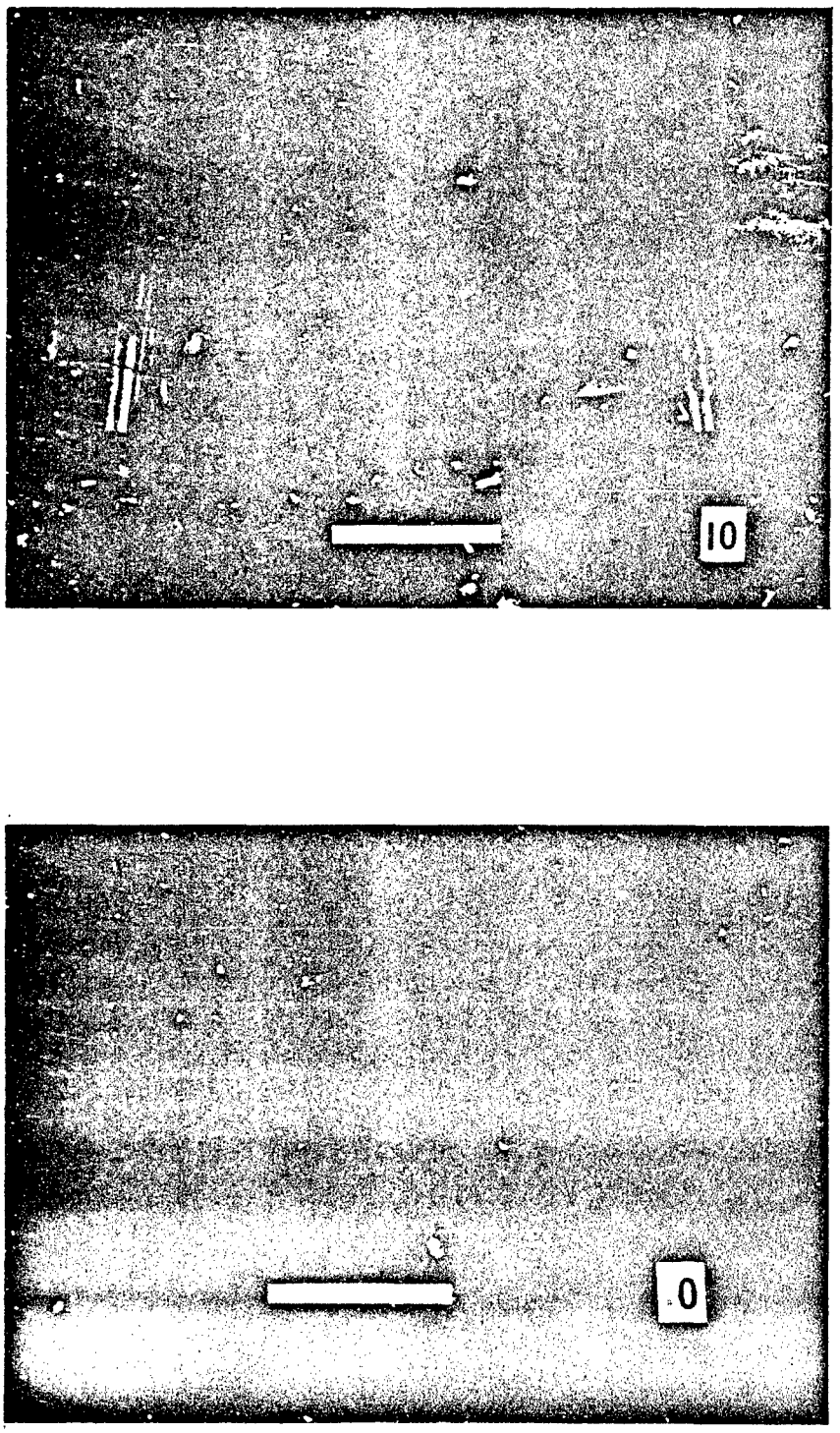

Figure 68. Typical Failure of Log-Covered Trench Shelter (8)

of the trench walls almost identical to the unmodified model shelter. Because of test schedule constraints, this modification was not attempted in a low pressure test. However, it is probable that survival rates at the low pressure would have increased using the longer poles.

Statistical Evaluation of Test Results

Two approaches to "certification" that a given shelter design provides acceptable protection for a certain range of overpressure loads were described earlier. Test data were collected for both approaches. The first option is to define a binomial experiment and use test results to crtify that there is a 90-percent confidence that shelter type A provides acceptable protection at least P_s percent of the time when exposed to a load of x psi. The second option is to perform a regression analysis on test results to certify that there is a 90-percent confidence that the response of shelter type A will be less than threshold value R (psi inside shelter) when exposed to a load of x psi. It is important to note that in the first option, the confidence interval is around P_s, which is a percentage or a probability number. In the second option, the confidence interval is around R, which is a structural response parameter.

The structural response parameter selected for the regression analysis was the level of overpressure attained inside the shelter. It was thought that this parameter would correlate with the probability of survival of the shelter; i.e., shelters that survived would experience lower inside overpressure than shelters that failed. Toward this end, pressure data were collected inside shelters during each experiment. It was found that inside and outside pressure levels were virtually equal, and that inside pressure did not correlate well with shelter survival probability. Consequently, the regression approach to generation of shelter survival confidence limits was not used in the analysis of post-test results.

The binomial experiment approach to confidence interval estimation was used to analyze the shelter test data. Estimated probability of survival is shown in Figure 69 for each of the six shelter types tested. Note the similarity in the survival characteristics of shelter types 2 and 8, types 3 and 5, and types 6 and 7.

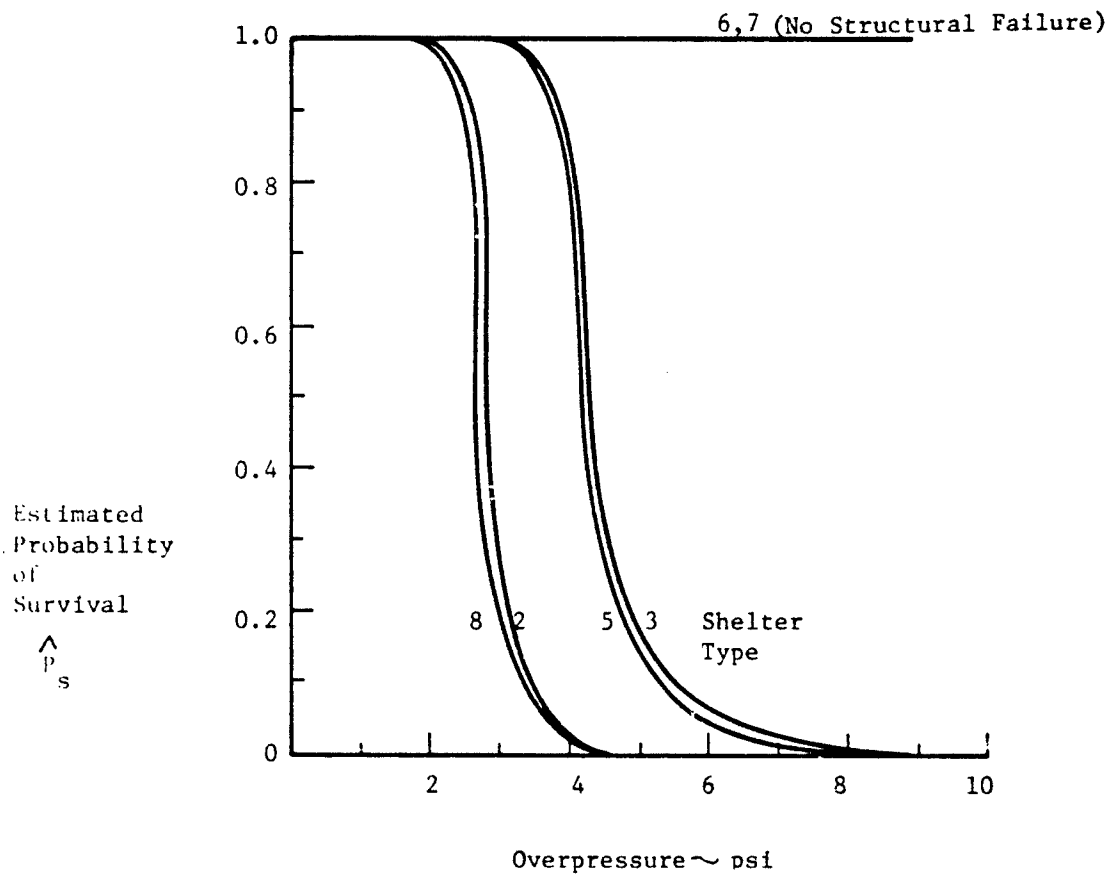

Figure 69. Shelter Survival Probability Estimates

The binomial sum and the beta integral can be shown to be equivalent, and the beta integral can be related to the F-distribution. Consequently, exact confidence limits for the binomial parameter P_s = probability of shelter survival can be expressed in terms of an F distribution as follows:

$$\text{Lower Limit: } P_s \geq 1 - \frac{(n-s+1)\, F_{\alpha/2}\,[2(n-s+1),2s]}{s+(n-s+1)\, F_{\alpha/2}\,[2(n-s+1),2s]}$$

$$\text{Upper Limit: } P_s \leq 1 - \frac{n-s}{n-s+(s+1)\, F_{\alpha/2}\,[2(s+1),\ 2(n-s)]}$$

where
- n = number of trials
- s = number of survivals in n trials
- P_s = probability of shelter survival
- $(1-\alpha)100$ = confidence level desired (percent)
- $F_{\alpha/2}\,[\nu_1,\nu_2]$ = F-statistic with ν_1 and ν_2 degrees of freedom.

Applying the above methodology to the shelter test results yields the 90-percent confidence intervals on P_s shown in Figure 70. The point of interest is really the lower boundary of the confidence interval. For example, the data shown for shelter type 3 indicate that there is at least 90-percent confidence that this shelter will survive a load of 2.8 psi 83 percent of the time. The varying size of the confidence intervals shown in Figure 70 is a direct reflection of the number of tests that were conducted for a given shelter type - applied load combination.

CONCLUSIONS

Each of the six expedient fallout shelters analyzed or tested offers some level of blast protection.

The car-over-trench shelter is expected to fail by overturning of the vehicle at 5.4 psi overpressure.

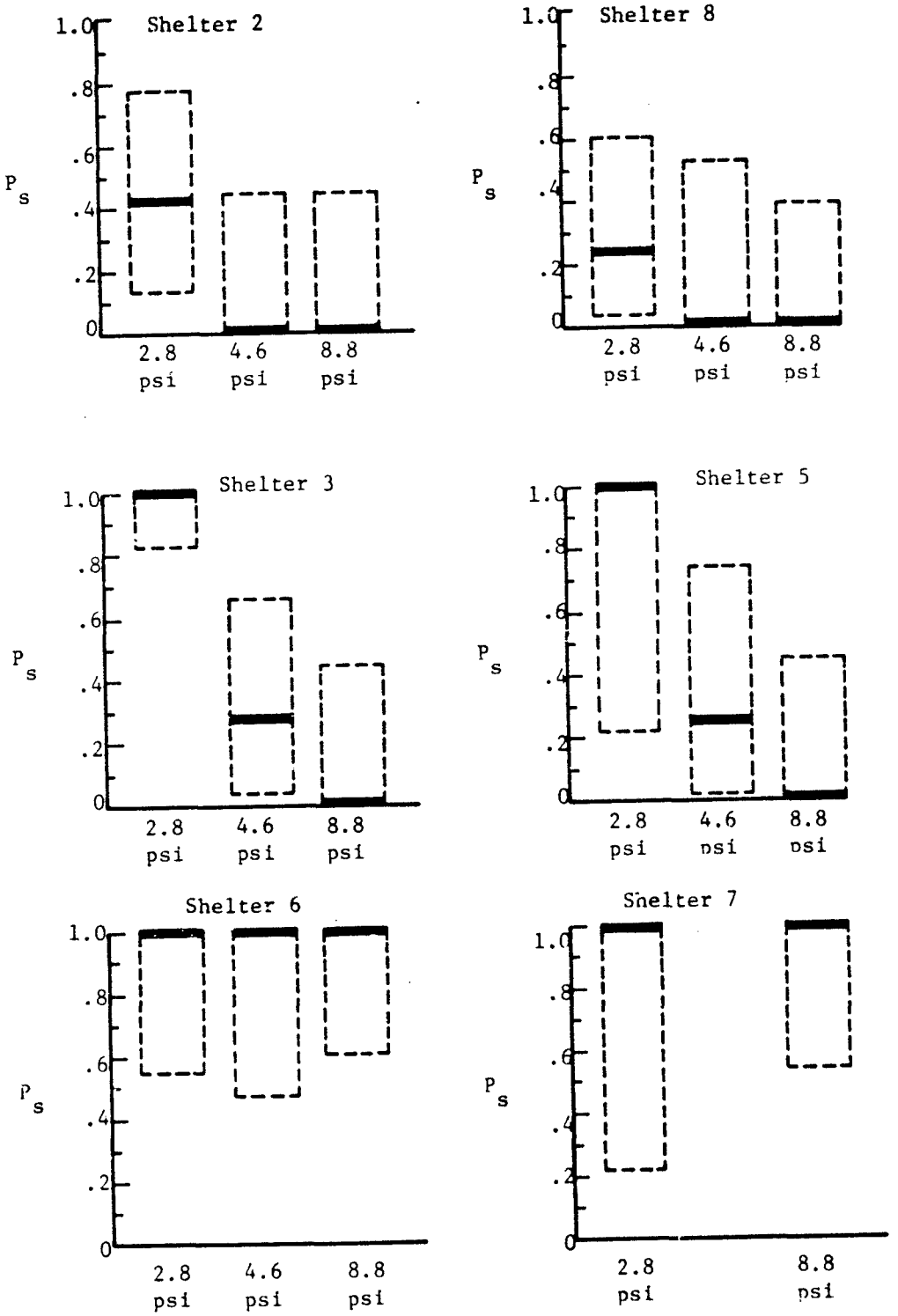

Figure 70. 90 Percent Confidence Intervals

Structural failures were determined analytically for six of the expedient shelters. Actual failure loads were found to be higher due to blast pressure leakage into the shelters.

Trench shelters fail by soil wall collapse in the 5 to 6 psi overpressure range. Soil failures were determined both analytically and experimentally, even though the soil passed the recommended thumb pressure test.

Pressures measured inside the expedient shelters were virtually the same as the external overpressures. The threshold for occupant lung damage is 8 psi overpressure. A survival rate of 99 percent is expected at 28 psi overpressure.

Replica modeling is appropriate for structural response provided the response is in the quasi-static loading realm. Replica modeling limits the Fort Cronkhite utility to a maximum of approximately 9 psi. Higher overpressures can be modeled by modifying the facility.

Multiple shelters properly spaced can be placed in each test without creating interference in the blast loadings.

Results from model tests were consistent with previous full-scale testing.

The small pole and aboveground ridge-pole shelters were structurally sound under all the imposed overpressures (up to 8.8 psi). Although none of the structures failed, fallout protection was degraded due to scouring of the soil overburden.

The aboveground door-covered and crib-wall shelters survived at 2.8 psi, experienced some failures at 4.6 psi, and failed at 8.8 psi. Modifying the crib-wall shelters by anchoring the roof poles prevented roof collapse, although soil scouring still occurred.

Only a few of the trench shelters (door-covered and log-covered) survived the 2.8 psi overpressure. The dominant failure was collapsing of the side walls. Shoring of the trench walls prevented collapsing of the soil and offers a significant increase in survivability.

RECOMMENDATIONS

Develop or improve designs to prevent scouring of shelter soil overburden. The first step is to quantify the amount of earth scouring for various shelter geometries, soil properties, and overpressure loadings. Load duration is a major factor to earth scouring.

Develop techniques for shoring trench walls. The payoff potential for shoring trench walls was demonstrated in limited testing. Guidelines should be incorporated into expedient shelter designs.

Develop techniques to tie down shelter roof components (logs or doors) to the walls and the walls of the aboveground shelters to the ground.

Replica modeling proved successful in evaluating the expedient shelters for overpressures less than 9 psi. Improvements to shelter designs also should be evaluated in modeled tests.

REFERENCES

1. "Guide for Increasing Local Government Civil Defense Readiness During Periods of International Crisis," Defense Civil Preparedness Agency, Civil Preparedness Guide (CPG) 1-7, April 1979.

2. Kearny, C. H., "Nuclear War Survival Skills," NWS Research Bureau, 1982.

3. Glasstone, S., and Dolan, P. J., (eds.), The Effects of Nuclear Weapons, 3rd Edition, U. S. Department of Defense and U. S. Department of Energy, Washington, D. C., 1977.

4. Haltiwanger, Hall, and Newmark, "Approximate Methods for the Vulnerability Analysis of Structures Subjected to the Effects of Nuclear Blast," Report No. U-275-76, June 1976.

5. Wilton, C., Kaplan, K., and Gabrielsen, B. L., "The Shock Tunnel: History and Results," SSI7618-1, March 1978.

6. Kearny, C. H., and Chester, C. V., "Blast Tests of Expedient Shelters in the DICE THROW Event," Oak Ridge National Laboratory, ORNL-5347, March 1978.

7. Kearny, C. H., Chester, C. V., and York, E. N., "Blast Tests of Expedient Shelters in the MISERS BLUFF Event," Oak Ridge National Laboratory, ORNL-5541, January 1980.

8. "Workbook for Predicting Pressure Wave and Fragment Effects of Exploding Propellant Tanks and Gas Storage Vessels," NASA CR 134906, September 1977.

9. Biggs, J. M., Introduction to Structural Dynamics, McGraw-Hill, Inc., 1964.

10. Lambe, T. W., and Whitman, R. V., Soil Mechanics, John Wiley and Sons, Inc., 1969.

11. White, C. S., "The Scope of Blast and Shock Biology and Problem Areas in Relating Physical and Biological Parameters," Annals of the New York Academy of Sciences, Volume 162, Art. 1, pp. 89-102, October 1968.

12. White, C. S., Jones, R. K., Damon, E. G., Fletcher, E. R., and Richmond, D. R., "The Biodynamics of Air Blast," DNA 2738T, Lovelace Foundation for Medical Education and Research, July 1971.

13. Richmond, D. R., Damon, E. G., Fletcher, E. R., Bowen, I. G., and White, C. S., "The Relationship Between Selected Blast Wave Parameters and the Response of Mammals Exposed to Air Blast," Annals of the New York Academy of Sciences, Volume 152, Art. 1, pp. 103-121, October 1968.

14. Damon, E. G., Yelverton, J. T., Luft, U. C., and Jones, R. K., "Recovery of the Respiratory System Following Blast Injury," Technical Progress Report to Defense Atomic Support Agency, DASA2580, Lovelace Foundation for Medical Education and Research, October 1970.

15. Bowen, I. G., Fletcher, E. R., and Richmond, D. R., "Estimate of Man's Tolerance to the Direct Effects of Air Blast," Technical Report to Defense Atomic Support Agency, DASA 2113, Lovelace Foundation for Medical Education and Research, October 1968.

16. Damon, E. G., Richmond, D. R., Fletcher, E. R., and Jones, R. K., "The Tolerance of Birds to Air Blast," Technical Report to Defense Agency, DNA 3314F, Lovelace Foundation for Medical Education and Research, July 1974.

17. von Gierke, H. E., "Biodynamic Models and Their Applications," Aerospace Medical Research Laboratory, Wright-Patterson AFB, Ohio, 1971.

18. Baker, W. E., Kulesz, J. J., Ricker, R. E., Bessey, R. L., Westine, P. S., Parr, V. B., and Oldham, G. A., "Workbook for Predicting Pressure Wave and Fragment Effects of Exploding Propellant Tanks and Gas Storage Vessels," November 1975.

19. Allahdadi, A., "Analytical and Experimental Assessment of a High-Explosive-Driven Shock Tube," AFWL-TR-81-201, February 1983.

20. Baker, W. E., Hokanson, J. C., and Cervantes, R. A., "Model Tests of Industrial Missiles," Final Report SwRI Project No. 02-9153-001, May 1976.

21. Baker, W. E., Westine, P. S., and Dodge, F. T., Similarity Methods in Engineering Dynamics, Spartan Books, Hayden Book Company, Inc., Rochelle Park, New Jersey, 1973.

22. Baker, W. E., Westine, P. S., Kulesz, J. J., Wilbeck, J. S., and Cox, P. A., Jr., "A Manual for the Prediction of Blast and Fragment Loading on Structures," DOE/TLC-11268, U. S. Army Corps of Engineers, Huntsville, Alabama, September 30, 1980.

23. Benson, K. A., "Mill Race: Cratering and Related Effects," AFWL-TR-82-76, January 1983.

24. Brode, H. L., "Review of Nuclear Weapons Effects," Annual Review of Nuclear Science, Volume 18, 1968.

25. Clark, R. O., and Allahdadi, F. A., "Explosive Driven Shock Waves in One Dimension," AFWL-TR-82-85, February 1983.

26. Coulter, G. A., "Translation and Impingement of Furniture Debris in a Model Apartment House Shelter," Memorandum Report ARBRL-MR-02835, May 1978.

27. Ethridge, N. H., "Blast Diffraction Loading on the Front and Rear Surfaces of a Rectangular Parallelepiped," BRL Memorandum Report No. 2784, September 1977.

28. Ethridge, N. H., Loretto, R. E., Wortman, J. D., and Bertrand, B. P., "HULL Hydrocode Computations of Flow Blockage and Its Relation to Overturning of Vehicles in a Large Blast Simulator," BRL Technical Report ARBRL-TR-02442, U. S. Army Ballistic Research Laboratory, Aberdeen Proving Ground, MD, November 1982.

29. Gill, H. L., "Active Arching of Sand During Dynamic Loading - Results of an Experimental Program and Development of an Analytical Procedure," Navy Civil Engineering Laboratory Technical Report R-541, September 1967.

30. Hendson, A. J., Jr., and Auld, H. E., "The Effect of Soil Properties on the Attenuation of Airblast-Induced Ground Motions," Proceedings International Symposium on Wave Propagation and Dynamic Properties of Earth Materials, August 1967.

31. Kaplan, K., and Price, P. D., "Accidental Explosions and Effects of Blast Leakage Into Structures," U. S. Army Armament Research and Development Program, Contractor Report ARLCD-CR-79009, June 1979.

32. Longinow, A., Ojdrovich, G., Bertram, L., and Wiedermann, A., "People Survivability in a Direct Effects Environment and Related Topics," Final Report Contract DAHC 20-68-C-0126, DCPA Work Unit 1614D, May 1973.

33. Longinow, A., Hahn, E. E., and Bertram, L. A., "Personnel Survivability in Blast Wind Environment," ASCE Journal of the Engineering Mechanics Division, Volume 103, April 1977.

34. Longinow, A., and Wiedermann, A., "Relative Structural Considerations for Protection From Injury and Fatality at Various Overpressures," Final Report DCPA Contract DCPA01-75-C-0325, June 1977.

35. Longinow, A., "Survivability in a Nuclear Weapon Environment," Final Report DCPA Contract DCPA01-77-C-0229, May 1979.

36. Longinow, A., "Probability of People Survival in a Nuclear Weapon Blast Environment," Final Report FEMA Contract DCPA01-79-C-0240, May 1980.

37. Longinow, A., and Joyce, R. P., "Load Tests of a Wood Floor Over a Basement," Final Report FEMA Contract DCPA01-78-C-0223, June 1980.

38. Longinow, A., Chu, K-H., and Thomopoulos, N. T., "Probability of Survival in Blast Environment," ASCE Journal of the Engineering Mechanics Division, Volume 108, April 1982.

39. Lottero, R. E., Wortman, J. O., Bertrand, B. P., and Kitchens, C. W., Jr., "Three-Dimensional Oblique Shock Diffraction Over a Rectangular Parallelepiped: Computational/Experimental Comparison," ARBRL-TR-02443, November 1982.

40. Lynch, F. X., "Adequate Shelters and Quick Reaction to Warning: A Key to Civil Defense," Science, Volume 142, 8 November 1963.

41. Reitter, T. A., McCallen, D. B., and Kang, S-W., "Literature Survey of Blast and Fire Effects of Nuclear Weapons on Urban Areas," UCRL-53340, June 1982.

42. Strode, J. D., Jr., "MISER BLUFF Event Phase II Test Execution Report, Events 1 and 2," POR 7012 (WT-7012), December 1979.

43. Tansley, R. S., and Bernard, R. O., "Shelter Upgrading Manual: Key Worker Shelters," FEMA Contract No. EMW-C-0153, Work Unit 1128A, May 1981.

44. Tansley, R. S., and Zaccor, J. V., "Testing of Shelter Design and Industrial Hardening Concepts at the MILL RACE Event," FEMA Contract No. EMW-C-0611, Work Unit 11280, January 1982.

45. Trimpi, R. L., and Cohen, N. B., "A Theory for Predicting the Flow of Real Gases in Shock Tubes with Experimental Verification," National Advisory Committee for Aeronautics Technical Note 3375, March 1955.

46. Wiehle, C. K., "Summary of Shelter Entranceways and Openings," Final Report OCD-DAHC 20-67-C-0136, OCD Work Unit No. 1157D, September 1967.

47. Wood Handbook: Wood as an Engineering Material, Agriculture Handbook No. 72, Forest Products Laboratory, Forest Service, U. S. Department of Agriculture, Washington, D. C., Revised August 1974.

APPENDIX A

SWEDISH SHELTERS

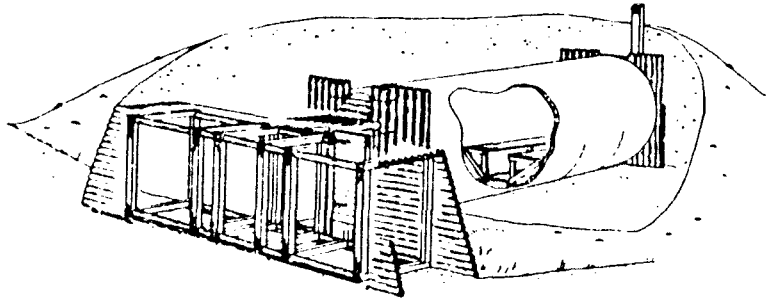

FRILIGGANDE SKYDD
häfte 2

RÖRSKYDD AV BETONG
MED TIMMERINGÅNG
FÖR 10-40 PERS.

FÖRHANDSUTGÅVA 1982-12-01

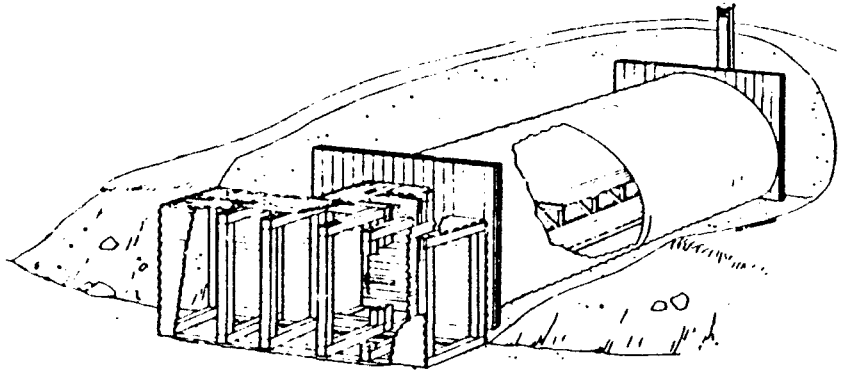

FRILIGGANDE SKYDD
häfte 3
RÖRSKYDD AV PLÅT
FÖR 10-40 PERS.

FÖRHANDSUTGÅVA 1982-12-01

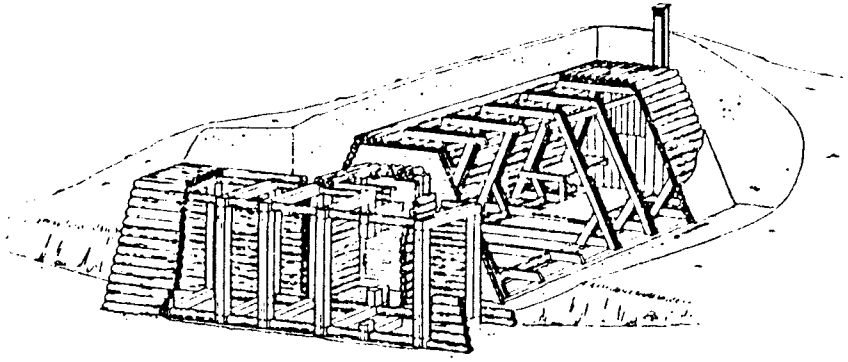

FRILIGGANDE SKYDD
häfte 4
VALVSKYDD AV TRÄRAMAR FÖR 10-40 PERS.

FÖRHANDSUTGÅVA 1982-12-01

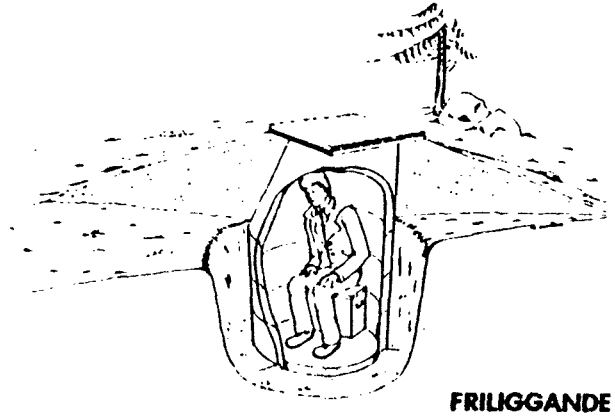

FRILIGGANDE SKYDD
häfte 5
ENMANSSKYDD AV BETONGRÖR

FÖRHANDSUTGÅVA 1982-12-01

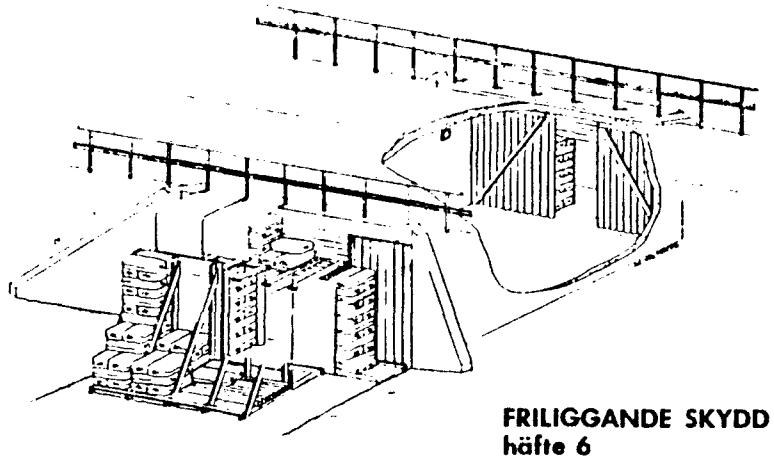

FRILIGGANDE SKYDD
häfte 6

SKYDD I VÄGTUNNEL
MED TIMMERVÄGG
FÖR CA 30-60 PERS.

FÖRHANDSUTGÅVA 1982-12-01

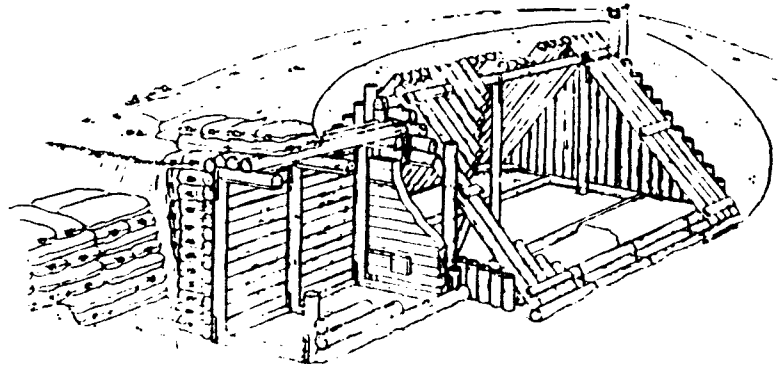

FRILIGGANDE SKYDD
häfte 7
SKYDD I TIMMERKOJA
FÖR 8 PERS.

FÖRKANDSUTGÅVA 1982-12-01

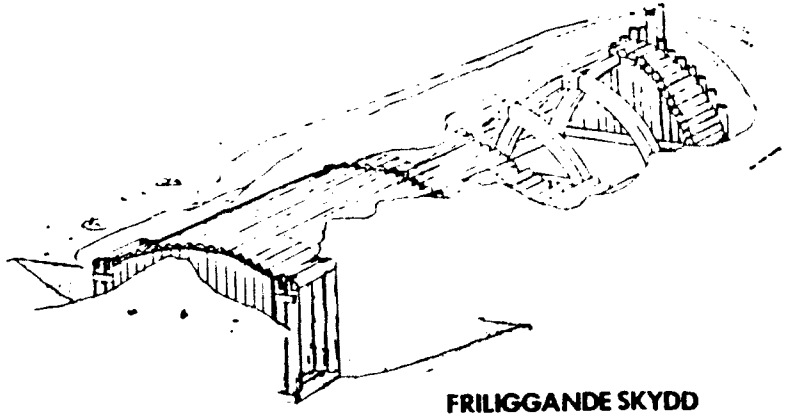

FRILIGGANDE SKYDD
häfte 8
VALVSKYDD MED BETONGBÅGAR
FÖR 10-40 PERS.

FÖRHANDSUTGÅVA 1982-12-01

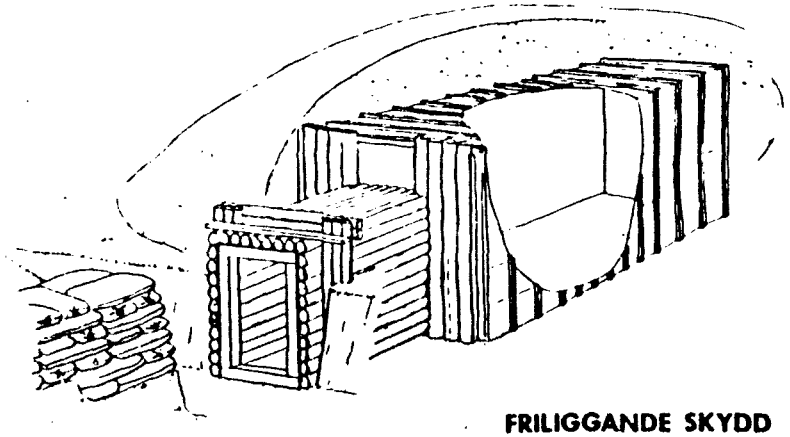

FRILIGGANDE SKYDD
häfte 9
SKYDD I CONTAINER
FÖR 10 PERS.

FÖRHANDSUTGÅVA 1982-12-01

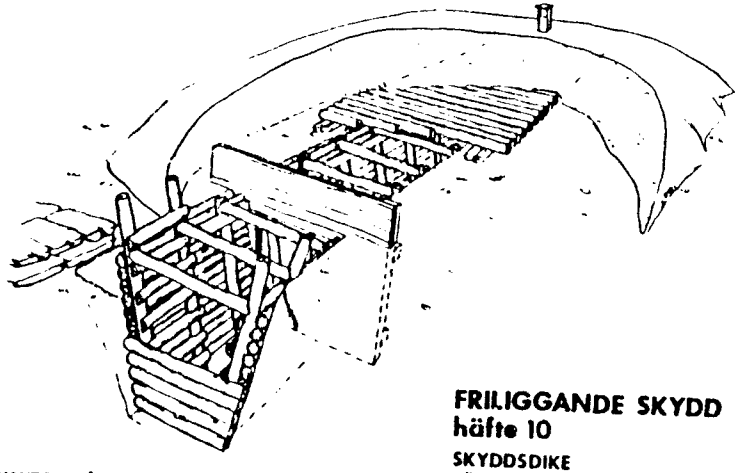

FRILIGGANDE SKYDD
häfte 10
SKYDDSDIKE
FÖR 10 PERS.

FÖRHANDSUTGÅVA 1982-12-01

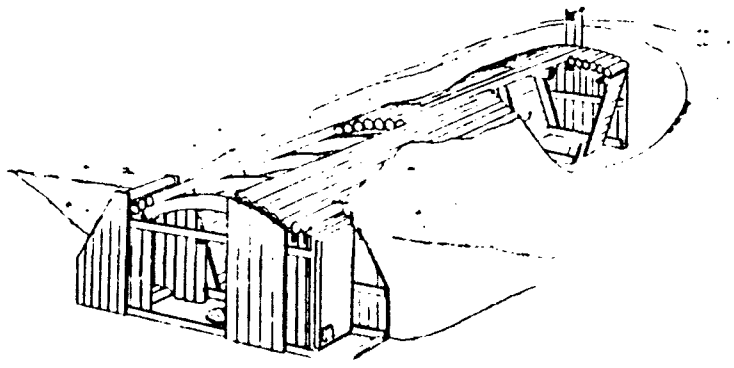

FRILIGGANDE SKYDD
häfte 11

SKYDDSDIKE MED BETONGBÅGAR
FÖR 10 PERS.

FÖRHANDSUTGÅVA 1982-12-01

APPENDIX B

EXAMPLE STRUCTURAL ANALYSIS

Given Real System - Crib-Walled Shelter

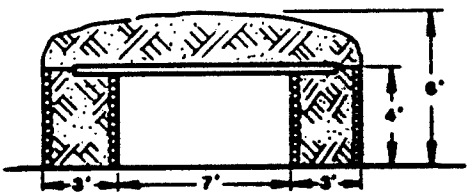

Poles: Young's Modulus E = 741,000 psi
Crushing Strength σ = 8,700 psi
Diameter = 4 inches
Density γ_p = 39 lb/ft^3
Soil: Density γ_s = 100 lb/ft^3

Idealized System

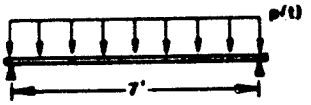

Moment of Inertia

$$I = \frac{\pi r^4}{4} = \frac{\pi(2)^4}{4} = 12.6 \text{ in}^4$$

Single Pole:

Total Weight (Soil + Pole) $W = (100 \times 2 \times 7 \times \frac{4}{12}) + (39 \times \frac{\pi 2^2}{144} \times 7)$

$= 467 + 24 = 491$ lbs.

$$\text{Total Mass } M = \frac{D}{g} = \frac{491}{386} = 1.27 \frac{\text{lb.sec}^2}{\text{in}} \quad (D = \text{Dead Load})$$

$$\text{Stiffness } K = \frac{384EI}{5\ell^3} = \frac{384(741,000)12.6}{5(7 \times 12)^3} = 1210 \text{ lb/in.}$$

$$\text{Maximum Bending Moment } M_{max} = \frac{\sigma I}{C} = \frac{8700(12.6)}{2}$$

$= 54,810$ in.-lb

$$\text{Maximum Resistance } R_m = \frac{8M}{L} \text{ (Ref. 9)} = \frac{8(54,810)}{7(12)}$$

$$= 5220 \text{ lb}$$

$$\text{Maximum Deflection } X_m = \frac{R_m}{K} = 4.3 \text{ in.}$$

$$\text{Dead Load Deflection } X_o = \frac{W}{K} = \frac{491}{1210} = .41 \text{ in.}$$

Failure Load Estimate

$$\frac{1}{2} R_m X_m - \frac{1}{2} D X_o = (P A + D)(X_m - X_o)$$

P - overpressure

A - Area under pressure loading

$$\frac{1}{2} (5220)(4.3) - \frac{1}{2} (491)(.41) = \{P(4x84) + 491\}(4.3 - .41)$$

$$11122 = (336 P + 491)3.89$$

$$P = \left(\frac{11122}{3.89} - 491\right) \frac{1}{336} = 7 \text{ psi}$$

Blast Analysis

For $P_{so} = 7$ psi, $t_d = 2.17$

Transformation Factors (Ref. 9)

Load $K_L = .64$

Mass $K_m = .50$

$$\text{Natural Period } \tau = 2\pi\sqrt{\frac{K_m M}{K_L K}} = 2\pi\sqrt{\frac{(.5)(1.27)}{(.64)(1210)}}$$

$$= .18 \text{ sec}$$

$$\frac{t_d}{\tau} = \frac{2.17}{.18} = 12 \qquad \therefore \text{ Dynamic Load Factor DLF} = 1.95$$

$$X_m = X_o + DLF\ X_{STATIC}$$

$$\text{where } X_{STATIC} = \frac{PA}{K} = \frac{P(4x84)}{1210}$$

$$4.3 = .41 + 1.95\left(\frac{336\ P}{1210}\right)$$

$$P = \left(\frac{4.3 - .41}{1.95}\right)\ \frac{1210}{336} = 7.18 \text{ psi}$$

Expected Failure Overpressure = 7.18 psi

APPENDIX C

TESTBED SOIL PROPERTIES

Professional Service Industries, Inc.
Shilstone Engineering Testing Laboratory Division

December 13, 1983

Southwest Research Institute
P.O. Box 28510
6220 Culebra Road
San Antonio, Texas 78284
Attn: Phillip Nash

Re: Various Classification Tests
Navato Loam Sample
Purchase Order No. 17157
SETL Project No. 312-35160

Gentlemen:

As authorized under the above referenced purchase order, various classification tests were conducted on the soil sample delivered to our laboratory by a representative of Southwest Research Institute on October 12, 1983. The classification tests requested included an Atterberg Limits analysis, grain size distribution analysis, moisture density relationship analysis, and an unconsolidated-undrained triaxial test. The results of these tests are presented on the attached report forms.

The moisture-density relationship for the soil sample, classified as a slightly gravelly sandy silty clay (CL), was determined in accordance with procedures outlined under ASTM designation D-698 (Standard Proctor). With the maximum dry density and optimum moisture content for the soil known, test specimens were remolded for unconsolidated-undrained triaxial testing. At the request of SWRI personnel, the test specimens were molded approximately 4 to 5 percent dry of optimum to simulate as closely as possible actual field conditions. It should be noted that the specimens were extremely friable at this moisture content, rendering testing difficult at best.

The Mohr's circles for specimens tested at various confining pressures have been plotted on an attached form. An examination of this figure reveals that the failure envelope for the specimens tested is curved, resulting in a cohesion intercept of approximately 650 pounds per square foot. A curved failure envelope is typical for partially saturated soils tested under triaxial conditions in which only total stresses are measured. If a linear failure envelope (dashed line on Mohr's circle graph) is assumed, the angle of internal friction for this material is approximately 25 percent.

8430 Western Avenue • San Antonio, TX 78216 • Phone: 512/342-9377

It should be noted that the test results reported are subject to change for different compaction procedures. Furthermore, changes in in situ moisture conditions (the material may become nearly or completely saturated with time in a natural environment) and whether the moisture change occurs with or without volume change can greatly affect the strength properties of the material.

We appreciate the opportunity to assist your organization on this project. Should you have questions concerning the test results, do not hesitate to contact one of the undersigned.

Very truly yours

SHILSTONE ENGINEERING TESTING
LABORATORY DIVISION

A. Scot Harrell, E. I. T.
Branch Manager

John W. Dougherty, P. E.
Senior Project Engineer

ASH:JWD/tr

Professional Service Industries, Inc.
Shilstone Engineering Testing Laboratory Division

REPORT OF MOISTURE DENSITY RELATIONSHIP OF SOIL

TESTED FOR: Southwest Research Institute

PROJECT: Navato Loam Sample
(P.O. No. 17157)

DATE: 10-14-83

OUR REPORT NO.: 312-35160

TEST DATA

Visual Classification: Light brown slightly gravelly s
silty clay (CL)

Sample Source: Delivered to laboratory by SWRI

Method of Test: ASTM D-698 (Standard Proctor)

Test Results:

Maximum Dry Density:	110.9	lbs/ft³
Optimum Moisture Content:	15.0	%

Atterberg Limits:
Liquid Limit: 33 , Plastic Limit: 17 , PI: 16

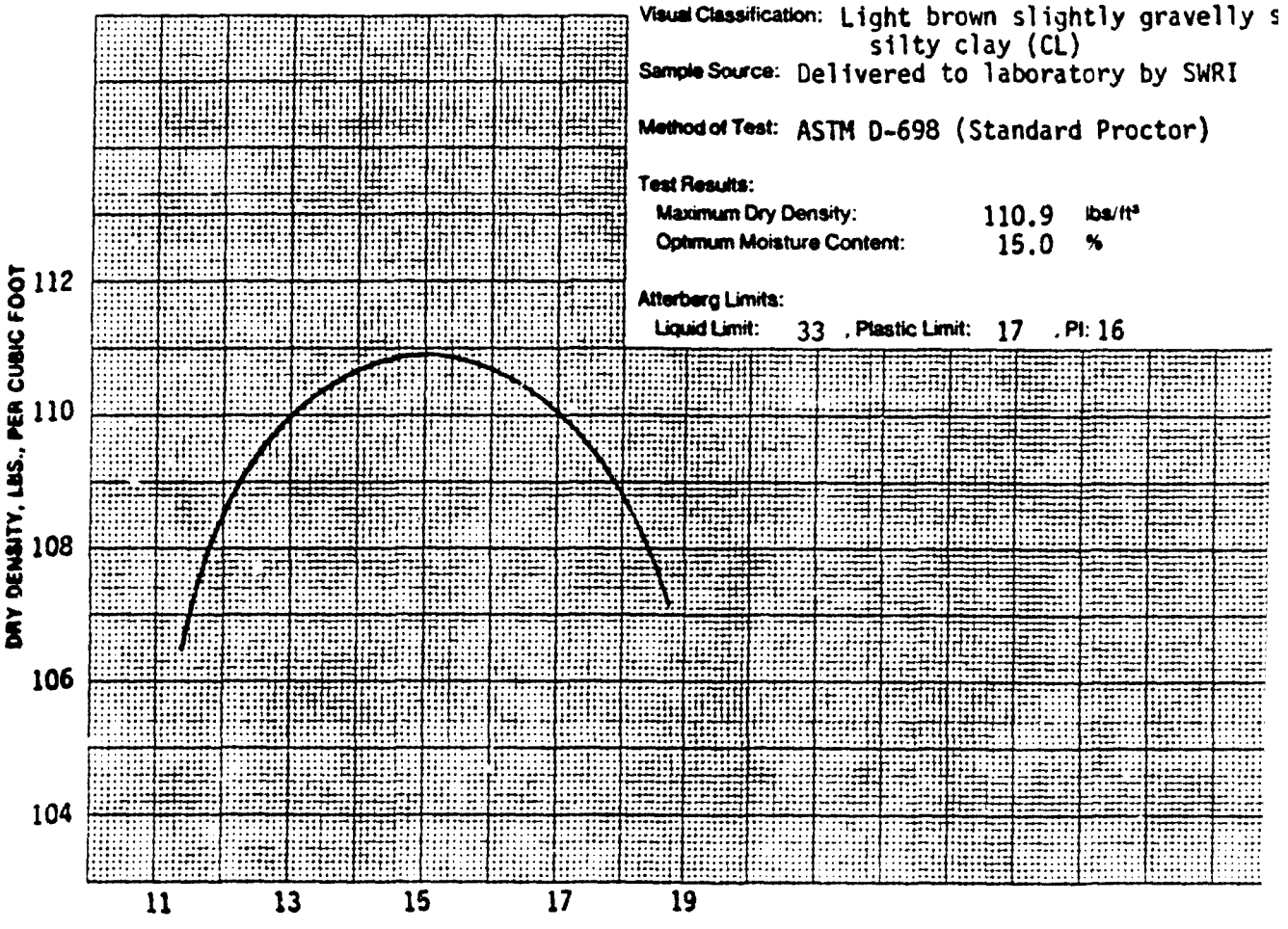

Respectfully submitted,
Professional Service Industr

C-4

Professional Service Industries

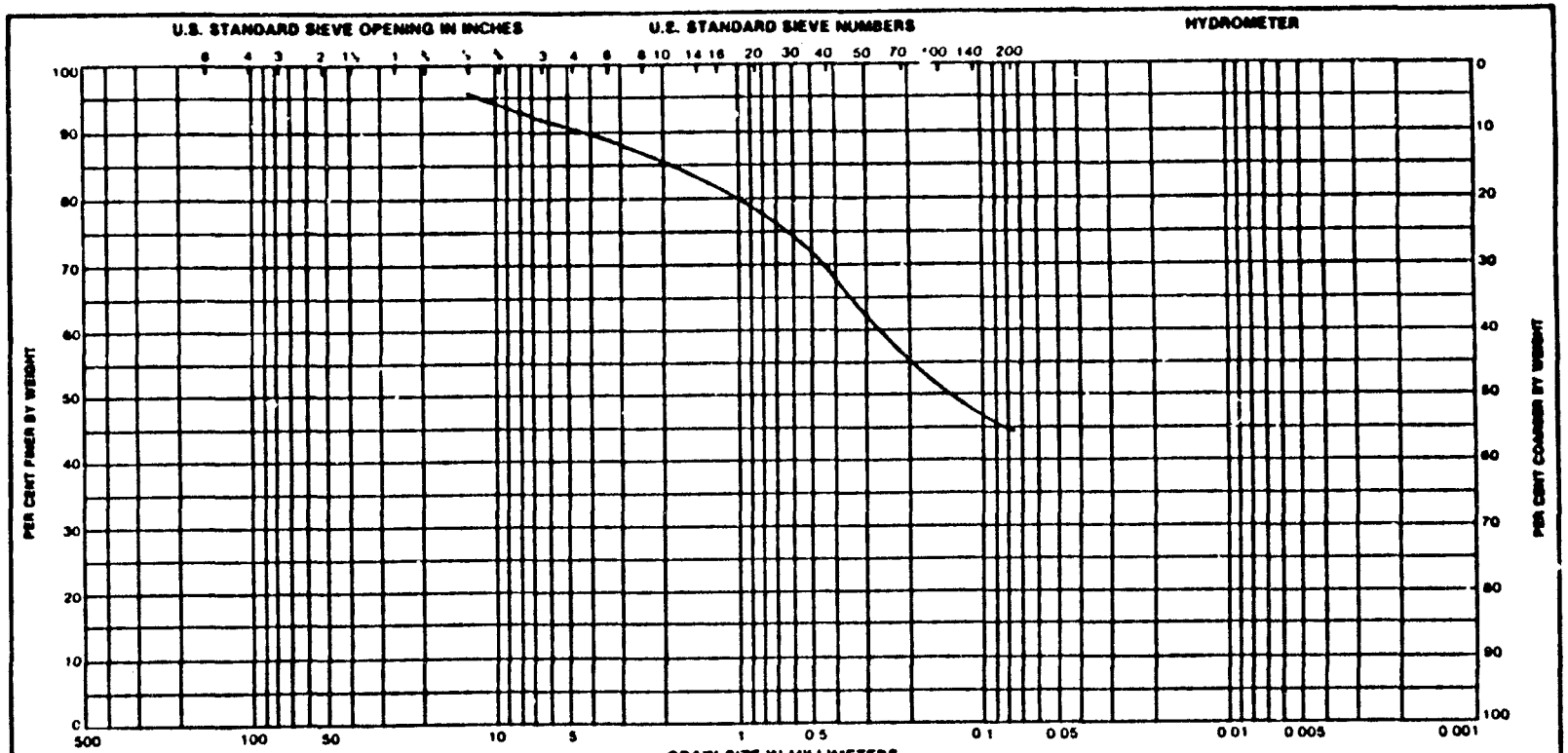

Boring No.	Sample No.	Elev. or Depth	Classification	Nat w %	LL	PL	PI	Project
-	-	-	Light brown gravelly sandy silty clay	-	33	17	16	Navato Loam Sample Southwest Research Institute

REPORT OF SOIL ANALYSIS

File No 312-35160

Specimen	①	②	③
Moisture Content, %	10.9	11.0	11.4
Dry Unit Weight, PCF	102.8	100.4	101.9
Degree of Saturation, %	47	48	49

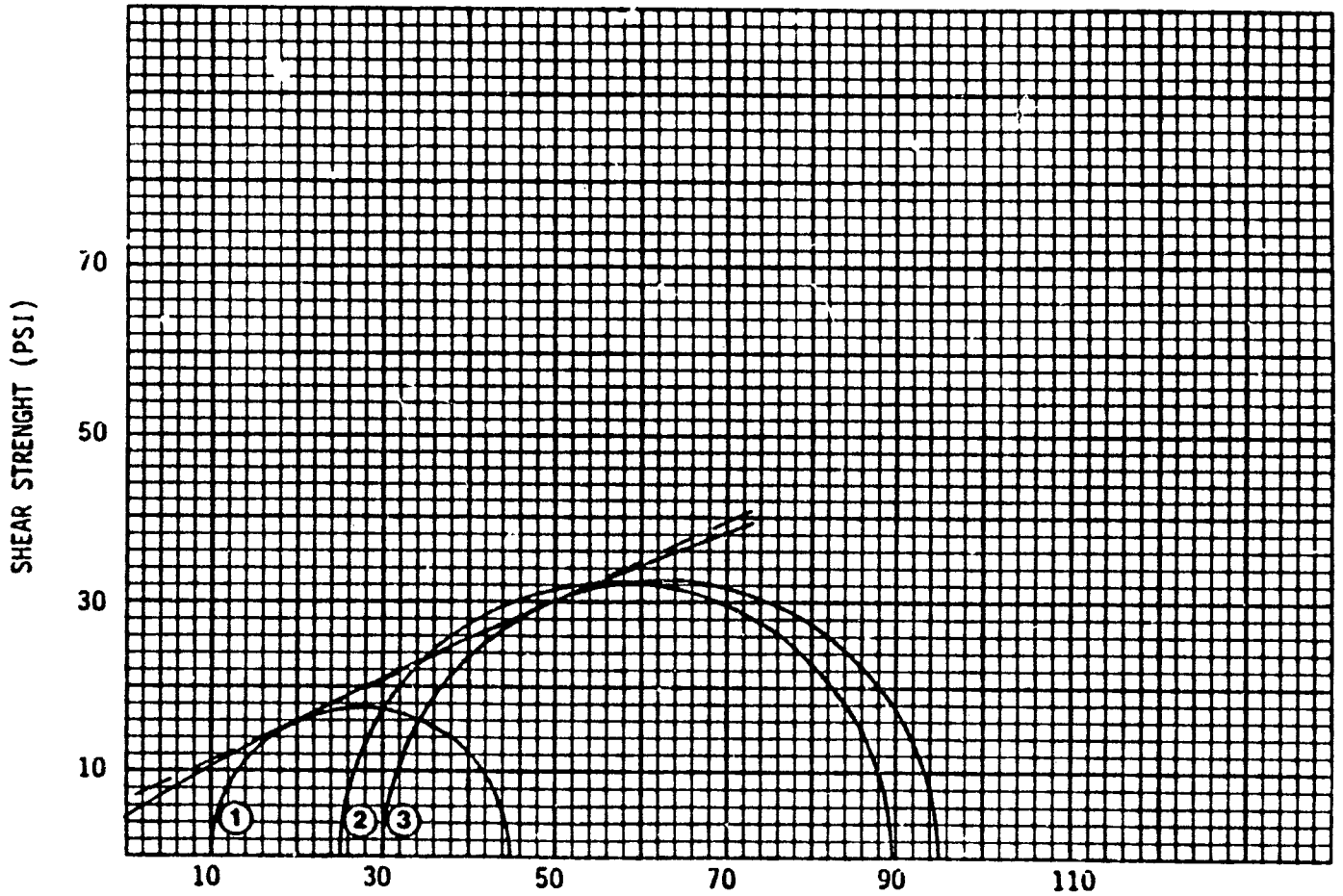

Mohr's Circles for Unconsolidated-Undrained Triaxial Test

APPENDIX D

SHELTER SPACING ANALYSIS

A quick-look analysis was conducted to make some determinations of the shock and flow parameters in the test section of the shock tunnel. The analysis includes:

1. Shock pressure increase due to the decrease in area caused by the presence of the test bed.
2. Shock parameters on the test bed.
3. Post diffraction phase boundary layer flow approximations.
4. Post diffraction phase interference effects to permit lateral and tandem spacing criteria for the post diffraction phase.

1. Shock Pressure

Based on the formulations presented by Wright (Ref. D1)

$$\frac{p_2}{p_1} = \left(\frac{h_2}{h_1}\right)^{-0.395} \qquad \text{(D-1)}$$

The unobstructed tunnel test section height is 8.5 ft and the test bed is 1.0 ft high. Thus, where $h_1 = 8.5$ ft and $h_2 = 7.5$ ft, $p_2/p_1 = 1.05$. This relationship gives the increase in the shock pressure above that which would be found if the test bed were not employed so as to decrease the cross sectional area.

2. Shock Parameters

As an example, a 10 psi shock overpressure corresponds to a pressure ratio of

$$\frac{p_1}{p_o} = \frac{10 + 14.69}{14.69} = 1.68$$

Consequently, the Shock Mach number is

$$M_1 = \frac{p_1/p_o + \mu}{1 + \mu}^{1/2} \qquad \text{(D-2)}$$

where $\mu = (\gamma-1)/(\gamma+1) = 0.167$. The ratio of specific heats, γ, was taken to be 1.4. Thus, for $p_1/p_o = 1.68$, $M_1 = 1.26$. Also, for $p_2/p_1 = 1.05$, $p_2/p_o = (1.05)(1.68) = 1.76$ and

$$M_2 = \frac{p_2/p_o + \mu}{1 + \mu}^{1/2} \qquad \text{(D-3)}$$

or, $M_2 = 1.29$. For an acoustic (sound) speed, $c_o = 1116$ ft/s, the shock speed ($U = Mc_o$)

$$U_1 = 1404 \text{ ft/s}$$
$$U_2 = 1435 \text{ ft/s} .$$

Flow (particle) velocity is determined from

$$\frac{u}{c_o} = \frac{(1-\mu)(\gamma-1)}{(1+\mu)(\gamma+\mu)}^{1/2} \qquad \text{(D-4)}$$

where $y = p/p_o$. Thus, for $p/p_o = p_1/p_o$ $u_1/c_o = 0.386$ or $u_1 = 431$ ft/s. For $p/p_o = p_2/p_o$, $U_2/c_o = 0.424$ or $U_2 = 473$ ft/s.

Temperature and density Rankine-Hugoniot relationships are, respectively

$$\frac{T}{T_o} = y \frac{1 + \mu y}{\mu + y} \qquad \text{(D-5)}$$

and

$$\frac{\rho}{\rho_o} \equiv \eta = \frac{\alpha + \gamma}{1 + \mu\gamma} \qquad \text{(D-6)}$$

So,

$$\frac{T_1}{T_o} = (1.68)\ \frac{1 + (0.167)(1.68)}{0.167 + 1.68} = 1.17$$

and

$$\frac{T_2}{T_o} = (1.76)\ \frac{1 + (0.167)(1.76)}{0.167 + 1.76} + 1.18$$

For $T_o = 529.7°R$ (70°F), $T_1 = 157°F$ and $T_2 = 166°F$. Also, using Eq. (D-6) $\rho_1/\rho_o = 1.44$ and $\rho_2/\rho_o = 1.49$. For $\rho_o = 0.00233\ lb_f - s^2/ft^4$, $\rho_1 = 0.00336\ lb/_f - s^2/ft^4$ and $\rho_2 = 0.00347\ lb_f - s^2/ft^4$.

3. Boundary Layer Parameter Approximations

By using average values of the shock parameters from the example just cited, boundary layer parameters may be approximated to get an idea of the depth of submergence of the model shelters within the boundary layer that develops behind the shock. These approximations may be useful for comparison to what full-scale results or measurements may be known. Clearly the following analysis is approximate, and it does not look at the way that the boundary layer develops and the influence that viscous effects might be expected to have on structural response.

For an average tempertaure of $(T_1 + T_2)/2 = 162°F$ the absolute viscosity $\bar{\mu} = 4.3 \times 10^{-7}\ lb_f - s/ft^2$. With an average velocity of $(u_1 + u_2)/2 = 452$ ft/s, an average Reynolds number per foot of tunnel is

$$R_{e/ft} = \frac{\rho u}{\mu} = \frac{(0.00342)(452)}{4.3 \times 10^{-7}} = 3.59 \times 10^6/ft \qquad \text{(D-7)}$$

In Eq (D-7) the average density given by $\rho = (\rho_1 + \rho_2)/2 = (0.00336 + 0.00347)/2.0$ is used. Considering a representative length of flow of x = 50.0 ft, the boundary layer thickness is approximated by

$$\frac{\delta}{x} = 0.37\ R_e^{-1/5} \tag{D-89}$$

to give

$$\delta = (50)(0.37)\left[(3.59 \times 10^6)(50)\right]^{-1/5} = 0.4 \text{ ft} \simeq 5 \text{ in.}$$

Assuming a 1/7th power-law profile for the velocity/boundary-layer-thickness relationship, the momentum thickness is given by

$$\theta = \int_0^\infty \frac{u}{U_1}\left(1 - \frac{u}{U_1}\right) dz \tag{D-9}$$

becomes

$$\theta = 0.097\ \delta \tag{D-10}$$

and the displacement thickness becomes

$$\delta^* = 0.125\ \delta \tag{D-11}$$

For δ = 5 in., $\theta \simeq$ 0.5 in. and $\delta^* \simeq$ 0.6 in. The momentum thickness, a characteristic of the "defeat" in the momentum transport due to a boundary layer is of key concern to the drag force that an object has when it is submerged in the boundary layer. If relative heights of an object and the boundary layer are very different between model- and full-scale, the model-

scale force measurements may not accurately represent what drag force would be found in full-scale. For this example, an object that projected several inches above the test bed would not be expected to be substantially effected by boundary layer influences insofar as drag on the object.

4. Post-Diffraction Spacing Criteria

The post-diffraction phase of a model test is the portion of the test following the time that the shock front arrives at the model and wave reflections, refractions and diffractions from or caused by the incident wave no longer are present at the model. The flow at the model is characterized by the velocity U_2, pressure p_2, density ρ_2, temperature T_2 and associated boundary layer parameters. Preceding sections in this appendix give predictions or estimates for these parameters. To access the spacing that is required between models to avoid interference during this drag phase, interferences drag data have been used. Data samples taken from Hoerner (Ref. D2) show that for spacing ratios less than some value, interference between the objects being considered is noticeable. Beyond some spacing ratio (based on a characteristic object dimension) the objects no longer interfere but respond as if isolated. Five examples of interference effects from Hoerner are presented on the following Figure D-1. By choosing the height as the characteristic dimension for side-by-side (lateral) spacing and for tandem (axial spacing, spacings side-by-side and fore and aft were prescribed. For example, bluff models approximately 4 in. high could be six to seven heights from one another in tandem (approximately 2 ft) and not interfere in the drag flow phase.

To access spacing from a tunnel wall, it was assumed that a mirror image of the model was tandem to the model.

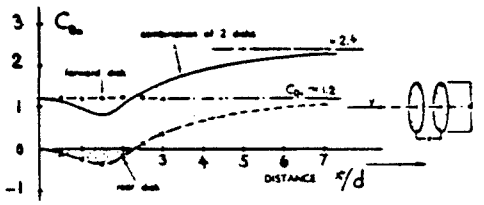

a) Interaction between two disks placed one behind the other

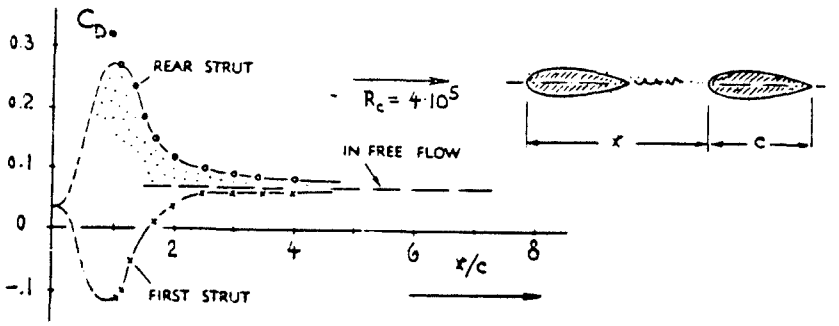

b) Drag of a pair of strut sections, one behind the other, in tandem

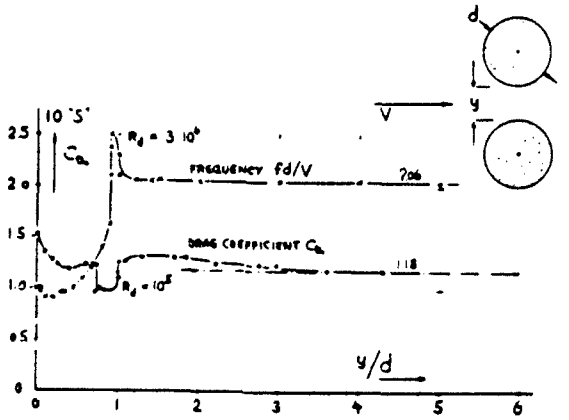

c) Drag (and vortex-street frequency) of a pair of circular cylinders placed side by side

Figure D-1. Five Examples of Interference Effects

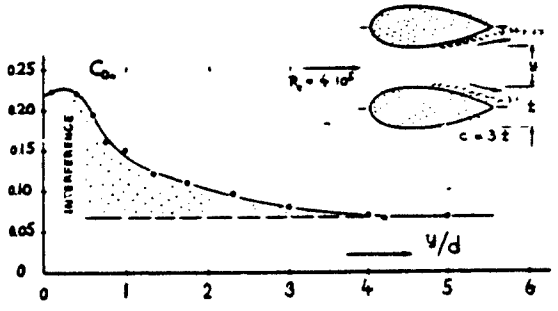

d) Drag of a pair of struts, one beside the other

Interference in B'Layer. Coming to the end of this chapter on surface imperfections, *figure* 30 presents a further example, showing that the drag of protuberances within the boundary layer has characteristics similar to those in free flow. A comparison of this illustration with figure 1 in the "interference" chapter suggests that the second hexagonal head is shielded by the first one. In closest position (at x/d = 0), the drag is ≈ 25% of that of two single heads. It should be noted, however, that beyond x/d = 5, an interference effect is no longer noticeable. This result too, is in agreement with experience in free flow.

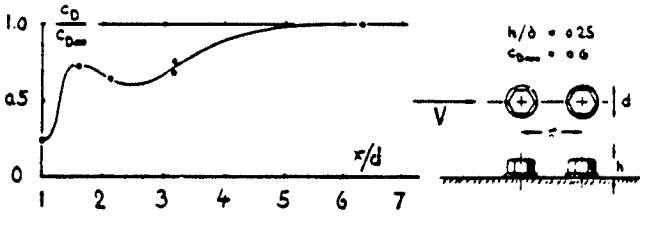

e) Interference effect between a pair of hexagonal bolt heads tested within the boundary layer of a wall

Figure D-1. Five Examples of Interference Effects (Cont'd.)

REFERENCES

D1. Wright, J. I., Shock Tubes, Spottiswoode, Ballantyne and Co. Ltd., London 1961, pp 1-120.

D2. Hoerner, Sighard F., Fluid-Dynamic Drag, published by the author, Midland Park, New Jersey 1958.

DISTRIBUTION LIST

(One copy unless otherwise specified)

Federal Emergency Management Agency
Attn: Assistant Associate Director
for Research
National Preparedness Programs
Directorate
Washington, D.C. 20472 (3)

Dr. David W. Bensen
Office of Research
National Preparedness Programs
Federal Emergency Management Agency
Washington, D.C. 20472 (45)

Mr. Don Bettge
Civil Defense Division
National Preparedness Programs
Federal Emergency Management Agency
Washington, D.C. 20472

Defense Technical Information Center
Cameron Station
Alexandria, VA 22314 (12)

Assistant Director
Energy & Natural Resources
Office of Science and Technology Policy
Executive Office Building
Washington, D.C. 20500

Mr. Carl Wiehle
Defense Intelligence Agency
Attn: CKW DB-4C2
Washington, D.C. 20301

Director, Defence Nuclear Agency
Attn: Michael Frankel
Washington, D.C. 20305

Command and Control Technical Center
Department of Defense
The Pentagon
Washington, D.C. 20301

Mr. Samuel Kramer
National Bureau of Standards
Room B-124, Bldg 225
Washington, D.C. 20234

Mr. William Parker
National Bureau of Standards
Building 224 - Room A-345
Washington, D.C. 20234

Dr. John Rockett
National Bureau of Standards
Center for Fire Research
Building 224 - Room B-260
Washington, D.C. 20234

Director
Department of Military
Application
Department of Energy
Washington, D.C. 20545

Los Alamos Scientific
Laboratory
Attn: Document Library
Los Alamos, NM 87544

R. G. Hickman
Lawrence Livermore National
Laboratory
University of California
Box 808, L-140
Livermore, CA 94550 (10)

Oak Ridge National Laboratory
Attn: Librarian
P.O. Box X
Oak Ridge, TN 37830

Emergency Technology Division
Oak Ridge National Laboratory
Attn: Librarian
Oak Ridge, TN 37830

Chief of Engineers
Department of the Army
Attn: DAEN-RDZ-A
Washington, D.C. 20314

Director, Army Materials and Mechanics
Research Center
Attn: Technical Library
Watertown, MA 02172

Assistant Secretary of the Army (RD&A)
Attn: Deputy ASA for (RD&S)
Washington, D.C. 20310

U.S. Army Training and Doctrine Command
Fort Monroe
Hampton, VA 23651

Director, U.S. Army Ballistic Research
Laboratory
Attn: Document Library
Aberdeen Proving Ground, MD 21005

Mr. William Taylor
Ballistic Research Laboratory
Aberdeen Proving Ground, MD 21005 (2)

Director, U.S. Army Engineer
Waterways Experiment Station
Attn: Document Library
P.O. Box 631
Vicksburg, MS 39180

Mr. W. L. Huff
USAE Waterways Experiment Station
P.O. Box 631
Vicksburg, MS 39180

U.S. Army Combined Arms Combat
Development Activity
Fort Leavenworth, KA 66027

Civil Engineering Center AF/PRECET
Attn: Technical Library
Wright-Patterson Air Force Base
Dayton, OH 45433

Air Force Weapons Laboratory
Attn: SUL Technical Library
Kirtland Air Force Base
Albuquerque, NM 87117

Dr. Conrad Chester
Oak Ridge National Laboratory
P.O. Box X
Oak Ridge, TN 37830

Dr. Clarence R. Mehl
Division 7112
Sandia National Laboratories
Box 5800
Albuquerque, NM 87185

National Council on Radiation
Protection and Measurements
7910 Woodmont Avenue
Bethesda, MD 20014

Mr. Phil Nash
Southwest Research Institute
6220 Culebra Road
San Antonio, TX 78284

Dr. Wilfred E. Baker
Wilfred Baker Engineering
218 E. Edgewood Place
San Antonio, TX 78209

Mr. C. Wilton
Scientific Service, Inc.
517 East Bayshore
Redwood City, CA 94063

Dr. William Christian
Underwriters' Laboratories,
Inc.
333 Pfingsten Road
Northbrook, IL 60062

Dr. Donald Drzewiecki
Calspan Corporation
P.O. Box 400
Buffalo, NY 14225

Mr. Clay P. Butler
SRI International
333 Ravenswood
Menlo Park, CA 94025

Mr. Dick Foster
SRI International
333 Ravenswood
Menlo Park, CA 94025

Air Force Weapons Laboratory
Civil Engineering Division
Kirtland Air Force Base
Albuquerque, NM 87117

Hudson Institute
Quaker Ridge Road
Croton-on-Hudson, NY 10520

Mr. Fred Sauer
Phyics International Company
2700 Merced Street
San Leandro, CA 94577

The Dikewood Corporation
1613 University Blvd, N.E.
Albuquerque, NM 87102

Dr. Anatole Longinow
IITRI
10 West 35th Street
Chicago, IL 60616

Mr. Leo A. Schmidt
Institute for Defense Analyses
Program Analysis Division
1801 N. Beauregard Street
Alexandria, VA 22311

The RAND Corporation
Attn: Document Library
1700 Main Street
Santa Monica, CA 90401

Director
Lovelace Foundation
5100 Gibson Blvd, S.E.
Albuquerque, NM 87108

Dr. Donald Sachs
Kaman Sciences Corp.
1911 Jefferson Davis Highway
Arlington, VA 22202

Center for Planning and Research
2483 E. Bayshore, Suite 104
Palo Alto, CA 94303

Dr. Fred Offensend
SRI International
333 Ravenswood
Menlo Park, CA 94025

Mrs. Ruth Schnider
Center for Planning and
Research
2473 E. Bayshore
Palo Alto, CA 94303

Mr. Walter Strope
Center for Planning and
Research
5600 Columbia Pike - Suite 101
Bailey's Crossroads, VA 22041

Dr. Dennis Holliday
R&D Associates
P.O. Box 9695
Marina del Ray, CA 90291

Research Triangle Institute
Attn: Mr. Ed L. Hill
P.O. Box 12194
Research Triangle Park,
North Carolina 22709

Mr. Robert Fristrom
Johns Hopkins Applied Physics
Laboratory
Johns Hopkins Road
Laurel, MD 20707

Dr. John Cockayne
Senior Scientist
Science Applications, Inc.
1710 Goodridge Drive
P.O. Box 1303
McLean, VA 22101

Mr. Marvin Drake
Science Applications, Inc.
1200 Prospect Street
La Jolla, CA 92037

Mr. Richard Laurino
Center for Planning and Research
2483 E. Bayshore
Palo Alto, CA 94303

Mr. John Rempel
Center for Planning and Research
2483 E. Bayshore
Palo Alto, CA 94303

Dr. Joseph E. Minor, Director
Institute for Disaster Research
Department of Civil Engineering
Box 4089
Lubbock, TX 79409

Professor R. K. Pefley
University of Santa Clara
Santa Clara, CA 95053

Dr. Ing. P.G. Seeger
Forschungsstelle fuer
Brandschuetztechnik
University of Karlsruhe (TH)
75 Karlsruhe 21
Postfach 63380
West Germany

Secretaire d'Administration
Ministere de l'Interieur
Direction Generale de la
Protection Civile
rue de Louvain, 1
1000 Brussels, Belgium

Canadian Defence Research Staff
Attn: Dr. K. N. Ackles
2450 Massachusetts Ave, N.W.
Washington, D.C. 20008

H. L. Murphy Associates
Box 1727
San Mateo, CA 94401

Mr. Harvey G. Ryland
Ryland Research, Inc.
5266 Hollister Avenue
Suite 324
Santa Barbara, CA 93111

Technology & Management
Consultants
330 Washington Street
Suite 613
Marina del Ray, CA 90291

Dr. Matthew Gibbons
5424 Lawton Avenue
Oakland, CA 94618

Jefe, Seccion de Estudios y
Planification
c/Evaristo San Miguel, 8
Madrid-8
Spain

Ministero dell Interno
Direzione Generale della
Protezione Civile
00100 Rome, Italy

Directeur de la Protection
Civile
Ministere de l'Interieur
36 Rue J. B. Esch
Grande-Duche de Luxembourg

Directeur Organisatie
Bescherming Bevoling
Ministry of Interior
Schedeldoekshaven 200
Postbus 20011
2500 The Hague, Netherlands

The Head of Sivilforsvaret
Sandakerveien 12
Postboks 8136
Oslo dep
Oslo 1, Norway

Dr. Don Scheuch
430 Golden Oak Drive
Portola Valley, CA 94025

Director Civilforsvarsstyrelsen
Stockholmsgade 27
2100 Copenhagen 0
Denmark

Direction de la Securite Civile
Ministere de l'Interieur
18 Rue Ernest Cognac
92 Levallois (Paris) France

Bundesministerium des Innern
Graurheindorfer Strasse 198
5300 Bonn 1
West Germany

Ministry of Social Service
11 Spartis Street
Athens, Greece

Almannavarnir Rikisins
Reykavik, Iceland

Stato Maggiore Difesa Civile
Centro Studi Difesa Civile
Rome, Italy

Civil Emergency Planning Directorate
North Atlantic Treaty Organization
1110 NATO, Belgium

Servico National de Proteccao
Civil
Rua Bela Vista a Lapa, 57
1200 Lisbon, Portugal

Civil Defense Administration
Ministry of Interior
Ankara, Turkey

Home Office
Scientific Advisory Branch
Horseferry House
Dean Ryle Street
London SW1P2AW
England